FUZZY LOGIC BASED MULTI-OBJECTIVE OPTIMIZATION OF ACTIVE SUSPENSION SYSTEM OF 4X4 IN-WHEEL MOTOR DRIVEN ELECTRICAL VEHICLE

Ömer BİNGÜL

T.C.
BURSA ULUDAĞ ÜNİVERSİTESİ
FEN BİLİMLERİ ENSTİTÜSÜ

FUZZY LOGIC BASED MULTI-OBJECTIVE OPTIMIZATION OF ACTIVE SUSPENSION SYSTEM OF 4X4 IN-WHEEL MOTOR DRIVEN ELECTRICAL VEHICLE

Ömer BİNGÜL
0000-0002-8113-4988

Dr. Öğr. Üyesi Ahmet YILDIZ
(Danışman)

YÜKSEK LİSANS TEZİ
OTOMOTİV MÜHENDİSLİĞİ ANABİLİM DALI

BURSA – 2021
Her Hakkı Saklıdır

ÖZET

Yüksek Lisans Tezi

FUZZY LOGIC BASED MULTI-OBJECTIVE OPTIMIZATION OF ACTIVE SUSPENSION SYSTEM OF 4X4 IN-WHEEL MOTOR DRIVEN ELECTRICAL VEHICLE

Ömer BİNGÜL

Bursa Uludağ Üniversitesi
Fen Bilimleri Enstitüsü
Otomotiv Mühendisliği Anabilim Dalı

Danışman: Dr. Öğr. Üyesi Ahmet YILDIZ

Bu tezde, 4x4 tekerlek içi motorlu bir elektrikli aracın doğrusal olmayan aktif süspansiyon sisteminin bulanık mantık tabanlı çok amaçlı optimizasyonu, süspansiyon sistemlerinin yuvarlanma açısı ve yük transferi gibi gerçek çalışma koşulları dikkate alınarak incelenmiştir. Bu bağlamda, on bir serbestlik derecesine sahip ikinci dereceden lastik ve kübik süspansiyon katılığına sahip doğrusal olmayan bir tam elektrikli araç modeli ve beş serbestlik dereceli bir koltuk-sürücü modeli oluşturulmuştur. Sürüş ve sağlık kriterlerini değerlendirmek için ISO 2731-1'de tanımlanan gereklilikler esas alınmıştır. Seçilen amaç fonksiyonları, weighted root mean square baş ivmesi, root mean square koltuk ivmesi, crest factor, titreşim doz değeri, root mean square baş ivmesinin root mean square koltuk ivmesine oranı, root mean square üst gövde ivmesinin root mean square koltuk ivmesine oranı, ve root mean square üst gövde ivmesidir. Bunlara ek olarak, nadiren incelenen rollover etkisi araştırılmıştır. Root mean square süpansiyon deplasmanı, root mean square tekerlek deplasmanı, root mean square tekerlek içi motor deplasmanı ve yuvarlanma açısı kısıtlar olarak seçilmiştir. Optimizasyon NSGA-II algoritması ile gerçekleştirilmiştir. Pasif sistem için tasarım değişkenleri; süspansiyon, tekerlek içi motor ve koltuğun yay katılıkları ve amortisör sönüm katsayılarıdır. Ardından, en iyi sürüş konforu ve sağlık kriterini sağlamak için proportional derivative kontrolcü ile birleştirilmiş bir bulanık mantık kontrolcü optimize edilmiştir. Sunulan optimizasyon sonuçlarının bulanık mantık kontrolcünün pasif sisteme karşılık olarak önemli bir gelişme gösterdiği ve yük transfer indeksinde devrilme koşuluyla ilgili olumsuz bir değişiklik göstermediği görülmektedir.

Anahtar Kelimeler: elektrikli araç, tekerlek içi motor, çok amaçlı optimizasyon, genetik algoritma, yuvarlanma etkisi
2021, xiv + 88 sayfa.

ABSTRACT

MSc Thesis

FUZZY LOGIC BASED MULTI-OBJECTIVE OPTIMIZATION OF ACTIVE SUSPENSION SYSTEM OF 4X4 IN-WHEEL MOTOR DRIVEN ELECTRICAL VEHICLE

Ömer BİNGÜL

Bursa Uludağ University
Graduate School of Natural and Applied Sciences
Department of Automotive Engineering

Supervisor: Asst. Prof. Dr. Ahmet YILDIZ

In this thesis, fuzzy logic based multi-objective optimization of a nonlinear active suspension system of 4x4 in-wheel motor-driven electrical vehicle is studied by considering real working conditions such as roll angle and load transfer of the suspension systems. In this regard, a nonlinear full electrical vehicle model with quadratic tire stiffness and cubic suspension stiffness with eleven degrees of freedom and a seat-driver model with five degrees of freedom implemented and optimized by the guidelines introduced in ISO 2731-1 to assess ride and health criteria. Selected objective functions are comprised of weighted root mean square head acceleration, root mean square seat acceleration, crest factor, vibration dose value, the amplitude of head root mean square acceleration to seat root mean square acceleration, the amplitude of upper torso root mean square acceleration to seat root mean square acceleration, and root mean square upper torso acceleration. In addition to these, rarely considered rollover effect was investigated. Root mean square suspension displacement, root mean square tire displacement, root mean square in-wheel motor displacement, and roll angle were selected as constraints. Optimization was carried out with NSGA-II algorithm. Design variables for the passive system are; stiffnesses and dampers of suspension, in-wheel motor, and seat. Then, a fuzzy logic controller coupled with a proportional derivative controller optimized for best ride comfort and health criterion. Presented optimization results demonstrated a significant improvement over the passive system with fuzzy logic controller, and the load transfer index showed no adverse change between models concerning the rollover condition.

Key words: electric vehicle, in-wheel motor, multi-objective optimization, genetic algorithm, rollover effect
2021, xiv + 88 pages.

ACKNOWLEDGEMENTS

Throughout the writing of this dissertation I have received a great deal of support and assistance.

First and foremost, I would like to express my sincere thanks to my supervisor, Asst. Prof. Dr. Ahmet YILDIZ for his guidance, motivation and continual support throughout my research. The achievement of this work would not be possible without his valuable expertise and helpful suggestions by making some sense of the confusion.

In addition, I would like to thank my parents for their love, encouragement, wise counsel, sympathetic ear and support throughout years. I would also like to thank to my friends who provided stimulating discussions as well as happy distractions to rest my mind outside of my research.

Ömer BİNGÜL
23/09/2021

TABLE OF CONTENTS

Page

ÖZET vi
ABSTRACT vii
ACKNOWLEDGEMENTS viii
ABBREVIATIONS x
LIST OF FIGURES xii
LIST OF TABLES xiv
1. INTRODUCTION 1
2. LITERATURE REVIEW 5
2.1. Introduction 5
2.2. Vehicle Suspension Systems 6
2.2.1. Passive suspension 6
2.2.2. Semi-active suspension 9
2.2.3. Active suspension 14
2.3. Electric Vehicle Suspension Systems 17
2.3.1. Centralized propulsion suspension system 18
2.3.2. In-wheel motor suspension system 20
2.4. Control Methods 23
2.4.1. Proportional integral derivative control 23
2.4.2. Fuzzy logic control 24
2.5. Optimization Methods 27
3. MATERIAL AND METHOD 31
3.1. Full Vehicle and Human Models 31
3.2. Active Suspension 40
3.2.1. PID controller 40
3.2.2. Fuzzy logic controller 42
3.3. Multi-Objective Optimization 45
3.3.1. Diversity preservation 50
3.3.2. Objective functions 53
3.3.3. Population size and stoppage criterion 59
4. RESULTS AND DISCUSSION 61
5. CONCLUSION 76
REFERENCES 77
CURRICULUM VITAE 88

ABBREVIATIONS

Notation	Description
ABC	Artificial Bee Colony
ABS	Anti-lock Brake Systems
ACO	Ant Colony Optimization
ADM	Advanced Dynamic Damper Mechanism
ANFIS	Adaptive Network-based Fuzzy Inference System
ANN	Artificial Neural Network
BBO	Biogeography-Based Optimization
BP	Back Propagation
CD	Crowding Distance
CF	Crest Factor
CS	Cuckoo Search
D	Derivative
DE	Differential Evolution
DOF	Degrees Of Freedom
EA	Evolutionary Algorithm
EHA	Electro-Hydrostatic Actuator
EKF	Extented Kalman Filter
EMS	Electromagnetic Suspension
ER	Electrorheological
ESC	Electronic Stability Control
EV	Electic Vehicle
FIS	Fuzzy Inference System
FL	Fuzzy Logic
FLC	Fuzzy Logic Controller
FTC	Fault Tolerant Control
GA	Genetic Algorithm
GP	Genetic Programming
HGCZ	Health Guidance Caution Zone
HIS	Hydraulically Interconnected Suspension
I	Integral
ICE	Internal Combustion Engine
IWM	In-wheel Motor
LHR	Likely Health Risk
LQ	Linear Quadratic
LQR	Linear Quadratic Regulator
LSRA	Linear Switched Reluctance Actuator
LTR	Load Transfer Ratio
MF	Membership Function
MIMO	Multiple-Input-Multiple-Output
MOEAs	Multi-Objective Evolutionary Algorithms
MOGA	Multi-Objective Genetic Algorithm
MOPSO-CD	Multi-Objective Particle Swarm Optimization
MR	Magnetorheological

NHR	No Health Risk
NNC	Neural Network Control
NPGA	Niched Pareto Genetic Algorithm
NSGA	Non-dominated Sort Genetic Algorithm
NSGA-II	Non-dominated Sort Genetic Algorithm II
P	Proportional
PD	Proportional Derivative
PHR	Potential Health Risk
PI	Proportional Integral
PID	Proportional Integral Derivative
PMA	Permanent-Magnet Actuator
PSA	Pattern Search Algorithm
PSO	Particle Swarm Optimization
RMS	Root Mean Square
SMC	Sliding Mode Control
SQP	Sequential Quadratic Programming
SRM	Switched Reluctance Motor
TCS	Traction Control System
TWLO	Two-Wheel Lift-Off
VDV	Vibration Dose Value
WBV	Whole Body Vibration

LIST OF FIGURES

Page

Figure 2.1 Trade-off nature of suspension systems 5
Figure 2.2 Passive suspension 6
Figure 2.3 Schematic of an anti-roll HIS 8
Figure 2.4 The assembled anti-roll HIS system 8
Figure 2.5 Schematic of a quarter-car suspension with skyhook control 9
Figure 2.6 Suspension system model: (a) passive, (b) semi-active 10
Figure 2.7 ER damper schematic configuration 11
Figure 2.8 Photograph of ER damper 11
Figure 2.9 Schematic of an MR shock absorber 12
Figure 2.10 Photo of an MR shock absorber 13
Figure 2.11 Bouc–wen model for MR shock absorber 13
Figure 2.12 Active suspension 14
Figure 2.13 An electrohydraulic actuator schematic 15
Figure 2.14 Photo of the pressure control unit 16
Figure 2.15 (a) Passive suspension system (b) electromagnetic suspension system 17
Figure 2.16 (a) Schematic configuration of double-sided LSRA module. (b) 3D model of LSRA 18
Figure 2.17 TOGG centralized propulsion electrical vehicle 18
Figure 2.18 Tesla model s 85d centralized propulsion electrical vehicle 19
Figure 2.19 REE board electrical vehicle chassis incorporating in-wheel motors . 20
Figure 2.20 Hiriko fold — a vehicle employing in-wheel motors 21
Figure 2.21 Frequency response of sprung mass acceleration and tire deflection . 22
Figure 2.22 Random response of sprung mass acceleration and tire dynamic force 22
Figure 2.23 Simulink model of a pid control system 25
Figure 2.24 A fuzzy pid controller schematic 27
Figure 2.25 (a) Schematic of the controller and (b) the general architecture of the controller 28
Figure 3.1 Full car model of 4x4 in-wheel motor driven electrical vehicle 31
Figure 3.2 Wan and schimmels human model 36
Figure 3.3 Wheel load difference and roll angle 38
Figure 3.4 Class c road input (velocity 90 $kmph$) 41
Figure 3.5 A controlled system diagram 42
Figure 3.6 Flc controller 44
Figure 3.7 Gaussian type membership functions of error input 45
Figure 3.8 Gaussian type membership functions of derivative of error input . . . 45
Figure 3.9 Gaussian type membership functions of output 46
Figure 3.10 Flow chart of the multi-objective optimization algorithm based on fast and elitist non-dominated sorting genetic algorithm 49
Figure 4.1 Objective values of selected members (1 and 2 scale x10 - 5 to 7 scale x100) 61
Figure 4.2 Minimum objective values of populations in all generations 62
Figure 4.3 k_p fuzzy logic controller (a) E, (b) delE, and (c) output membership functions 65

Figure 4.4 k_d fuzzy logic controller (a) E, (b) delE, and (c) output membership functions 66
Figure 4.5 (a) k_p and (b) k_d surfaces of the fuzzy logic controller 67
Figure 4.6 Time response of human model 69
Figure 4.7 Comparison of AR_h, AR_{ut}, VDV_h, A_{ut} 70
Figure 4.8 Sprung mass displacement graphs 71
Figure 4.9 Suspension deflections 72
Figure 4.10 Tire deflections 73
Figure 4.11 Control forces of active suspension 74
Figure 4.12 A_{wh} graph (health guidance caution zone) 75

LIST OF TABLES

Page

Table 3.1 Road roughness values classified by ISO 8608 (2016) (degree of roughness $S(\Omega) \times 10^{-6}$) 40
Table 3.2 Constants of full vehicle and human model 58
Table 3.3 Design variable range for passive suspension elements 60
Table 3.4 Design variable range of fuzzy logic controlled proportional and derivative gains 60
Table 3.5 Design variable range for fuzzy logic controller 60
Table 4.1 Minimum objective values 61
Table 4.2 Selected passive design variables for passive and fuzzy logic controlled systems 63
Table 4.3 Selected membership function design variables of fuzzy logic controller 64
Table 4.4 Fuzzy logic controller k_p rules of selected population member 64
Table 4.5 Fuzzy logic controller k_d rules of selected population member 64
Table 4.6 Comparison of selected members 68
Table 4.7 Vertical wheel forces and load transfer index 69
Table 4.8 Time limits for vibration exposure 75

1. INTRODUCTION

Electic Vehicles (EVs) attracted more research interest in recent years as the next generation transportation vehicles as fossil fuel-powered vehicles wreak havoc on the environment by causing global warming. U.S Environmental Protection Agency states that EVs provide a massive improvement against Internal Combustion Engines (ICEs) from 12-30% to 77% in terms of energy efficiency (DOE and EPA, 2021). More importantly, tens of millions of people suffer, and millions of people lose their lives due to air pollution every year. Air pollution increases respiratory morbidity and mortality, which caused 3.7 million people to lost their lives just in 2012 due to poor air quality (Jiang, Mei, & Feng, 2016). ICEs, as one of the major reasons for poor air quality in cities, presents a big environmental impact with high emissions and fine particulate matter pollution.

As the impact of ICEs on the environment and public health has become more clear, more effort than ever before is being made to accelerate the development of EVs. As stated by a report made by Edison Electric Institute, while the US housed 1 million EVs in 2018, 18.7 million EVs expected to be on US roads with annual sales exceeding 3.5 million, more than 20% of annual automobile sales, by 2030. While there is so much inclining to EVs in the world, Turkey showed their interest by the foundation of Turkey's Automobile Joint Venture Group Inc., also known as TOGG. As the construction of Turkey's EV production factory in Gemlik/Bursa continuing and the first production car is expected to hit the roads in 2022, production capacity is expected to reach one hundred thousand by 2027 (Türkiye Elektrikli ve Hibrid Araçlar Derneği, 2020). Moreover, as stated in March 2021, the New Generation Commercial Vehicle and Battery Production facility in Kocaeli, a venture of Ford Otosan, was announced and expected to reach a production capacity of two hundred ten thousand commercial EVs and hundred thirty thousand EV battery by 2027 as Turkey's second EV production facility (Anadolu Ajansı, 2021). EVs has numerous benefits compared to ICEs such as higher efficiency, enhanced comfort, lower cost of ownership, and zero greenhouse gas emissions. All these advantages of EVs and environmental effects of ICEs drive the industry to EVs.

While there is so much attention to EVs and their main differences to ICEs are their electric motor and battery system, their suspension system requires as much research concentration. A vehicle's handling capabilities are significantly affected by the suspension system's dynamic behavior, meaning that performance improvements of suspension systems positively affect the comfort, forestall fatigue, health risks, and decrease traffic accidents (D. Cao, Song, & Ahmadian, 2011).

It is possible to identify suspensions as passive, semi-active, and active (Hrovat, 1997). Passive suspensions comprise spring and dampener elements. Passive systems comprise the superiority of being an unsophisticated design, easy application, no energy consumption, and high-reliability (W. Sun, Gao, & Shi, 2020). However, they are insufficient in promoting comfort and handling due to the inability of variable spring and shock absorber characteristics to handle different road conditions and conflicting performance expectations (Naudé & Snyman, 2003).

Semi-active suspensions have shock absorbers that have changeable characteristics. This means that damping coefficients or spring stiffness can be adjusted at a specific range, and due to their low energy consumption and high reliability, they are available in numerous vehicles (Paulides, Encica, Lomonova, & Vandenput, 2006). Nonetheless, the resulting damping or spring forces have the constraints of a passive suspension system and can only provide limited improvement in comfort, although they accommodate significant improvement over passive suspension systems (W. Sun et al., 2020).

Active suspensions consist of the same damper and spring elements as passive systems. In addition to these, an actuator is present in these types of suspensions, which separates these systems from the other two. Active suspensions systems have high energy consumption and can produce forces independent of relative suspension displacement or velocity. Although due to their cost, size, and implementation difficulties, active suspensions are not popular (Li, Liu, Gao, & Shi, 2012).

Suspension system design is also essential in EVs in precisely the same way they are in ICEs. EVs also comprise passive, semi-active and active suspensions, and moreover, they provide advantages over traditional ICE vehicles in terms of efficiency, lightweight

designability, and environmentally by zeroing greenhouse gas output. Electric motors, compared to ICEs, contain a much fewer number of parts which in turn gives them the advantage of being easier to design and manufacture, more prolonged lifespan makes them economically desirable, much less noise and vibration creation during operation enhance comfort, instantaneous speed control provides more performance output.

For EVs two approaches are possible for the positioning the electric motor, just like the ICEs, the electric motor can be positioned on the sprung mass, vehicle body, and also due to not having strict size restrictions of ICEs, electric motors can be positioned on the unsprung mass, inside wheels. In-wheel Motor (IWM) EV design allows the vehicles to be more compact (Nagaya, Wakao, & Abe, 2003). Nevertheless, this design also increases the unsprung mass's weight, drastically affecting comfort, handling, and health criteria (Nagaya et al., 2003).

Many studies have been carried out on the optimization of EVs and IWM configurations (TOKSOY & YILDIZ, 2020; Yildiz & Özel, 2021). Compared to IWMs, EVs with centralized propulsion have the advantage of longer motor lifespan due to lower motor vibration, higher comfort, and better road handling due to lower unsprung mass (Liu, Gu, & Zhang, 2017). Although centralized propulsion systems have these advantages, IWM propulsion systems have been extensively researched owing to their native advantages such as simplicity, efficiency, swift and accurate torque generation without adverse effects on drive-shaft, ease of X-by-wire implementation, enhancing of Electronic Stability Control (ESC) system, Traction Control System (TCS), and Anti-lock Brake Systems (ABS) performance (Murata, 2012a). While IWMs have many upsides, some significant disadvantages prevent them from being used in production cars, such as an increase in the wheels' mass leads to decreased comfort and road-holding abilities. Nagaya et al. (2003) developed an IWM system which is defined as Advanced Dynamic Damper Mechanism (ADM) to reduce these adverse effects. The motor acted as a dynamic vibration absorber isolated from the unsprung mass by attaching the motor to the wheel via a passive suspension mechanism. It was found that this system reduced fluctuations in dynamic tire loads, vibrations in the motor, wheel, and vehicle body.

While EVs and IWMs provide many improvements, the design phase of any suspension system contains compromises because comfort, reliability, and safety requirements are most of the cases trade-off objectives, and determination of suspension characteristics is a choice that needs to be made in suspension design (H. Chen & Guo, 2005). Due to suspension systems compromising nature, multi-objective optimization would benefit the suspension systems development phase in acquiring optimal suspension.

W. Sun et al. (2020) defines the successful development of active suspension systems in two stages. W. Sun et al. states that foremostly creating a dynamic model of the vehicle, and secondly designing and optimizing the active system's control strategy has a crucial impact on comfort, health, and safety. W. Sun, Li, Huang, and Zhang (2017) states that three external sources that cause dynamic vehicle responses are the road excitation, inertia accelerations caused by acceleration/deceleration and turning.

W. Sun et al. mentions that comfort and stability are connected with different Degrees Of Freedom (DOF) movements; for instance, the vehicle body movement can be perilous when the sprung mass roll causes disproportionate load distribution on tires, resulting in side-slip or rollover of the vehicle. Considering that active suspension improves stability on top of the ride comfort, the frequently incorporated quarter or half car models are not sufficient for active suspension analysis.

This thesis further studies the multi-objective parameter optimization of an EVs active suspension to address the above issues. In addition to the aforementioned studies, with facts stated by W. Sun et al. (2017), a nonlinear full electrical vehicle model with quadratic tire stiffness and cubic suspension stiffness with eleven DOF and a seat-driver model with five DOF is established. Also, in addition to more traditional comfort and safety objectives widely used in literature, rarely considered real working conditions of the suspension systems such as roll angle and load transfer are investigated. Then, multi-objective optimization of a Proportional Derivative (PD) Fuzzy Logic Controller (FLC) is carried out with a fast and elitist Non-dominated Sort Genetic Algorithm II (NSGA-II). Subsequently, responses of optimized passive and FLC controlled systems are matched against each other. Key findings are presented in the conclusion.

2. LITERATURE REVIEW

2.1. Introduction

EVs compared to conventional ICEs provides many benefits such as high driving performance, efficiency, and environmental friendliness. IWM configuration with numerous advantages is attracting more research interests. Regardless of its benefits, IWM technology has its drawbacks, such as incrementing wheels mass causes critical deterioration in comfort and road-holding capabilities. Such compromises in suspension systems, as shown in Fig. 2.1, affect not only conventional ICE vehicles with their more than a century-long existence but also EVs regardless of their suspension type.

Extensive research of conventional vehicle suspension systems has been carried out concerning control strategies, structural design, and dynamic performance (D. Cao et al., 2011). Based on the studies related to IWM EVs, active suspension control is imperative for IWM configuration.

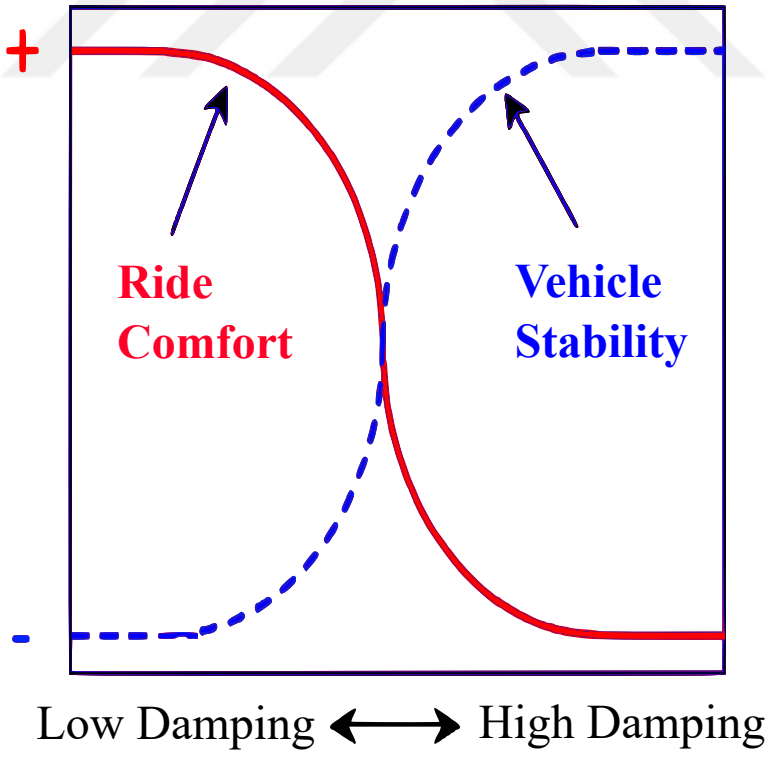


Figure 2.1. Trade-off nature of suspension systems (Simon & Ahmadian, 1998)

2.2. Vehicle Suspension Systems

Vehicle suspension systems are comprised of springs, shock absorbers, and mechanical linking parts that connect the vehicle's body to wheels. Suspension systems provide the wheel-road contact, also preventing the body from rolling motion in cornering conditions in addition to its primary purpose of isolating road-induced vibration (Gillespie, 1992). From the system control perspective, categorization of suspensions is possible in three distinctive classes: passive, semi-active, and active suspensions.

2.2.1. Passive suspension

Passive suspensions have well-known spring and damper elements that their characteristics cannot be changed from their designed values. These systems provide numerous advantages over semi-active and active suspensions, such as unsophisticated design, low cost, and high reliability. A passive suspension schematic is shown in Fig. 2.2.

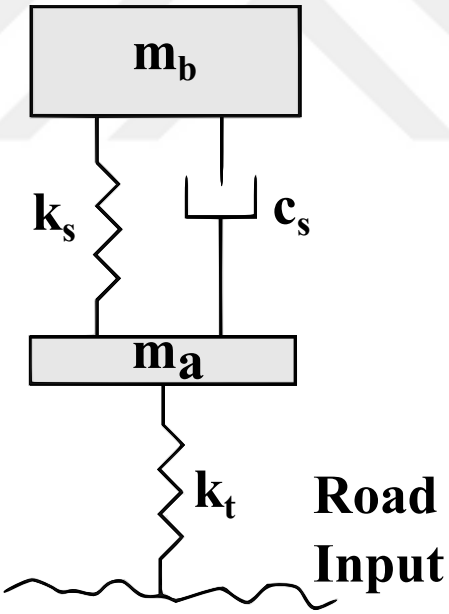


Figure 2.2. Passive suspension (Ahmadian, 2001)

Under the specifications of ISO 8608 (2016), vehicle ride comfort is usually assessed with a random road profile or bump profile. For the prevention of mechanical suspension system failures and ride comfort deterioration, suspension deflection constraint is utilized. Dynamic tire forces are directly linked to road-holding abilities, and tire deflection values

are generally constrained and optimized for a good-performing suspension system. For the improvement of vehicle vibration, passive suspension parameter optimization can be carried out with a Genetic Algorithm (GA) (Mitra et al., 2016). Factors affecting dynamic vehicle responses are irregularities in roadways, vehicle speed, and passive systems characteristics.

Regarding cornering conditions, anti-roll torsional bars are implemented to improve vehicle stability, such as roll angle. While torsional anti-roll bars improve roll stiffness and provide a better cornering dynamic characteristic with a connection between the left and right wheels, deterioration in road holding ability and ride comfort are undesired side effects of such systems. Compared to a suspension system with spring elements, an anti-roll bar comprised suspension system demonstrates improved performance, and independent suspension systems outperform rigid axle suspension systems (Cole, 2000). D. Cao, Rakheja, and Su (2010) stated that conflicting parameters such as comfort and handling performances could be improved with passive interconnected suspension systems.

Interconnected suspension systems can generate forces in all other wheels through mechanical or hydraulic links between wheels with the displacement of one wheel. These systems can potentially overcome the compromising nature of comfort and handling performance (W. A. Smith & Zhang, 2010). N. Zhang, Smith, and Jeyakumaran (2010) researched hydro-pneumatic suspension systems comprehensively. On a different approach to interconnected suspension systems, Hydraulically Interconnected Suspensions (HISs) attracted many researchers' attention. W. A. Smith and Zhang (2010) proposed a HIS system that replaces the typical shock absorbers. In Figs. 2.3 and 2.4 an anti-roll HIS is presented. It is seen that four cylinders placed at each wheel are interconnected by hydraulic lines, accumulators, damper valves, flexible hoses, and pipelines. W. A. Smith, Zhang, and Hu (2011); Wang, Zhang, and Du (2012) presented a simulation and experimental study of an SUV comprising HIS system subjected to various steering maneuvers, and the results indicated that roll performance improvements and prevention of vehicle rollover are achievable through implementation of these systems.

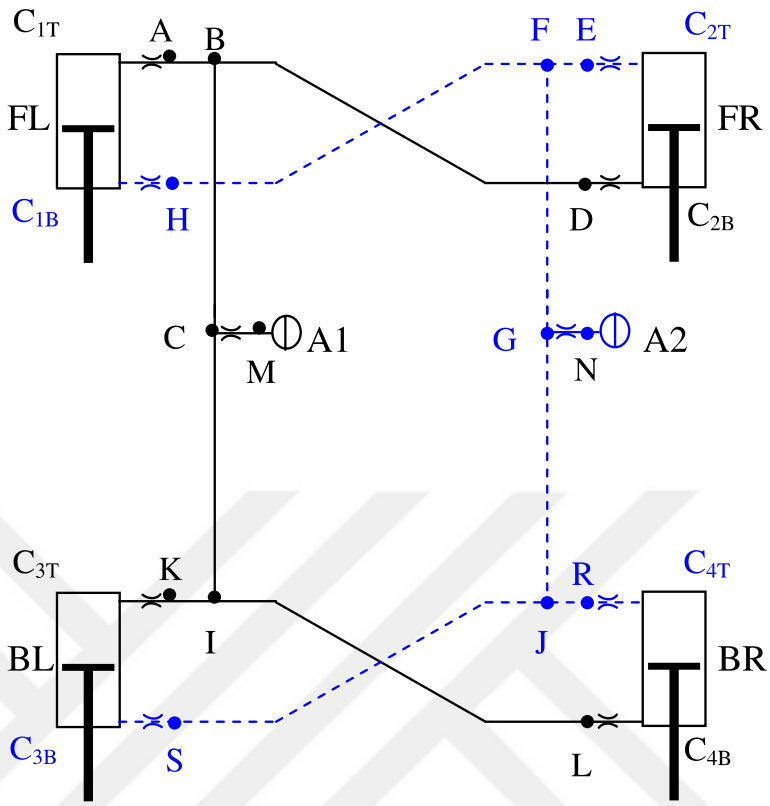


Figure 2.3. Schematic of an anti-roll HIS (W. A. Smith et al., 2011)

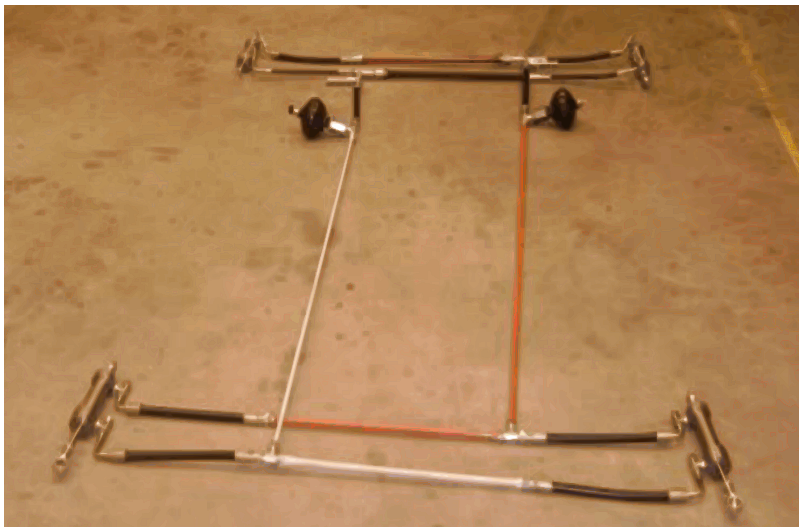


Figure 2.4. The assembled anti-roll HIS system (Wang et al., 2012)

2.2.2. Semi-active suspension

By comparison to passive suspensions, optimal suspension can be achieved with controlled suspensions, improving comfort and handling. The first semi-active suspension concept was presented by Karnopp and Crosby (1974) presenting the skyhook algorithm to enhance vehicle suspension systems. A skyhook quarter car schematic is shown in Fig. 2.5. Generally, in semi-active suspension systems, shock absorber constitutes a variable characteristic over passive systems fixed-rate shock absorber or active suspension systems actuator. Force generated by damper can either be regulated by changing area of the orifice, which in turn changing fluid flow resistance, or by another variation such as changing the fluid viscosity such as in Electrorheological (ER) and Magnetorheological (MR) shock absorbers (Gopala Rao & Narayanan, 2009). A comparison of passive and semi-active suspensions is shown in Fig. 2.6. As a competitor to active suspension systems, semi-active systems provide advantages, including cost savings by simple design and energy efficiency.

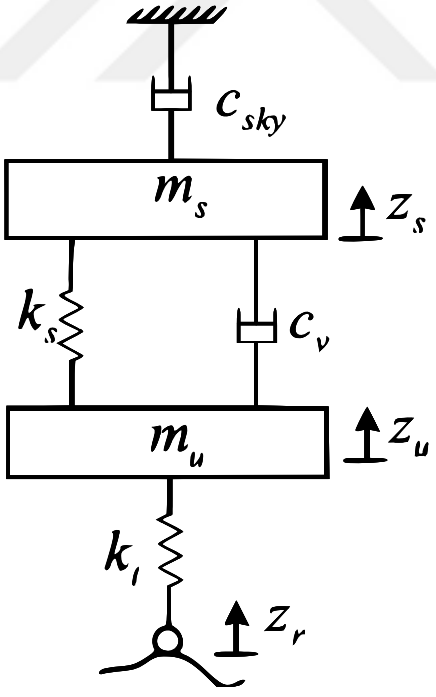


Figure 2.5. Schematic of a quarter-car suspension with skyhook control (Nguyen et al., 2009)

Choi and Han (2007) states semi-active ER suspension systems are capable methods of promoting comfort and road-handling, and with low latency to electric field stimulation, ER fluids offer almost instantaneous control times. In their study, they proposed a continuously variable ER damper controlled by a skyhook controller. To demonstrate performance of their suspension, Choi and Han experimented with four independent skyhook controllers. ER shock absorber proposed in K. G. Sung, Han, Lim, and Choi (2007) is shown in Figs. 2.7 and 2.8. Choi, Choi, and Park (1998) proposed an Sliding Mode Control (SMC) for an ER suspension. K. G. Sung, Han, Cho, and Choi (2008) proposed and experimentally tested a fuzzy moving SMC controlled ER suspension on a quarter car model. As these studies indicate, ER suspension systems coupled with an efficient controller improve the comfort criteria of vehicles.

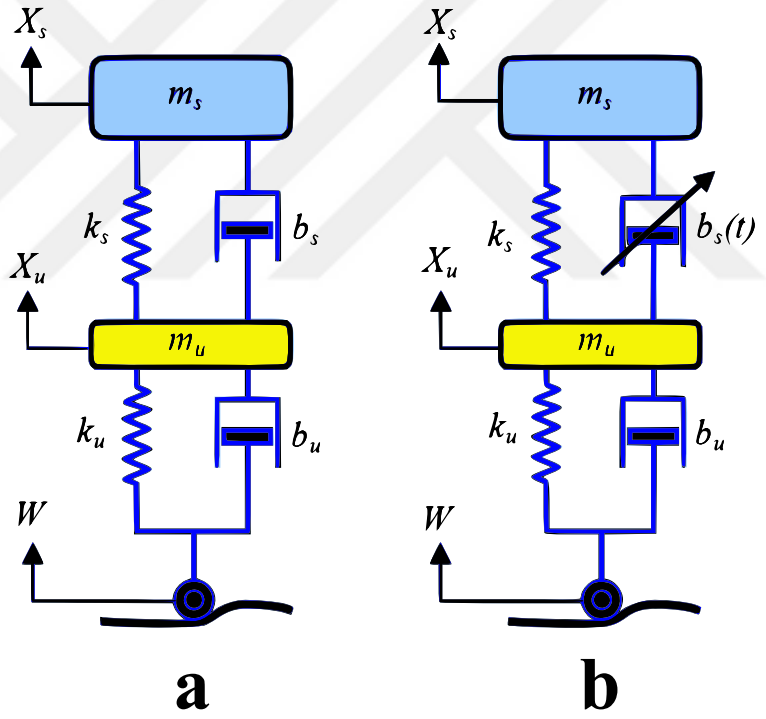


Figure 2.6. Suspension system model: (a) passive, (b) semi-active (Mihai & Andronic, 2014)

With higher viscosity, MR fluids yields better strength than ER fluids. Choi, Lee, and Park (2002) presented a cylindrical MR shock absorber based on Bingham model of MR fluid from several MR fluid models such as polynomial model, LuGre friction model, algebraic model, Bouc-Wen hysteresis model, and neural network model.

Figs. 2.9 and 2.10 shows Choi et al. model's schematics.

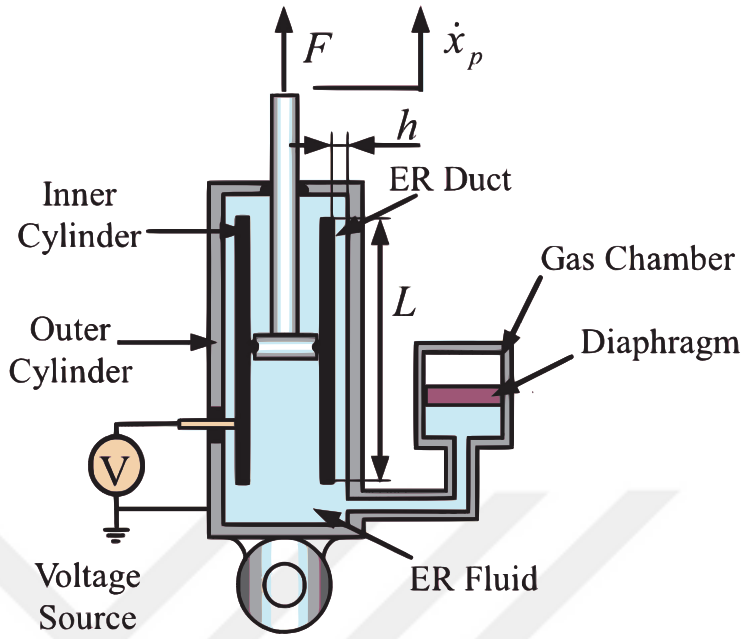


Figure 2.7. ER damper schematic configuration (K. G. Sung et al., 2007)

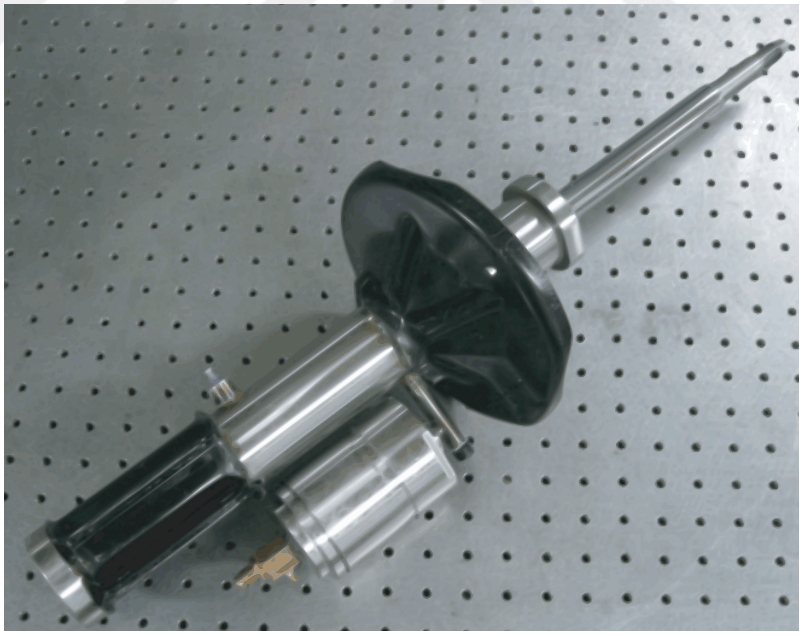


Figure 2.8. Photograph of ER damper (K. G. Sung et al., 2007)

Yıldız, Sivrioğlu, Zergeroğlu, and Çetin (2015) proposed a nonlinear adaptive control of a semi-active MR damper system with modified dynamic LuGre frictional model, conducted experiments to improve the MR damper, and analyzed the performance of the MR shock absorber suspension. Balamurugan, Jancirani, and Eltantawie (2014) presented a

modified algebraic model and analyzed the performance of the MR damper, and thus a controller with low computational complexity is realized through their studies. Du, Yim Sze, and Lam (2005) proposed a polynomial model to characterize the dynamical behavior of an MR shock absorber, and with comfort, handling, and suspension displacement objectives.

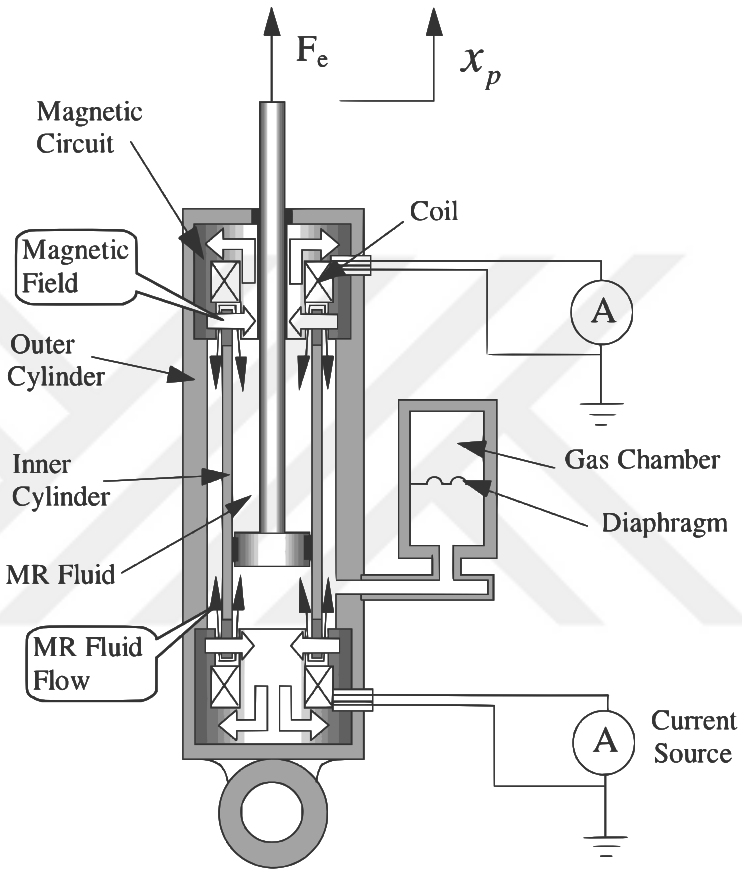


Figure 2.9. Schematic of an MR shock absorber (Choi et al., 2002)

Numerous control methods are deployed as semi-active MR shock absorber suspension such as nonlinear adaptive control, sky-hook control, model-following SMC, H∞ and fuzzy Proportional Integral Derivative (PID), etc. Xu, Ahmadian, and Sun (2014) presented an MR damper capable of variable spring and damping characteristics. Xu et al. proposed two independent Fuzzy Logic (FL) and an on/off controller to control yaw moment and stiffness-damping characteristics, respectively. Maciejewski, Glowinski, and Krzyzynski (2014) presented an adaptive PID capable of self-tuning for semi-active MR shock absorber with four different controlling schemes for example PID, Proportional (P),

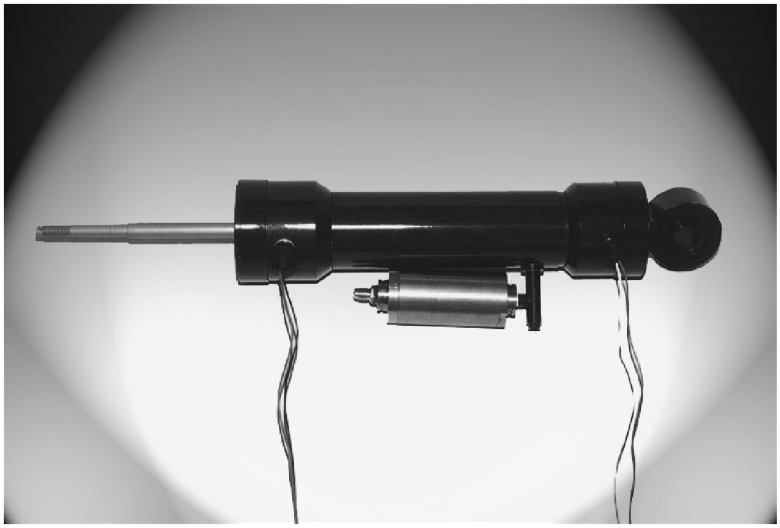


Figure 2.10. Photo of an MR shock absorber (Choi et al., 2002)

Proportional Integral (PI) and PD. Yokoyama, Hedrick, and Toyama (2001) presented a semi-active SMC, where measurement of damper force isn't required, and sliding mode is achieved at the same time with high robustness against system and road disturbance uncertainties. Since MR shock absorbers contain fluid, this fluids are represented with mathematical models such as presented in Fig. 2.11.

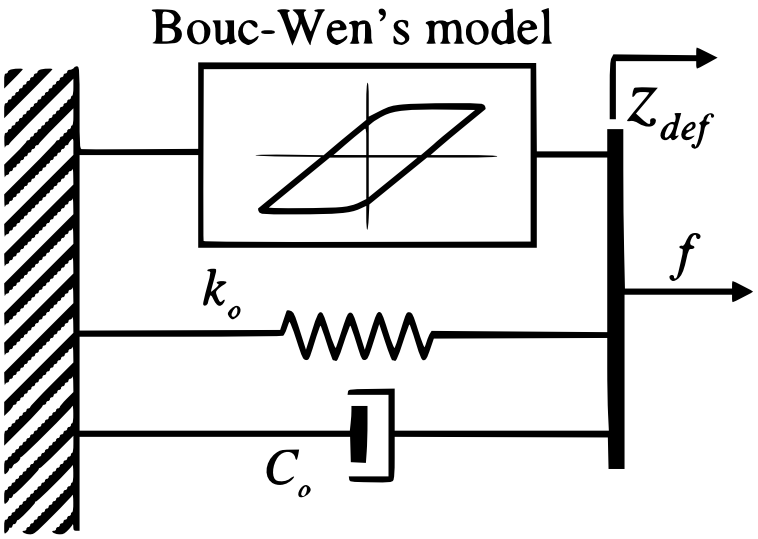


Figure 2.11. Bouc–wen model for MR shock absorber (El Majdoub et al., 2014)

2.2.3. Active suspension

Active suspensions offer state-of-the-art control through sensory input and adequate response to vehicle motion and road-induced vibrations. An active suspension schematic is presented in Fig. 2.12. Differentiating part of these systems from semi-active suspensions are their actuators. For the isolation of the road-induced vibrations and vehicle dynamic stabilization, Electro-Hydrostatic Actuator (EHA) systems are typically selected as the active suspension system actuators. Though, superior control algorithm construction for such systems present difficulties due to highly nonlinear EHA behavior. Fig. 2.13 demonstrates an EHA schematics. Du and Zhang (2009) proposed an FLC for EHA system comprising nonlinear actuator characteristics and variations in sprung mass under control input constraints. W. Sun, Gao, and Yao (2013) presented a study with a full vehicle model EHA suspension system controlled by an adaptive robust control design based H∞ controller to enhance comfort and handling performance. Bello, Shafie, and Khan (2015) proposed a two control loop approach for half vehicle nonlinear EHA system in which an inner loop PID controller for EHA force control and an outer loop PID for suspension parameters. W. Sun, Pan, and Gao (2016) presented a study with a half-car EHA suspension system with a constrained adaptive back-stepping strategy to improve vertical and pitch motions in a system in which parameter uncertainties and actuator nonlinearities existed.

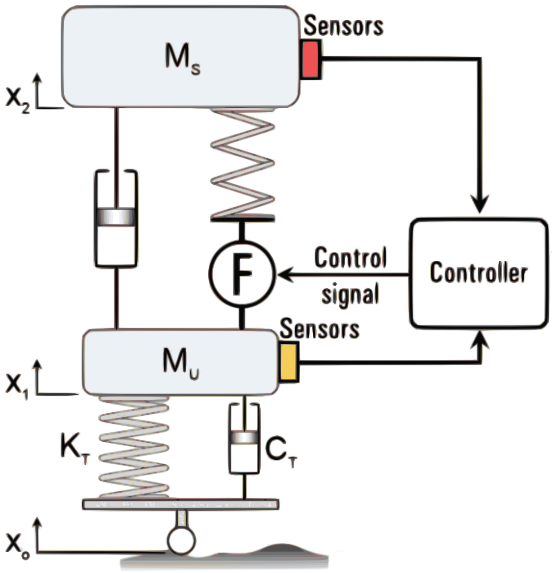


Figure 2.12. Active suspension (Elattar et al., 2016)

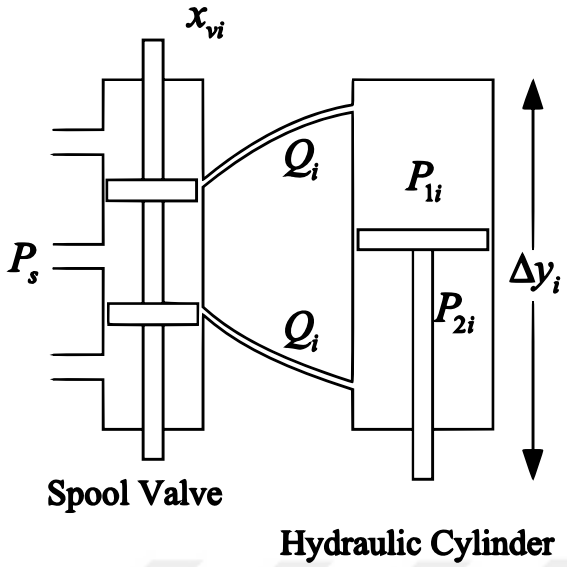


Figure 2.13. An electrohydraulic actuator schematic (W. Sun et al., 2013)

Another approach to an EHA system would be to employ control on a HIS systems pressure and fluid flow, for example, with electronic valves and pressure control unit. Fig. 2.14 shows a pressure control unit that can generate anti-roll moments by roll angle estimations. It is known that vehicle body motions caused by road-induced excitation are bounce, pitch, roll, and warp. In theory HIS systems could be used to decouple different vehicle vibration modes (M. C. Smith & Walker, 2005). Shao, Zhang, Du, and Wang (2013) proposed switching HIS with a fuzzy controller, and as a result, effective reduction of pitch and roll motion was achieved. Lam, Wang, and Zhang (2013) experimentally studied the proposed fuzzy controlled HIS system. N. Zhang, Wang, and Du (2014) presented a study in which vehicle motion decoupling has been carried out by the motion-mode energy method. Du, Zhang, and Wang (2014) proposed actively switching the interconnection configuration of the suspension system with a switched control of HIS system in order to decouple and eliminate vehicle body motion modes.

Isa, Mahadi, Ramli, and Abidin (2011) conducted a review of literature on Electromagnetic Suspension (EMS) systems for conventional vehicles. Application area of EMS systems has a broad scope such as from conventional ICE vehicles to EVs, from regenerative suspension systems to maglev trains, and many more. Yoshimura, Kume, Kurimoto, and Hino (2001) presented an SMC for an EMS that is outperforming Linear Quadratic (LQ)

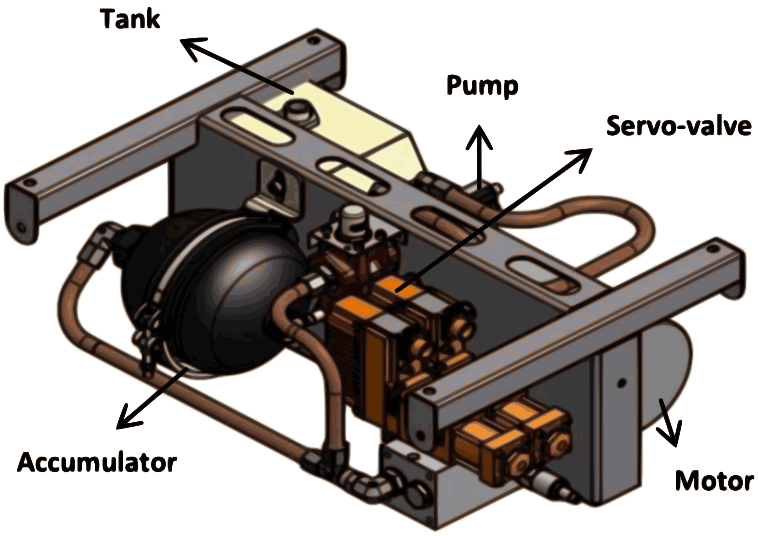


Figure 2.14. Photo of the pressure control unit (Zhu et al., 2013)

controlled EMS systems. Sinha and Pechev (2004), for magnetically levitated vehicles comprising EMSs, proposed nonlinear state and output feedback controllers. H. K. Sung, Lee, and Bien (2005) proposed a fault-tolerant controller for EMSs that demonstrate dynamic characteristics of maglev systems. Martins, Esteves, Marques, and da Silva (2006) experimentally revealed that linear Permanent-Magnet Actuator (PMA) actuators incorporated in vehicle active suspension systems are indeed very suitable for vehicle suspension system usage. Gysen, Paulides, Janssen, and Lomonova (2010) proposed an EMS system comprised of brushless tubular PMA and a spring as shown in Fig. 2.15 (b). Van Der Sande et al. (2013) presented a study in which the computer simulations and experimental results validated effectiveness of presented robust H∞ controller for a PMA EMS system and apart from the promising performance improvements some disadvantages such as high cost, complex assembly, and maintenance problems pointed out for PMA systems. As a substitute for EMS systems, Linear Switched Reluctance Actuator (LSRA) offers promising benefits such as high performance, simple structure, and low cost. J. Lin et al. (2013) presented a study in which an EMS based LSRA system demonstrated promising results, and from two controllers compared, nonlinear PD controller outperformed linear PD controller. The double-sided LSRA used in study of J. Lin et al. is presented in Fig. 2.16. J. Lin, Cheng, Xue, Cheung, and Zhang (2014) proposed a tracking differentiating method for inductance derivative estimation of LSRA system. J. Lin, Cheng, Zhang,

Cheung, and Xue (2015) proposed an EMS system with an LSRA due to LSRA systems high-force linear application potential and an adaptive SMC algorithm being able to compensate nonlinear nature of suspension systems, and through simulations, he proposed the system on a nonlinear quarter vehicle model.

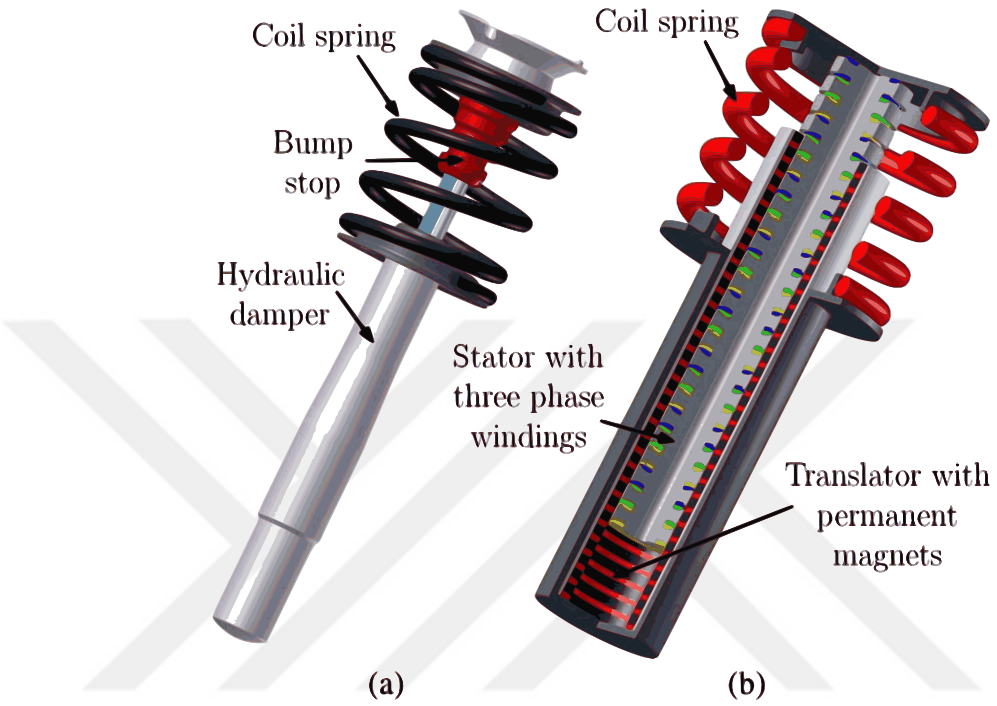


Figure 2.15. (a) Passive suspension system (b) electromagnetic suspension system (Gysen et al., 2010)

2.3. Electric Vehicle Suspension Systems

Suspension system design of land vehicles presents challenges regardless of vehicle type, while so, EVs present a not seen before rigorous design challenges against ICEs with their IWM propulsion systems. Consideration of many systems and requirements is needed to be made in the design phase of IWM EVs. While centralized propulsion systems may benefit from a more versatile and traditional suspension design, IWM propulsion systems require a more advanced suspension system to overcome the unwanted effects of increased unsprung mass. Regardless of its' design challenges, IWM systems are considered to be the future of EVs. Needless to say, centralized propulsion systems currently occupy the majority of the contemporary EV market.

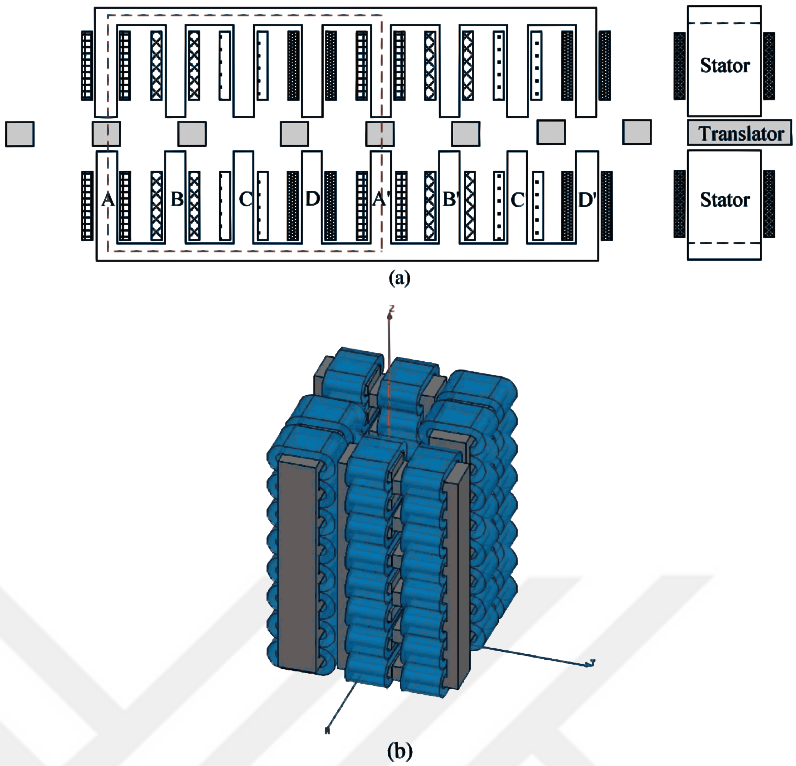


Figure 2.16. (a) Schematic configuration of double-sided LSRA module. (b) 3D model of LSRA (J. Lin et al., 2013)

2.3.1. Centralized propulsion suspension system

Centralized propulsion in EVs offer many advantages such as motor durability, less challenging suspension design and cost. Compared to central propulsion system EVs, IWM technology is still thin on the ground. Two EVs with centralized propulsion systems is shown in Figs. 2.17 and 2.18.

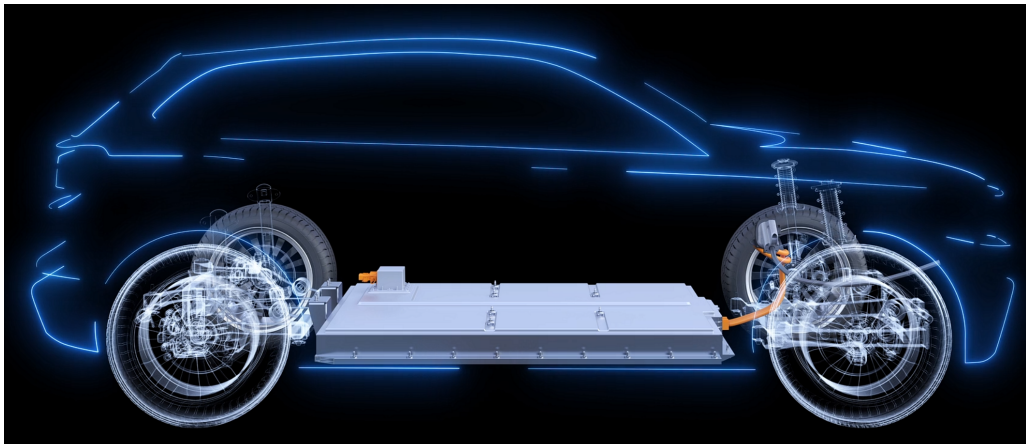


Figure 2.17. TOGG centralized propulsion electrical vehicle (TOGG, 2020)

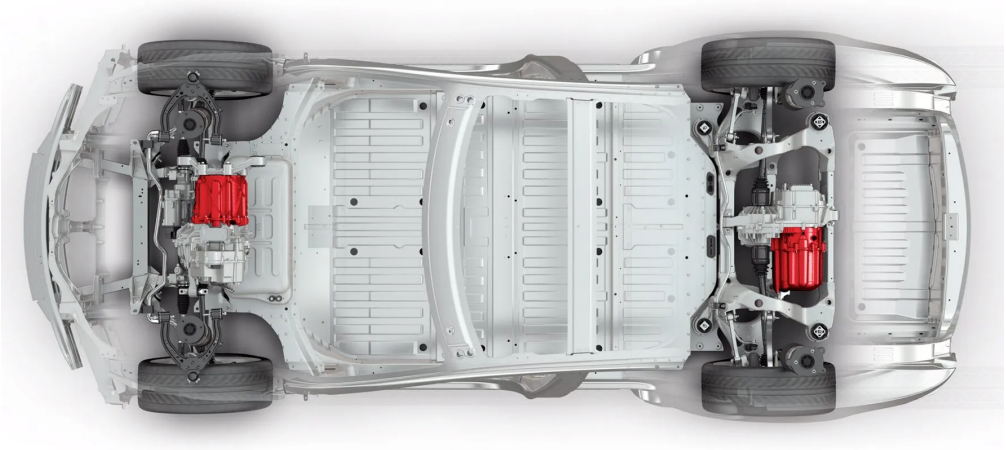


Figure 2.18. Tesla model s 85d centralized propulsion electrical vehicle

J.-T. Cao, Liu, Li, Brown, and Dimirovski (2007) presented an enhanced half-vehicle model for active control of suspension by the introduction of a state vector of vehicle pitch angle, which allowing the exploration of the effects of vehicle acceleration. By addition of correlation of acceleration and pitch angles into LQ controller as an additional parameter, J.-T. Cao et al. constructed an improved LQ controller. Hsu, Coker, and Huang (2011) investigated dynamic analysis of an EV creating the vehicle suspension system via a multi-body dynamics software, Altair MotionView / MotionSolve. Hsu et al., through simulation of dynamical properties and kinematic performance of both an ICE and an EV, optimized the front and rear suspension of the EV by improving the dynamic properties. Peng, He, and Feng (2013) proposed a collaborative control system for an EV with a controller comprised of centralized and hierarchical architecture. In the study of Peng et al., while the suspension and steering system was controlled by the centralized controller to enhance handling in addition to comfort, braking was controlled by the hierarchical controller to improve the proportional distribution of braking force and regenerative braking to improve braking performance. Kaldas, Çalişkan, Henze, and Küçükay (2013) proposed a FL control concept for a semi-active suspension. In the study of Kaldas et al., with an eleven DOF full vehicle model, improvement of vehicle ride and performance is targeted by optimizing the Membership Functions (MFs) and control rules of the FLC via a GA and significant improvements observed in terms of comfort and handling. Abu Bakar et al. (2014) found that the SAS-Skyhook algorithm provided the most significant improvement in ride comfort. Bakar and Aziz (2014) evaluated ride comfort of an ICE vehicle

converted to an EV. Bakar and Aziz employed a seven DOF vehicle model subjected to random road input in order to improve the ride comfort of the converted vehicle, and it was found that conversion of an ICE vehicle to EV does not affect ride comfort significantly, but to enhance comfort further, an active suspension has been integrated, and in overall 65% improvement has been observed. J. Zhang, Yang, Hu, Fu, and Zhai (2021) proposed a model predictive control strategy to improve EV ride comfort by incorporating a four DOF half vehicle model with braking accelerations taken into consideration, and results indicated improvements in vertical body velocities, pitch angle, and pitch angle velocities more than 70%.

2.3.2. In-wheel motor suspension system

EV propulsion systems can be configured to be either central motor or IWM driven layout based on vehicle design. Although central motor propulsion systems occupy EV market currently, IWM driven propulsion configuration has a rising research interest for their advantages (Murata, 2012b). IWM driven layout can improve vehicle dynamics in conditions of vehicles various acceleration scenarios. As a case in point, IWM enhances performance of TCS, ABS, and ESC (Murata, 2012b). Even though IWM configuration has numerous upsides, unwanted side effects of such systems exist mostly related to inadvertent increases in wheel mass. Due to deterioration in comfort, handling performance, and reliability of incorporating IWM systems, actively control of suspension is fundamental for implementation of IWM systems into EVs. An IWM EV platform and a vehicle employing IWM is shown in Figs. 2.19 and 2.20.

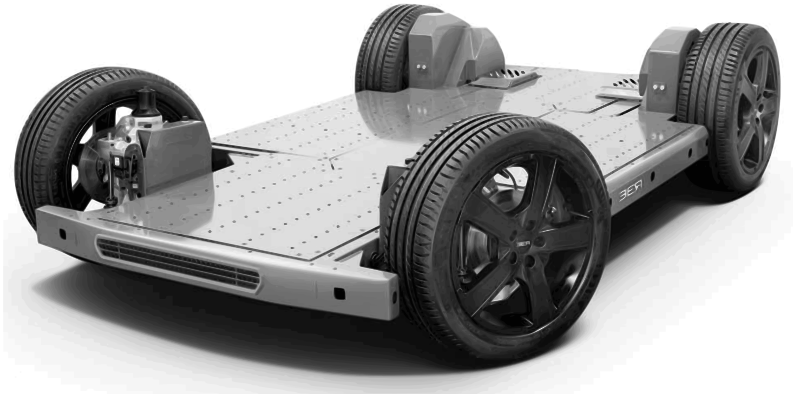


Figure 2.19. REE board electrical vehicle chassis incorporating in-wheel motors



Figure 2.20. Hiriko fold — a vehicle employing in-wheel motors

IWM layout can improve performance in the circumstances, for example, driving, turning, acceleration and braking conditions. To improve comfort, IWM can be positioned to play the role of a high-frequency dynamic absorber, also called ADM, and provide control over vehicles pitch performance (Murata, 2012b). Although, improvements in vehicle pitch performance are not solely a consequence of IWM layout. Furthermore, any vehicle with independent front and rear axle torque control can demonstrate improved pitch motion of the vehicle body. Fig. 2.21 shows changes in the sprung mass acceleration, suspension displacement, and tire displacement on a quarter vehicle model caused by an increase in sprung mass due to implementation of IWM. Increases in the unsprung mass cause negligible changes in the natural frequency of the sprung mass. That being said, negative effects such as comfort and road handling performance deterioration can be observed due to a rise in response frequency range as a consequence of unsprung mass increase. As presented in Fig. 2.22, vehicle body acceleration and tire dynamic forces is smaller in ADM EV compared to conventional IWM EV configurations. Kulkarni, Ranjha, and Kapoor (2018) presented a study on a quarter vehicle model with an IWM Switched Reluctance Motor (SRM) EV. Kulkarni et al. simulated his vehicle model and compared the results with an ICE conventional vehicle. Vos, Besselink, and Nijmeijer (2010) proposed pos-

sible improvements for IWM EVs such as ride performance and safety criteria with an investigation on the effects of IWM implementation on comfort and road handling characteristics by experiments and found the main disadvantage is an increase in dynamic wheel loads.

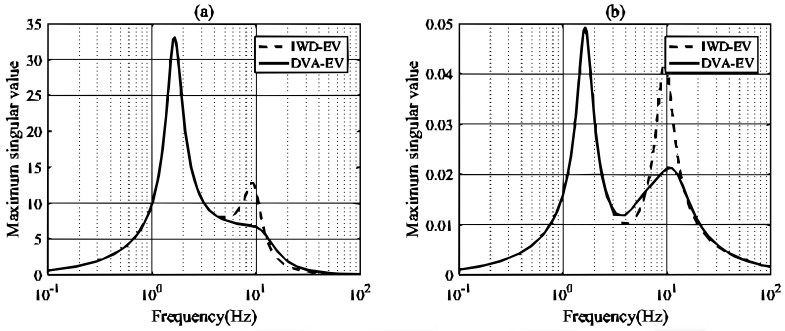


Figure 2.21. Frequency response of sprung mass acceleration and tire deflection (Shao, 2018)

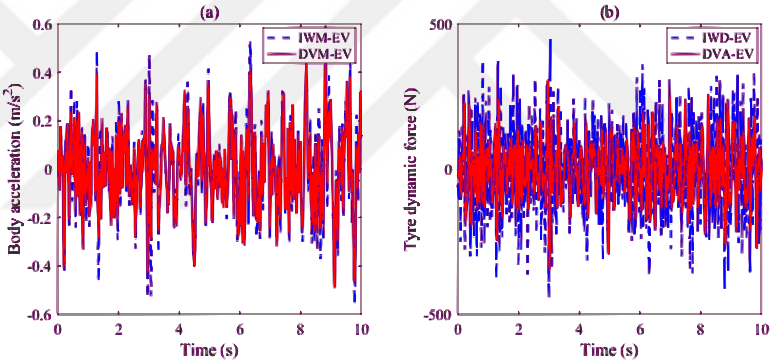


Figure 2.22. Random response of sprung mass acceleration and tire dynamic force (Shao, 2018)

The design phase carried out by experience does not ensure optimal dynamic behavior or system control. Hence, an optimization algorithm based IWM EV suspension design would benefit and improve vehicles' comfort and ride handling. Optimal vehicle comfort and ride handling of active suspensions can be achieved through incorporating parameters of vehicle suspension, IWM and controller to optimization phase. Due to the existence of conflicting control objectives in suspension design, multi-objective parameter optimization would not only benefit but is also required. Liu et al. (2017) proposed ADM to be incorporated for IWM EV with various control strategies. Liu et al. incorporated a fuzzy PID and a Linear Quadratic Regulator (LQR) control method for IWM and suspension

damper, respectively. Meng, Qian, and Liu (2018) proposed considering the active suspension system of an EV as a dual-rate sampled-data state-feedback control problem and implemented a linear hybrid stabilizer to achieve asymptotic stabilization. Quynh, Cuong, Liem, Long, and Dung (2019), in order to analyze effects of IWM system on EVs, presented a study in which a quarter car model induced by road excitation simulated and vertical vehicle body acceleration objective was observed. In study of Quynh et al., quarter model including an ADM IWM and a fixed IWM model compared. Quynh et al. revealed that increased unsprung mass without an ADM IWM system increased vertical body acceleration by 8.6% and any increase to IWM mass also increased vertical body accelerations, thus reducing comfort and ride handling. Nevertheless, to researches being done, predominant attention of the active suspension control studies focuses on conventional ICE vehicles, leaving IWM EVs relatively a new area that needs attention.

2.4. Control Methods

In the history of active suspension control applications, many approaches have been studied by researchers to improve comfort and ride handling (Ding, Wang, Meng, & Chen, 2020). As a result of the conflicting nature of performance requirements such as comfort, handling, and suspension displacement, a variety of control strategies such as LQR, Adaptive sliding control, $H\infty$ and robust H∞ control, SMC, FL, preview control, PI control, optimal control, and neural network methods have been studied to deal with the trade-off performance criteria for active suspension system control. Nonetheless, by their nature, some of these methods are resource-intensive and may underperform in unfamiliar conditions.

2.4.1. Proportional integral derivative control

In a system that needs to be controlled in various situations, the PID controller has been the most simple and successful solution in many cases. PID controllers can provide the desired control signal for specific process requirements by tuning the three weighting parameters. However, it should be noted that the use of PID controllers does not guarantee optimal system control. Kirli (2015) investigated a novel active suspension with six DOF half vehicle model, compared the proposed controller with a PID controller, and

designed an active suspension system that required only the measurement of front-wheel displacement to achieve full-body control. C. Lin, Liu, and Ren (2015) proposed a neural network-based PID control of a semi-active suspension comprising an MR damper for a commercial vehicle to improve comfort and stability. Tan, Lu, and Zhang (2016) proposed a dual-loop PID controller for a fourteen DOF rear IWM EV and controller optimized by Particle Swarm Optimization (PSO), the proposed controller improved comfort comparing to a passive suspension system. Jin, Yu, and Fu (2016) simulated and experimentally validated the effects of increase of unsprung mass in IWM EVs and proposed a PID controlled semi-active air-suspension system to enhance comfort. Ahmed and Özkan (2017) presented a fuzzy PID controller responsible for vehicle stability control targeting handling and stability of the vehicle. Djellal and Lakel (2018) proposed a PID controlled active suspension system to achieve a long life span via preventing brutal controller actions by simulating a passive and active suspension with constant and adapted reference for a quarter car model subjected to different road inputs. Daniyan, Mpofu, and Osadare (2018) presented a PID controlled active suspension system design for a railcar suspension by tuning the controller via Ziegler–Nichols method and achieved reducing noise, vibration, and miscellaneous disturbances. Haemers et al. (2018) proposed a Multiple-Input-Multiple-Output (MIMO) PI control for a full-car electromechanical active suspension exposed to random road excitation. Haemers et al. optimized the controller using a GA considering actuator constraints. Termous, Moreau, Francis, and Shraim (2018) compared PID and fractional first-generation CRONE controller controlling an anti-roll moment system to enhance comfort of EVs. Pillai, Pon Selvan, and Madara (2019) presented a PID tuning study where PID constants optimized via neural network for an EV to enhance efficiency of the suspension. Tian and Nguyen (2020) using an eight DOF vehicle model evaluated the control performance of a PID controller, shown in Fig. 2.23, for road vehicles with obvious improvement in objectives such as Root Mean Square (RMS) seat acceleration, pitch and roll motions of sprung mass compared to passive suspension.

2.4.2. Fuzzy logic control

Every control system aims to produce desired control signals for a given input signal. In the simplest case, a controller takes its cues from a look-up table, which dictates what

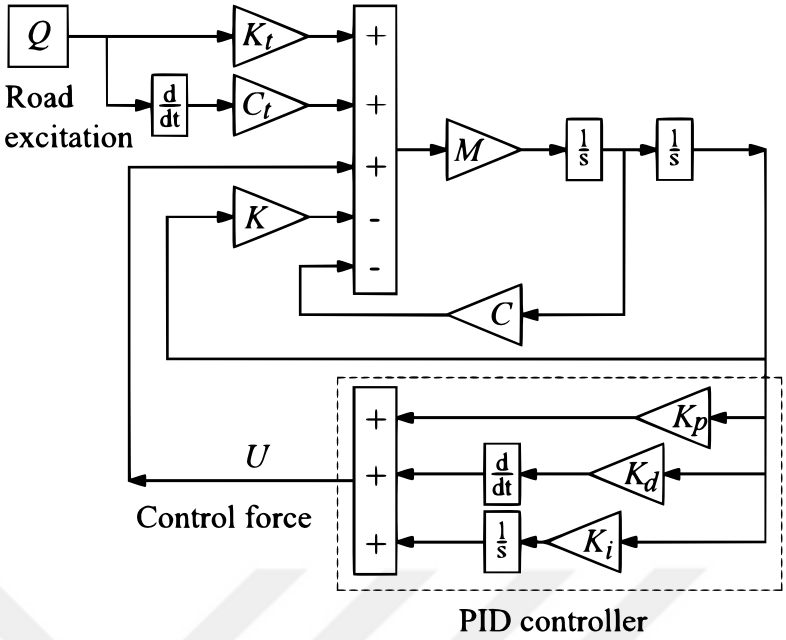


Figure 2.23. Simulink model of a pid control system (Tian & Nguyen, 2020)

output to produce for every input set. The usual alternative to look-up tables is to have the controller execute a mathematical formula. While this method work in simple systems, their implementation and real-time application may be infeasible. FL overcomes the disadvantages of table-based and formula-based control. Furthermore, FLC offer higher accuracy and smoother control even for complex and highly nonlinear control problems. Hence, FLCs finds themselves an area of use in many engineering applications, particularly in cases of existing non-linearity. Due to their nature, FLC offer highly customizable controlling solutions for many fields.

Chiou and Liu (2009) optimized MFs and rule table of an FLC by a GA for an active vehicle suspension to achieve optimal balance between comfort and vehicle stability. He, Wang, Zhang, Yang, and Xu (2010) proposed an FLC for a semi-active skyhook controller and co-simulated the vehicle model on ADAMS and Simulink to demonstrate the efficiency of the established controller, concluding that integrated chassis control systems can greatly improve vehicle comfort and handling. Yang and Zhao (2012) designed a fuzzy controller to enhance comfort and stability criteria such as body acceleration and suspension distortion of a two DOF quarter car model with a semi-active suspension using Matlab fuzzy toolbox. Y. Q. Sun, Zhao, and Xiang (2013) suggested an FL controller

for an active suspension system to enhance comfort and vehicle handling. Y. Q. Sun et al. by using a quarter-car active suspension and incorporating vertical acceleration, suspension stroke, and tire deflection objectives, demonstrated the effectiveness of FLC controllers under varying suspension component characteristics. Marzbanrad, Soleimani, Mahmoodi-k, and Rabiee (2015) presented a paper in which an FLC controller is optimized to achieve vehicle path following, roll, and handling performances. Shao, Naghdy, and Du (2017) through modeling a quarter-car model with ADM IWM demonstrated advantages of their fuzzy $H\infty$ controller. Harun, Ab Rahim, Abdul Halim, and Abdullah (2019) compared performance of passive suspension against LQR and FL controlled systems of a two DOF car model and concluded FL controller outperformed LQR. X. Q. Sun, Cai, Yuan, Wang, and Chen (2018) experimentally validated a fuzzy SMC to control an electronic air suspension system for vehicle height and leveling adjustments to achieve improved roll and pitch angles for a bus. Sosthene, Josee, and Hui (2018) proposed an FLC for active force tracking of a semi-active quarter-car suspension comprising an MR shock absorber, and results indicated improvements by 10% in ride comfort and 30% in vehicle stability. Senthil Kumar, Sivakumar, Kanagarajan, and Kuberan (2018) proposed a hybrid intelligent controller based on a combination of a neural network and FL, and a half car model with a sinusoidal road profile used for the design of Adaptive Network-based Fuzzy Inference System (ANFIS), which is able to handle better actuator dynamics and parameter-wise uncertainties of the hydraulic actuator. Mahmoodabadi and Nejadkourki (2020) presented active control for a quarter car model via an optimal fuzzy adaptive robust PID controller, as shown in Fig. 2.24, with two objectives for PSO algorithm. His fuzzy system comprised a singleton fuzzifier, center average defuzzifier, and for regulation of control parameters, a product inference engine.

Ren, Chen, and Zhou (2020) proposed an interval type-2 fuzzy state-feedback controller considering yaw moment control problem for EV systems under uncertain states such as sensor failures and actuator saturation. Ren et al. defined the parameter uncertainties through lower and upper bounds of MFs. Yatak and Şahin (2021) presented a hybrid fuzzy controller to improve comfort and road handling characteristics of a full vehicle model, which are trade-off objectives. Yatak and Şahin implemented two-interval type-2 FL con-

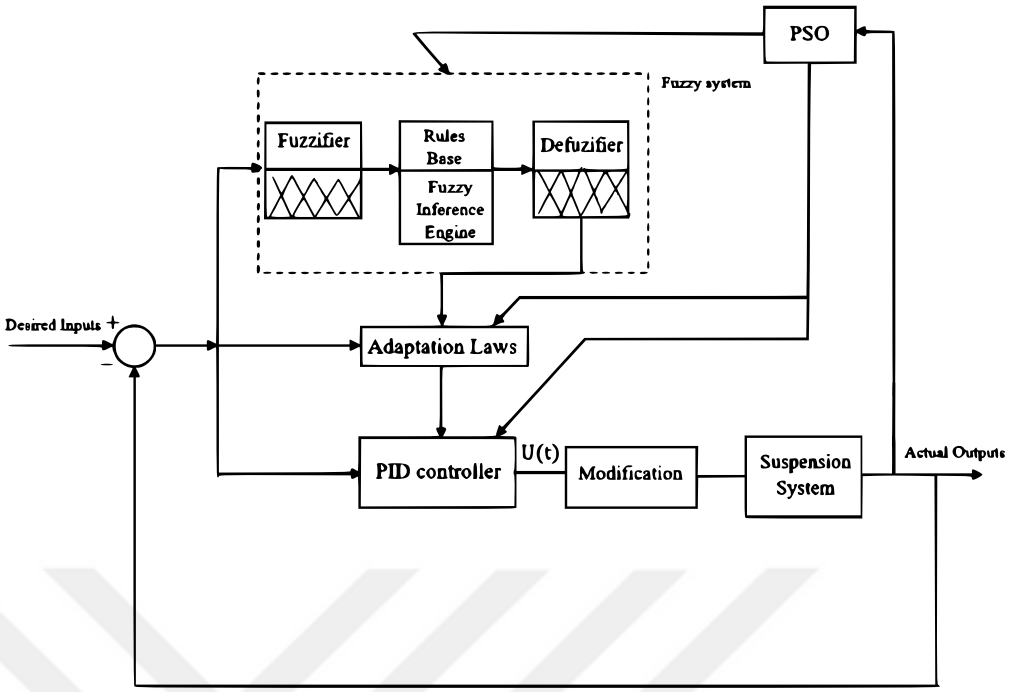


Figure 2.24. A fuzzy pid controller schematic (Mahmoodabadi & Nejadkourki, 2020)

trollers for each tire, with wheels subjected to random excitation defined by ISO 8608 (2016), and with objectives such as RMS acceleration, Crest Factor (CF) and road holding. Taghavifar (2021) proposed an Extented Kalman Filter (EKF) based PID type-2 fuzzy Neural Network Control (NNC) for an IWM EV exposed to class E off-road type random road excitation to improve comfort and handling criteria, which are a challenging task due to increased unsprung mass. The proposed controller by Taghavifar, shown in Fig. 2.25, optimized using Back Propagation (BP) and gradient descent methods and demonstrated an improvement in road holding and ride comfort criteria. Through conducted studies, the effectiveness of fuzzy methods is seen, and as stated by Ivanov (2015), interest in fuzzy methods increasingly accelerates in vehicle control systems.

2.5. Optimization Methods

Traditional optimization methods such as expert directed tuning fail to achieve optimal control for FLCs and implementation of Evolutionary Algorithms (EAs) solves this problem by their source of inspiration from nature. Patil and Palanichamy (1985) presented a study showing that compared to seat response, body parts such as head, torso, and pelvis are affected greatly from road-induced vibrations. Ergo, vehicle suspension sys-

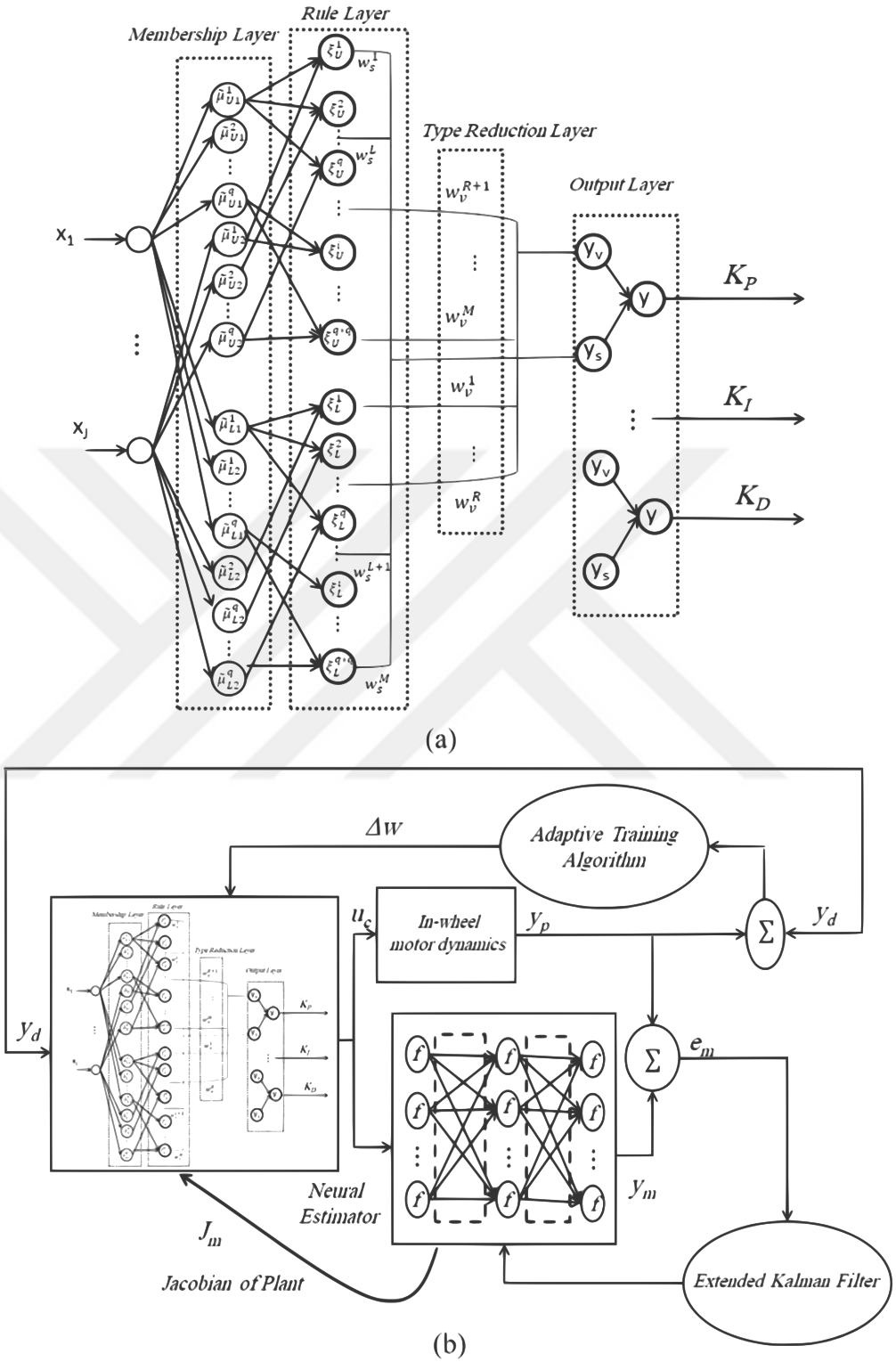


Figure 2.25. (a) Schematic of the controller and (b) the general architecture of the controller (Taghavifar et al., 2020)

tems should be optimized to reduce the effects of vibrations affecting the body parts, as mentioned above. Patil and Palanichamy presented multi-objective optimization of a quarter car model comprising nonlinearities and a four DOF human model. Patil and Palanichamy defined non-linearities as modeling the quarter car model with cubic suspension and quadratic tire stiffness. Objective functions of Patil and Palanichamy were frequency weighted RMS head acceleration, Vibration Dose Value (VDV), CF, the amplitude ratio of head RMS acceleration to seat RMS acceleration, the amplitude ratio of upper torso RMS acceleration to seat RMS acceleration, suspension deflection, and dynamic tire deflection. In addition to this optimization, Patil and Palanichamy compared the performance of two multi-objective optimization algorithms by conducting the same optimization in these two optimization methods, NSGA-II and Multi-Objective Particle Swarm Optimization with Crowding Distance (MOPSO-CD). Baumal, McPhee, and Calamai (1998) presented an optimization of passenger seat acceleration objective with constraints, for example handling and suspension deflection with a GA-based algorithm. Verros, Natsiavas, and Papadimitriou (2005) demonstrated a comparison between passive linear and dual-rate suspension shock absorbers and semi-active skyhook suspension on a quarter car model with random road input in their suspension stiffness and damper optimization study. Papageorgiou (2006) conducted a meta-heuristic optimization of RMS vertical body acceleration and road handling objectives on a quarter car model using Multi-Objective Genetic Algorithm (MOGA) and bilinear matrix inequalities techniques. Gündoğdu (2007) presented an optimization of a two DOF quarter car model with a two DOF driver model. In study of Gündoğdu, a single-objective GA optimization conducted with each objective has equal importance through a non-dimensional expression derived from head acceleration, crest factor, suspension deflection, and tire deflection. Gomes (2009) presented optimization of dynamic vehicle load and suspension deflection objectives of a two DOF quarter car model using PSO. Kuznetsov, Mammadov, Sultan, and Hajilarov (2011) presented optimization of comfort criteria defined in ISO 2631-1 (1997) of a three DOF driver model consists of a two DOF quarter car model and a one DOF driver model with an algorithm for global optimization problems. Özcan, Sönmez, and Güvenç (2013) performed optimization of a lightweight commercial vehicle. RMS body acceleration, tire forces, and body roll objectives were optimized using half and quarter car models. Mashadi, Mahmoudi-

Kaleybar, Ahmadizadeh, and Oveisi (2013) proposed a PID controller for a vehicle path tracking problem, and through optimization of the controller gains by GA, an effective patch following controller has been developed. Nagarkar, Vikhe Patil, and Zaware Patil (2016) presented an optimization of seat acceleration, head acceleration, and suspension deflection objectives of a quarter car model by converting the multi-objective nature of the optimization problem into uni-objective optimization by weighting the parameters as mentioned earlier. Nagarkar et al. used GA optimization method for this human-car suspension system optimization. Yildiz (2021) proposed using EAs such as PSO, GA, and the Differential Evolution (DE) for the optimization of trunk lid mechanisms. Yildiz observed that EAs perform variably in criteria such as optimization duration and performance of the optimized system. Through his observations Yildiz concluded best average error value is performed by GA. Yildiz (2019b) presented a study in which a nonlinear suspension optimization for a half vehicle model was carried out by PSO technique. A five DOF model is built by Yildiz to analyze ride comfort, and optimization was realized by PSO. Yildiz (2019a) comparatively conducted an optimization of an EV suspension system with PSO, GA, and DE. Study of Yildiz presented a half-vehicle model consisting of seat and suspension with cubic non-linearities in springs.

3. MATERIAL AND METHOD

3.1. Full Vehicle and Human Models

Full-car models with seven degrees of freedom offer higher accuracy in the design phase compared to half and quarter car models, which disregards pitch and or roll motions of the sprung mass. The full-car model consists of a sprung mass, which is the body of the vehicle, and four unsprung masses connected to it at each corner, which are wheels. Sprung mass is free for heave, pitch, and roll motions. In contrast, unsprung masses are only unrestricted for vertical movement. Unsprung masses are connected to sprung mass with spring and damper elements, and their connection to the road is only with spring elements, without a damper.

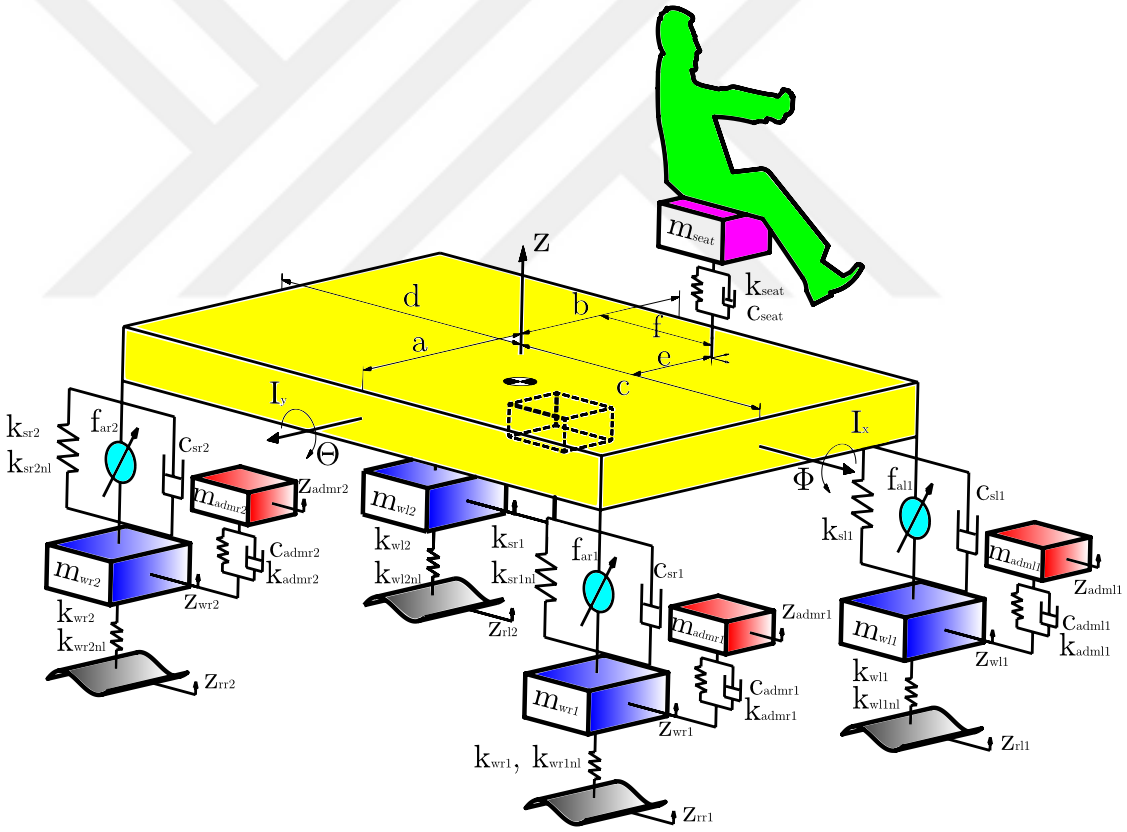


Figure 3.1. Full car model of 4x4 in-wheel motor driven electrical vehicle

In Fig. 3.1, M, I_x, and I_y stand for the mass of the sprung mass, and moment of inertia for roll and pitch motions, respectively. m_{wi}, k_{si}, c_{si}, f_{si}, m_{admi}, k_{admi}, c_{admi}, k_{wi} represents mass of the unsprung masses, spring, damper and actuator elements connecting

unsprung masses to sprung mass, mass of IWMs, spring and damper elements connecting IWM's to unsprung masses, and spring elements connecting unsprung masses to road, respectively. Z, Θ, and Φ represent heave, pitch, and roll motions of the sprung mass. z_{wi} and z_{admi} represents the vertical displacements of the unsprung masses and IWMs. a, b, c, and d represent the distances between the center of gravity of sprung mass and unsprung masses. e and f represent the distance of the seat to the center of gravity of the sprung mass. Motions of the equation for the full vehicle model are obtained under the assumption that pitch and roll angles are small, and thus lateral displacement due to pitch and roll motions is neglected. Spring elements used in many parts of automobiles exhibit nonlinear behavior and must be modeled accordingly (Fidanciogullari & Yildiz, 2021). Thus, quadratic nonlinearity in the tire and cubic nonlinearity in suspension stiffness is defined. k_{winl} and k_{sinl} represents nonlinear spring elements of wheel and suspension, respectively. Subscript $i = r1, r2, l1, l2$ represents right front, right rear, left front and left rear corners of the vehicle.

Equations of the full vehicle model are defined as following. Eqs. (3.1) to (3.4) shows the forces acting on suspension system.

$$\begin{aligned} f_{sr1} &= k_{sr1}(Z - \Theta \cdot c - \Phi \cdot a - Z_{wr1}) \\ &+ c_{sr1}(\dot{Z} - \dot{\Theta} \cdot c - \dot{\Phi} \cdot a - \dot{Z}_{wr1}) \\ &+ k_{sr1nl}(Z - \Theta \cdot c - \Phi \cdot a - Z_{wr1})^3 \end{aligned} \tag{3.1}$$

$$\begin{aligned} f_{sl1} &= k_{sl1}(Z - \Theta \cdot c + \Phi \cdot b - Z_{wl1}) \\ &+ c_{sl1}(\dot{Z} - \dot{\Theta} \cdot c + \dot{\Phi} \cdot b - \dot{Z}_{wl1}) \\ &+ k_{sl1nl}(Z - \Theta \cdot c + \Phi \cdot b - Z_{wl1})^3 \end{aligned} \tag{3.2}$$

$$
\begin{aligned}
f_{sr2} = {} & k_{sr2}(Z + \Theta \cdot d - \Phi \cdot a - Z_{wr2}) \\
& + c_{sr2}(\dot{Z} + \dot{\Theta} \cdot d - \dot{\Phi} \cdot a - \dot{Z}_{wr2}) \\
& + k_{sr2nl}(Z + \Theta \cdot d - \Phi \cdot a - Z_{wr2})^3
\end{aligned} \tag{3.3}
$$

$$
\begin{aligned}
f_{sl2} = {} & k_{sl2}(Z + \Theta \cdot d + \Phi \cdot b - Z_{wl2}) \\
& + c_{sl2}(\dot{Z} + \dot{\Theta} \cdot d + \dot{\Phi} \cdot b - \dot{Z}_{wl2}) \\
& + k_{sl2nl}(Z + \Theta \cdot d + \Phi \cdot b - Z_{wl2})^3
\end{aligned} \tag{3.4}
$$

Eqs. (3.5) to (3.8) as seen below, denotes forces acting between wheel and road.

$$
\begin{aligned}
f_{wr1} = {} & k_{wr1}(Z_{wr1} - Z_{rr1}) \\
& + k_{wr1nl}(Z_{wr1} - Z_{rr1})^2
\end{aligned} \tag{3.5}
$$

$$
\begin{aligned}
f_{wl1} = {} & k_{wl1}(Z_{wl1} - Z_{rl1}) \\
& + k_{wl1nl}(Z_{wl1} - Z_{rl1})^2
\end{aligned} \tag{3.6}
$$

$$
\begin{aligned}
f_{wr2} = {} & k_{wr2}(Z_{wr2} - Z_{rr2}) \\
& + k_{wr2nl}(Z_{wr2} - Z_{rr2})^2
\end{aligned} \tag{3.7}
$$

$$
\begin{aligned}
f_{wl2} = {} & k_{wl2}(Z_{wl2} - Z_{rl2}) \\
& + k_{wl2nl}(Z_{wl2} - Z_{rl2})^2
\end{aligned} \tag{3.8}
$$

Eqs. (3.9) to (3.12) denotes forces acting between wheel and IWM also called ADM.

$$f_{admr1} = k_{admr1}(Z_{admr1} - Z_{wr1}) + c_{admr1}(\dot{Z}_{admr1} - \dot{Z}_{wr1}) \tag{3.9}$$

$$f_{adml1} = k_{adml1}(Z_{adml1} - Z_{wl1}) + c_{adml1}(\dot{Z}_{adml1} - \dot{Z}_{wl1}) \tag{3.10}$$

$$f_{admr2} = k_{admr2}(Z_{admr2} - Z_{wr2}) + c_{admr2}(\dot{Z}_{admr2} - \dot{Z}_{wr2}) \tag{3.11}$$

$$f_{adml2} = k_{adml2}(Z_{adml2} - Z_{wl2}) + c_{adml2}(\dot{Z}_{adml2} - \dot{Z}_{wl2}) \tag{3.12}$$

Eqs. (3.13) to (3.15) are the Equations of Motion for the sprung mass with three DOF, which are heave, pitch, and roll motions.

$$M\ddot{Z} = -f_{sr1} - f_{sl1} - f_{sr2} - f_{sl2} - f_{ar1} - f_{al1} - f_{ar2} - f_{al2} + f_{seat} \tag{3.13}$$

$$I_y\ddot{\Theta} = +f_{sr1} \cdot c + f_{sl1} \cdot c - f_{sr2} \cdot d - f_{sl2} \cdot d + f_{ar1} \cdot c + f_{al1} \cdot c - f_{ar2} \cdot d - f_{al2} \cdot d - f_{seat} \cdot f \tag{3.14}$$

$$I_x\ddot{\Phi} = +f_{sr1} \cdot a + f_{sr2} \cdot a - f_{sl1} \cdot b - f_{sl2} \cdot b + f_{ar1} \cdot a + f_{ar2} \cdot a - f_{al1} \cdot b - f_{al2} \cdot b + f_{seat} \cdot e \tag{3.15}$$

Eqs. (3.16) to (3.19) are the Equations of Motion for wheels.

$$M_{wr1}\ddot{Z}_{wr1} = f_{sr1} - f_{wr1} + f_{admr1} + f_{ar1} \tag{3.16}$$

$$M_{wl1}\ddot{Z}_{wl1} = f_{sl1} - f_{wl1} + f_{adml1} + f_{al1} \tag{3.17}$$

$$M_{wr2}\ddot{Z}_{wr2} = f_{sr2} - f_{wr2} + f_{admr2} + f_{ar2} \tag{3.18}$$

$$M_{wl2}\ddot{Z}_{wl2} = f_{sl2} - f_{wl2} + f_{adml2} + f_{al2} \tag{3.19}$$

Eqs. (3.20) to (3.23) are the Equations of Motion of ADM.

$$M_{admr1}\ddot{Z}_{admr1} = -f_{admr1} \tag{3.20}$$

$$M_{adml1}\ddot{Z}_{adml1} = -f_{adml1} \tag{3.21}$$

$$M_{admr2}\ddot{Z}_{admr2} = -f_{admr2} \tag{3.22}$$

$$M_{adml2}\ddot{Z}_{adml2} = -f_{adml2} \tag{3.23}$$

Eqs. (3.24) and (3.25) denotes forces acting on seat and Equations of Motion for Seat.

$$f_{seat} = k_{seat}(Z_{seat} - Z_{0_{seat}}) + c_{seat}(\dot{Z}_{seat} - \dot{Z}_{0_{seat}}) \tag{3.24}$$

$$M_{seat}\ddot{Z}_{seat} = -f_{seat} + f_p \tag{3.25}$$

For the human model to be used in this study, the Wan and Schimmels (1995) four DOF human model was selected for its high-performing characteristic. Biomechanical parameters of the Wan and Schimmels model acquired from Abbas (2010). With 92% goodness of fitness, this model gives a good approximation of a human body response. The human model is presented in Fig. 3.2

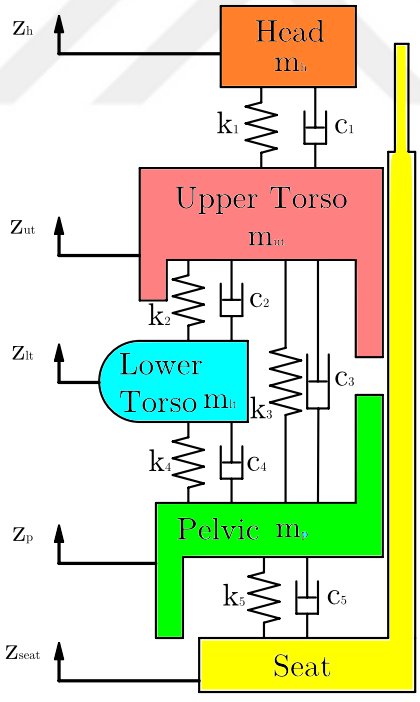


Figure 3.2. Wan and schimmels human model

Eqs. (3.26) to (3.30) are the forces acting on the human models masses.

$$f_p = k_5(Z_p - Z_{seat}) + c_5(\dot{Z}_p - \dot{Z}_{seat}) \tag{3.26}$$

$$f_{ltp} = k_4(Z_{lt} - Z_p) + c_4(\dot{Z}_{lt} - \dot{Z}_p) \tag{3.27}$$

$$f_{utp} = k_3(Z_{ut} - Z_p) + c_3(\dot{Z}_{ut} - \dot{Z}_p) \tag{3.28}$$

$$f_{utlt} = k_2(Z_{ut} - Z_{lt}) + c_2(\dot{Z}_{ut} - \dot{Z}_{lt}) \tag{3.29}$$

$$f_h = k_1(Z_h - Z_{ut}) + c_1(\dot{Z}_h - \dot{Z}_{ut}) \tag{3.30}$$

Eqs. (3.31) to (3.34) denotes the Equations of Motion for the human model.

$$M_p\ddot{Z}_p = -f_p + f_{ltp} + f_{utp} \tag{3.31}$$

$$M_{lt}\ddot{Z}_{lt} = -f_{ltp} + f_{utlt} \tag{3.32}$$

$$M_{ut}\ddot{Z}_{ut} = -f_{utp} - f_{ltp} + f_h \tag{3.33}$$

$$M_h\ddot{Z}_h = -f_h \tag{3.34}$$

Roll angle χ is shown in Fig. 3.3 and defined as following in Eq. (3.35).

$$\chi = \frac{F_M h'}{C_f + C_r - W h'} \tag{3.35}$$

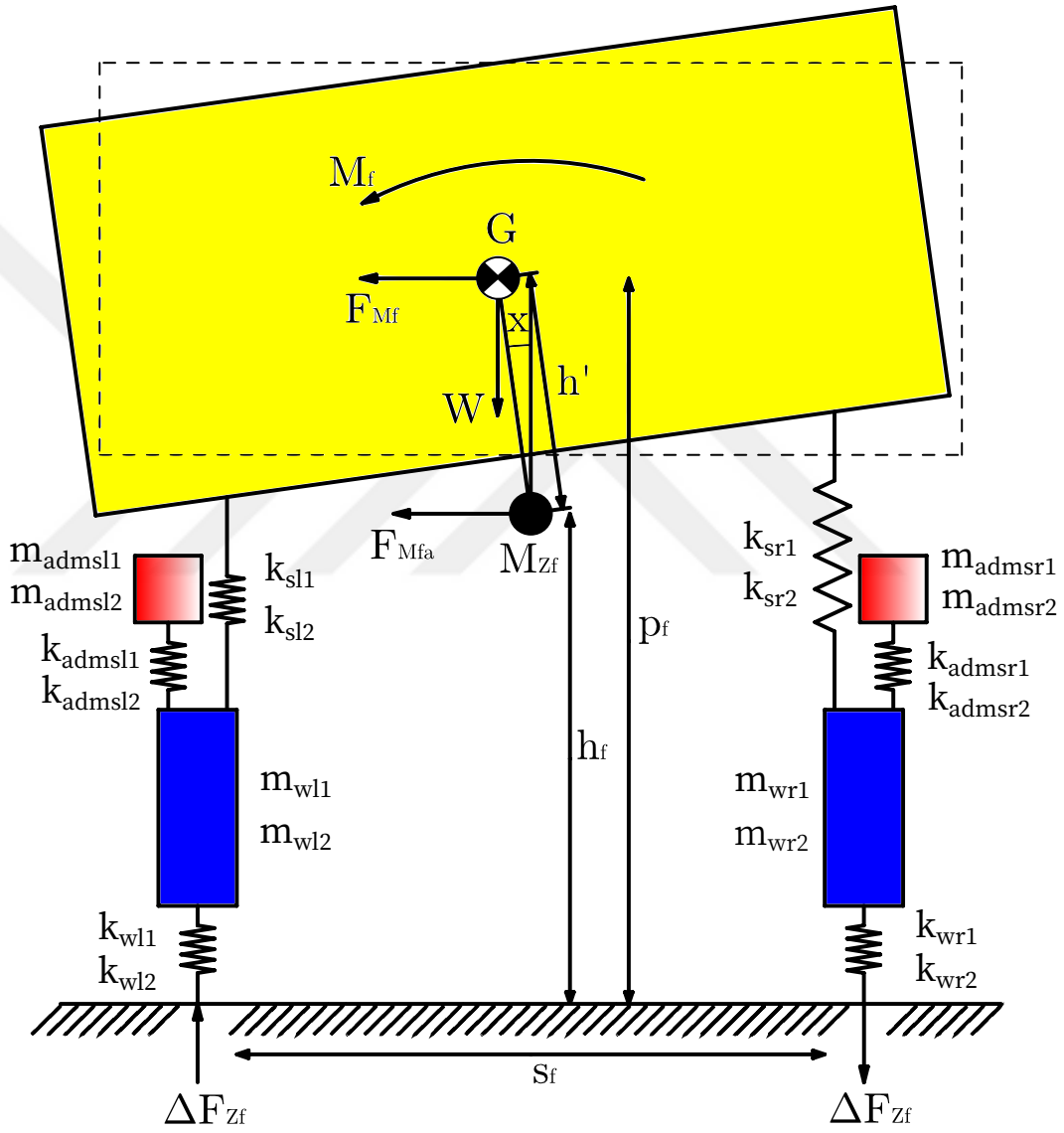


Figure 3.3. Wheel load difference and roll angle

Here F_m is the centripetal force acting on vehicles center of gravity and formulated as $F_M = mv^2/R$. In this formula, m, v, and R are the mass of sprung mass, the vehicle speed, and the vehicle's cornering radius, respectively. C_f, C_r, h', and W are front and

rear axle stiffnesses, the distance between the roll axis and center of gravity of sprung mass, and the weight of the sprung mass. Calculation of front and rear axle stiffness is made by equation $C_{f,r} = (t^2 \cdot K_{f,r})/2$, where t is lateral distance between two wheels and $K_{f,r}$ is spring stiffness for front and rear wheels.

Lateral load distribution affects the vehicle cornering characteristic. Load Transfer Ratio (LTR) is considered as the most reliable rollover indicator regardless of vehicle configuration and operating conditions (Lee, Yakub, Kasahara, & Mori, 2013). Equation of LTR is shown in Eq. (3.38). For the calculation of LTR, the following equations are utilized. Eqs. (3.36) and (3.37) defines the difference of normal loads acting on the front and rear tires during cornering conditions.

$$\Delta F_{Zf} = \frac{mv^2}{R}\left\{\frac{l_r}{l}\frac{p_f}{s_f} + \frac{m_f}{m}\frac{h_f}{s_f} + \frac{C_f h'}{(C_f + Cr - Wh')s_f}\right\} \tag{3.36}$$

$$\Delta F_{Zr} = \frac{mv^2}{R}\left\{\frac{l_f}{l}\frac{p_r}{s_r} + \frac{m_r}{m}\frac{h_r}{s_r} + \frac{C_r h'}{(C_f + Cr - Wh')s_r}\right\} \tag{3.37}$$

Here ΔF_{Zf} and ΔF_{Zr} are the difference of normal loads between right and left tires for the front and rear wheels. m, $m_{f,r}$, v, R, $l_{f,r}$ and l are vehicle mass, front and rear axle mass, vehicle speed, cornering radius, the distance between the front and rear wheels to CG of the vehicle, and distance between the front and rear wheels. $p_{f,r}$, $s_{f,r}$ and $h_{f,r}$ are front and rear roll axis height, the distance between right and left wheels, and front and rear CG height of the sprung mass, respectively.

$$LTR = \frac{F_r - F_l}{F_r + F_l} \tag{3.38}$$

Here F_r and F_l are defined as the vertical tire forces affect the left and right side wheels. The Two-Wheel Lift-Off (TWLO) happens if LTR reaches 1 or -1. LTR is calculated

to detect the change between passive and FL controlled suspensions considering rollover condition.

Eq. (3.39) is the differential equation of the road model. Table 3.1 shows the road roughness values classified by ISO 8608 (2016) and road condition to be used in this study is selected as Class C road with a degree of road roughness of $256 \times 10^{-6} m^2/(cycle/m)$. Seleceted vehicle velocity for the simulations and optimizations is 90 $kmph$. Fig. 3.4 represents the class C road model used in this study.

$$\dot{z}_r(t) + 2\pi n_0 v z_r(t) = \sqrt{S_q(n_0) v} w(t) \tag{3.39}$$

Table 3.1. Road roughness values classified by ISO 8608 (2016) (degree of roughness $S(\Omega) \times 10^{-6}$)

Road class	Range	Geometric mean
A (very good)	<32	16
B (good)	32–128	64
C (average)	128–512	256
D (poor)	512–2048	1024
E (very poor)	2048-8192	4096
F	8192-32768	16384
G	32768-131072	65536
H	131072<	262144

3.2. Active Suspension

3.2.1. PID controller

PID controllers find themselves a wide area of use in industrial applications through implementation ease and high-performance gains. A PID controller adjusts the control signal to minimize the error value. The controller attempts to achieve this objective through a feedback loop based on three constant gains. These three gains are P as present error, Integral (I) as the accumulation of past errors, and Derivative (D) as a future prediction of error through error change rate. The controller adjusts a suspension system continuously by accumulating these weighted error values by changing a damper element's damping rate via adjusting a valve position or power input to an actuator.

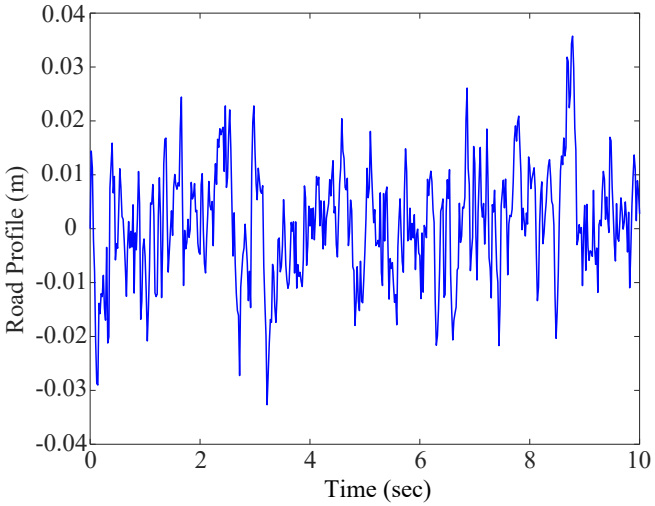


Figure 3.4. Class c road input (velocity 90 $kmph$)

In some applications, only one or two parameters may be enough for the desired system control. Such controllers as PI, PD, or P may be preferred in some situations. The equation and diagram of the PD part of the controller used in this study can be seen in Eq. (3.40) and Fig. 3.5.

PID controllers can be used in any process in which the system can be mathematically represented. There are lots of methods for tuning PID controllers, such as the trial and error method, which is time-consuming for processes with long run times and hard to find optimal values, Ziegler-Nichols method, which may result in a system with over-shoot and instability, gradient method, hill climbing, etc (P. C. Chen & Huang, 2005). All these methods, although useful in some systems, do not guarantee optimal control. Optimization of PID controllers by using Artificial Neural Networks (ANNs) got popular with development of intelligent control theory (Jianhua, 2008). However, this technique's implementation and performance limits its widespread application due to the necessity of massive collected data, time-consuming training process, and being prone to catching local optimums, etc (Niu, 2014).

$$u(t) = K_p e(t) + K_d \frac{de(t)}{dt} \tag{3.40}$$

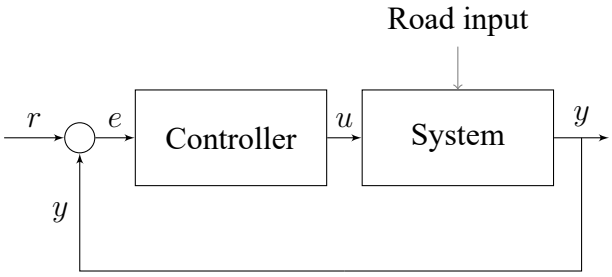


Figure 3.5. A controlled system diagram

In contrast, EAs offer feasible optimization solutions for PID controller parameters. Inspired by the biological and natural evolution process, EAs offer advantages such as global optimization, parallel processing, randomized search space, and fast convergence. Among EAs such as Genetic Programming (GP), Ant Colony Optimization (ACO), Artificial Bee Colony (ABC), Cuckoo Search (CS), PSO, DE, Biogeography-Based Optimization (BBO), etc., GAs offer a very high probability of finding the best solution.

3.2.2. Fuzzy logic controller

FL, unlike classical control strategies working with crisp numbers, instead deal with fuzzy inference. Being similar to human language and feelings in terms of their uncertainty, FL controller fuzzificates inputs and outputs via predetermined MFs. Based on the value of the crisp input, MFs create a different output. As a result, it can be considered as the response of the system is dependent to MFs of the FL controller, which can be considered as a range of inputs.

Human language, with its ambiguous structure, presents a somewhat FL without the realization of its existence in our lives. While human beings deal with uncertainty on a daily basis, machines typically do not operate in such a sense. For instance, a human can define a variable as too big or small with no specific numerical value. On the other hand, machines can only understand binary which can also be called crisp data. Nevertheless, computers can process ambiguous data with FL techniques, and to understand these techniques, Fuzzy Inference System (FIS) knowledge is required.

Implementation of FL techniques to standard computers requires three operation steps. These steps are fuzzification, fuzzy inference, and defuzzification. Fuzzification is the

first step to FL in which conversion of crisp data to fuzzy data through MFs is carried out. Secondly, in order to procure fuzzy output of the system, the fuzzy inference process step combines MFs with the control rules. Lastly, in the defuzzification process, each fuzzified input data are converted to corresponding crisp data from the lookup table.

As referred before, computers can process crisp data such as binary, and to achieve processing of ambiguous data, such as cold, very cold, or mildly cold, conversion of crisp data to linguistic values are critical. This conversion process converts crisp data to fuzzy data and is named fuzzification. A required number of fuzzy languages can be created to achieve desired control accuracy, such as positive big, positive small, zero, negative small, and negative big for a five fuzzy language system.

Following the fuzzification, the fuzzy inference step is crucial, and processing of the MFs is required to do so with various methods and control rules. The control rules that make up the lookup table are the core determiner of a fuzzy inference process, and making or breaking the system is directly associated with the human decision-making process and intuition. For example, for a vehicle speed controlling scheme, the control rules can be such as if the vehicle speed is low and the distance to the destination is high. Hence the vehicle speed should be set to high, which is how human beings' decision-making process works. As MFs are processed according to the lookup table, each output is then aggregated into a single output for the final defuzzification process with various methods such as weighted means, medians, max, sum, t-norms, t-conorms, etc.

As the last step, aggregated value is defuzzified, and to accomplish this task, various methods such as bisector of area, center of area, center of gravity, etc, are utilized, and a crisp value is outputted as a control signal.

In brief, FIS converts the crisp values into fuzzy values for the fuzzy inference process and outputs crisp values. Input and output values are required to be crisp values, but the fuzzy inference process in-between must work on fuzzy values. The reason for this lies in human intuition and language, which lacks crisp definitions for quantities for qualities.

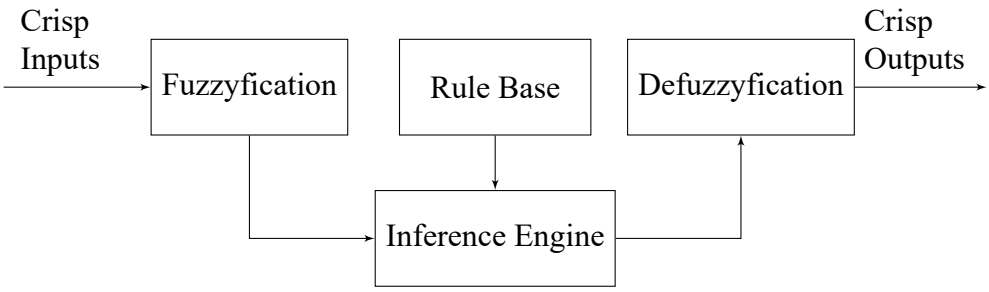


Figure 3.6. Flc controller

The FLC model optimized in this study is Mamdani fuzzy inference system. Mamdani method uses a set of linguistic rules to solve a control problem, and its structure is demonstrated in Fig. 3.6. Traditionally, for this controller type, controller design starts with a rule base created by an expert. After, optimization of membership functions is being carried out for achieving optimal control. However, many studies showed that rule bases created by an expert while performs satisfactory results, further optimization of this controller's rule base resulted in better-performing controllers. Hence, in this study, rule bases are also optimized for achieving the best results. For the optimization of the rule base, a 15 rule structure is defined.

FL deals with degrees of membership for any input and output for any controlling decision. Therefore membership function type choice is an important decision to make for any control problem.

The Gaussian membership function is defined in Eq. (3.41). In this equation, the parameters α and σ defines the features of fuzzy sets. For optimizing the FLC, α and σ will be designated as design parameters.

$$\mu(x) = exp\left(-\frac{(x-\alpha)^2}{2\sigma^2}\right) \tag{3.41}$$

FLC has two inputs and one output. The first input e is the error signal, which is the vertical displacement of the independent suspension system, the second input de is derivative of the error signal, which is the vertical velocity of the independent suspension system. The

output control signal of the FLC is the gain terms for independent PD system. By this configuration, system control outside of FLC control parameters is insured.

Constructed FLC is as follows; Fig. 3.7 shows that for error input 5 Gaussian membership functions, Fig. 3.8 shows that for derivative of error input 3 Gaussian membership functions and as seen in Fig. 3.9 for output 7 Gaussian membership functions exist. Input range of error is $[-2\ +2]$, input range of derivative of error is $[-1\ +1]$ and output range is $[0\ +6]$. While these are the ranges controller operates, actual input and output ranges are wider.

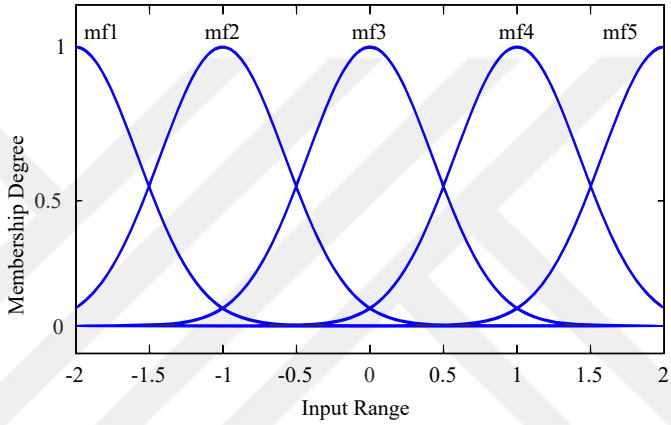


Figure 3.7. Gaussian type membership functions of error input

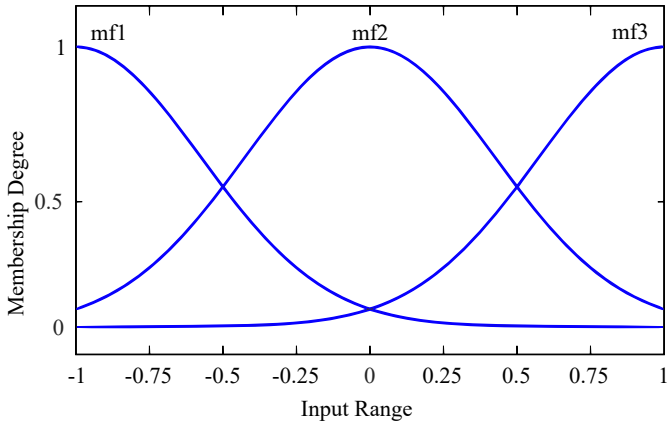


Figure 3.8. Gaussian type membership functions of derivative of error input

3.3. Multi-Objective Optimization

Optimization problems with multi-objective nature require a set of optimal solutions, known as Pareto-optimal. This phenomenon differentiates multi-objective problems from

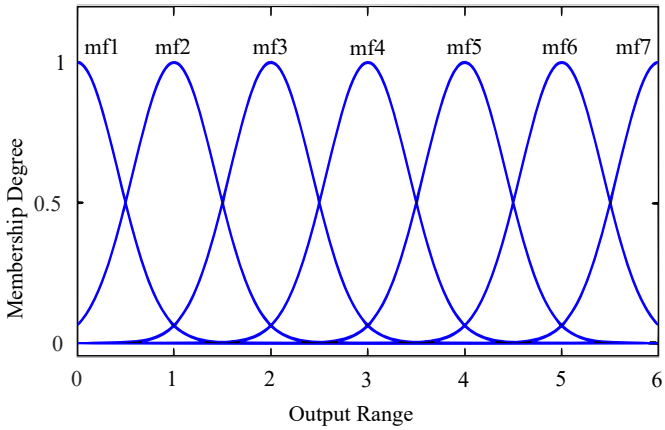


Figure 3.9. Gaussian type membership functions of output

single-objective problems. Pareto-optimal solutions cannot be said to be better than each other without further information. Consequently, it is desired to find as many Pareto-optimal solutions as possible. Classical optimization methods solve the multi-objective optimization problems by converting the multi-objective optimization problem to a uni-objective or by solving the problem one objective at a time. Application of classical methods requires multiple simulation runs, with no guarantee of finding the optimal solution. Also, uni-objective optimization methods eliminate control over the optimization space by their single-dimensional solution space nature. Multi-Objective Evolutionary Algorithms (MOEAs) offer to find multiple Pareto-optimal solutions in a single optimization run. By working with a large number of population, EAs present a diverse set of Pareto-optimal solutions.

During the advancement of EAs, numerous different methods were suggested. Srinivas and Deb (1994)'s Non-dominated Sort Genetic Algorithm (NSGA) , Fonseca and Fleming (1993)'s MOGA , and Abido (2003)'s Niched Pareto Genetic Algorithm (NPGA) attracted much attention by converting simple EAs to MOEAs through additional operators. These operators' conventional features were to assign a fitness value to population members through non-dominated sorting and preservation of diversity in non-dominated fronts. Although these MOEAs showed promising results in multi-objective optimization problems, requirements for their improvement introduced elitism to MOEAs. Elitism is a characteristic that the best generation members will be kept in population for the next generation.

Implementation of this approach improved convergence times as shown in (Zitzler, Deb, & Thiele, 2000).

FAST NON-DOMINATED SORTING

for each $p \in P$

  $S_p = \emptyset$

  $n_p = 0$

  for each $q \in P$

    if $(p \prec q)$ then If p dominates q

      $S_p = S_p \cup \{q\}$ Add q to the set of solutions dominated by p

    else if $(q \prec p)$ then

      $n_p = n_p + 1$ Increment the domination counter of p

  if $n_p = 0$ then p belongs to the first front

    $p_{rank} = 1$

    $F_1 = F_1 \cup \{p\}$

$i = 1$ Initialize the front counter

while $F_i \neq \emptyset$

  $Q = \emptyset$ Used to store the members of the next front

  for each $q \in S_p$

    $n_q = n_q - 1$

    if $n_q = 0$ then q belongs to the next front

      $q_{rank} = i + 1$

      $Q = Q \cup \{q\}$

  $i = i + 1$

  $F_i = Q$

In a straightforward approach to fast non-dominated sorting, for identifying the non-dominated front with a population size of N, each solution can be compared with other solutions to find if it is non-dominated. This process requires $O(MN)$ comparison for each solution, while M is the number of objectives. With a total complexity of $O(MN^2)$, all solutions' sorting process for the first front is accomplished. This process at this far founds first non-dominated front. Before finding the next front, the first front solutions are discarded, and the procedure so far is repeated until there is no front assigned individual is left. Because there is a maximum number of N front is possible for N population size, the computational complexity of this operation at worst conditions is overall $O(MN^3)$.

While this process is sufficient for Pareto-fronts' discovery, Deb, Pratap, Agarwal, and Meyarivan (2002) presented a more efficient way of non-dominated sorting in their paper. To accomplish this, for each solution, two calculations need to be made. Domination count n_p, which is the number of solutions that dominate the solution p, and S_p which is a set of solutions dominated by solution p. This process overall has a computational complexity of $O(MN^2)$. The flow chart and algorithm of this method are shown in Fig. 3.10 and above.

This process in detail works like this. All solutions in the first front, which is non-dominated, will have their domination counts as zero. For each non-dominated solution p, which $n_p = 0$ for p, each member of S_p is visited and their domination numbers (n_p) reduced by one. By doing this, if any member of the S_p reaches a domination count of zero, these solutions will be put into a separate list Q. This list becomes the second front. By repeating the same procedure, the third front will be identified. This process will be repeated until all fronts are identified.

For solutions that are not the member of the first front, domination count (n_p) can be at most $N - 1$. For this reason, before the domination count of any solution p becomes zero, each solution p will be visited at most $N - 1$ times. After the domination count (n_p) becomes zero for any solution p, a non-domination level (front) will be assigned to each solution and will never be revisited. On account of $N-1$ solutions such as this exists, total complexity is $O(N^2)$ for one objective, therefore total complexity will be $O(MN^2)$.

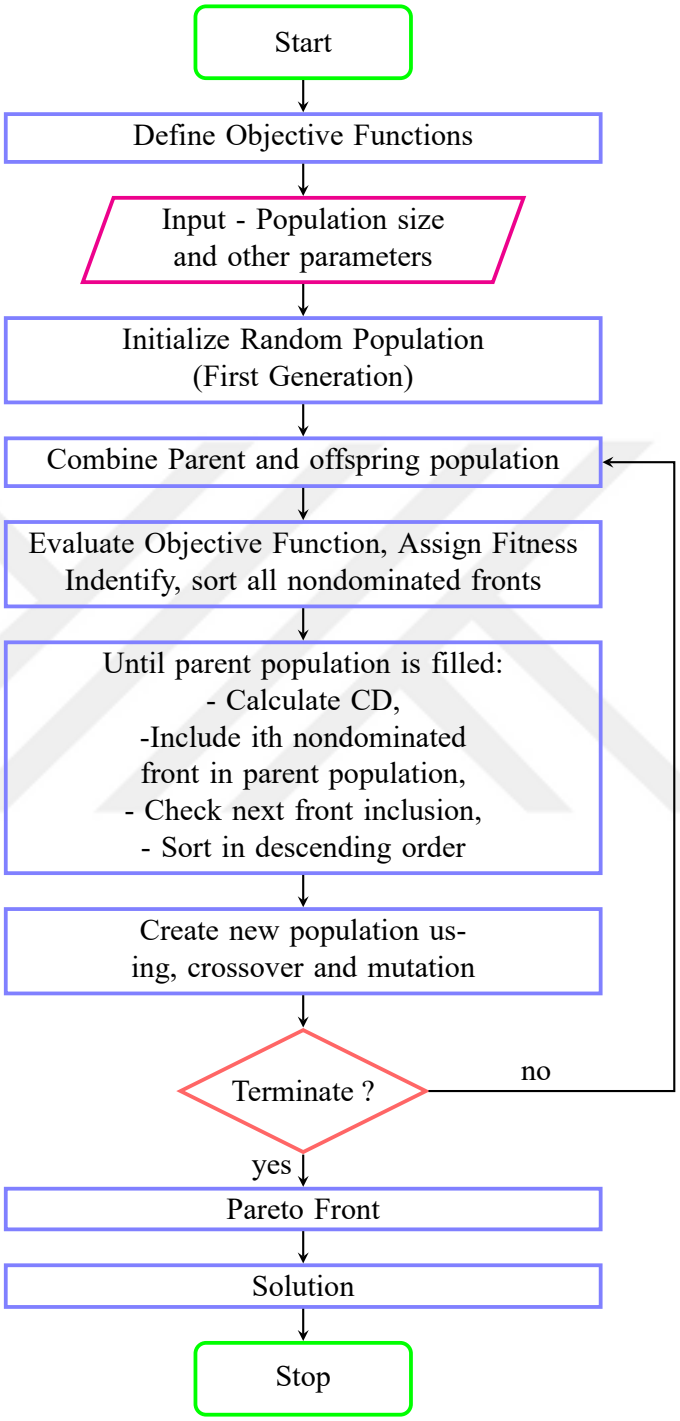


Figure 3.10. Flow chart of the multi-objective optimization algorithm based on fast and elitist non-dominated sorting genetic algorithm

3.3.1. Diversity preservation

EAs offer convergence to the Pareto optimal set, but it is also required to preserve a good diversity among the solution set. NSGA-II accomplishes this task via a Crowding Distance (CD) operator. To achieve preservation of diversity among the population, NSGA-II does not require any predefined value. The CD of a member is the average distance between $2M$ members on either side of this member, M being the objective number. Calculation of CD firstly requires sorting the population in ascending order for each objective. Following this, boundary solutions of each objective are assigned an infinite distance value. The rest of the population are assigned an absolute distance value equal to the difference between two adjacent solutions. After completing the first objective, this process is repeated for all other objectives. The Sum of each individual's objectives distance values is the total CD for that solution. Before calculating CD, normalization is applied to each objective function, dividing the two adjacent neighbors' difference value for each objective to that objectives' solution space range. The algorithm to compute CD is shown here.

CROWDING DISTANCE ASSIGNMENT

$l = |\mathcal{I}|$ number of solutions in $\mathcal{I}$

for each i, set $\mathcal{I}[i]_{distance} = 0$ initialize distance

for each objective m

$\mathcal{I} =$ sort$(\mathcal{I}, m)$ sort using each objective value

$\mathcal{I}[1]_{distance} = \mathcal{I}[l]_{distance} = \infty$ so that boundary points are always selected

for $i = 2$ to $(l - 1)$ for all other points

$$\mathcal{I}[i]_{distance} = \mathcal{I}[i]_{distance} + \frac{(\mathcal{I}[i+1].m - \mathcal{I}[i-1].m)}{(f_m^{max} - f_m^{mix})}$$

In this algorithm, m notation refers to m_{th} objective and i notation is i_{th} individual in the set $\mathcal{I}$. f_m^{max} and f_m^{mix} are the max and min values of the m_{th} objective. This sorting algo-

rithm has a computational complexity of $O(MNlogN)$, for M independent sortings and N population size. After the assignment of CD for all population members, comparison step is carried out by their proximity to other solutions. A smaller CD would mean that a solution is, in a sense, more crowded by other solutions. Crowded comparison operator compares this value.

The crowded comparison operator accomplishes to acquire a uniformly distributed Pareto optimal front by guiding the selection process at various stages of the algorithm. This operator carries out the selection process by comparing non-domination rank and CD for every population member. Selection process prefers the solution with lower rank (front) in case two solution has different ranks. When solutions have the same rank, solutions in the less crowded region will be preferred instead. The crowded comparison operator is shown below.

CROWDED COMPARISON OPERATOR

$i \prec_n j$ if ($i_{rank} < j_{rank}$

or $((i_{rank} = j_{rank})$

and $(i_{distance} > j_{distance}))$

NSGA-II algorithm starts the optimization process by creating a random population. After a non-domination-based sorting of the population, each solution is assigned a rank, also named front, equal to its non-domination count. The following steps are binary tournament selection, recombination, and mutation, to create an offspring population Q_0 of size N. With elitism, by comparing the current population with previously found non-dominated solutions, the process differs between the initial generation and others.

After the first generation, the process is conducted as follows. First step is to combine current (P_t) and previous (Q_t) generation to create a new population (R_t), which has a population size of $2N$. The second step is to sort the population R_t according to non-domination. Elitism is warranted by including previous and current generation population

in R_t. At this stage, solutions in the first front (F_1) are the best solutions and have priority over any other solution. If the size of F_1 is smaller than N, all members of F_1 is guaranteed to be chosen for the next population (P_{t+1}). If that is not the case, until N number of members is chosen for P_{t+1}, the following non-dominated front members will be chosen next and so on. Generally, the sum of all members from first to the last rank would be greater than N, and sorting would be needed for the last chosen rank (F_l). To choose exactly N members in total for P_{t+1}, for the last non-dominated chosen rank, solutions are sorted using crowded comparison operator and members chosen in descending order, starting from best, until N member P_{t+1} population is reached. To create the new population Q_{t+1} by selection, crossover and mutation, this N size P_{t+1} population is now used. Although selection criteria are based on a crowded comparison operator, binary tournament selection operator is still used for crossover selection and constraint handling. The main algorithm loop is shown below.

MAIN LOOP

$R_t = P_t \cup Q_t$	combine parent and offspring population
$\mathcal{F} =$ fast-non-dominated-sort(R_t)	$\mathcal{F} = (\mathcal{F}_1, \mathcal{F}_2, \ldots)$, all nondominated fronts of R_t
$P_{t+1} = \emptyset$ and $i = 1$	
until $\lvert P_{t+1}\rvert + \lvert\mathcal{F}_i\rvert \leq N$	until the parent population is filled
crowding-distance-assignment$(\mathcal{F}_i)$	calculate crowding distance in $\mathcal{F}_i$
$P_{t+1} = P_{t+1} \cup \mathcal{F}_i$	include i_{th} nondomination front in the parent pop
$i = i + 1$	check the next front for inclusion
Sort$(\mathcal{F}_i, \prec_n)$	sort in descending order using $\prec_n$
$P_{t+1} = P_{t+1} \cup \mathcal{F}_i[1 : (N - \lvert P_{t+1}\rvert)]$	choose the first $(N - \lvert P_{t+1}\rvert)$ elements of $\mathcal{F}_i$
$Q_{t+1} =$ make-new-pop(P_{t+1})	use selection, crossover and mutation to create a new population
$t = t + 1$	increment the generation counter

3.3.2. Objective functions

Optimization problems, while requiring many aspects for a successful optimization, objective functions are one of the critical factors. The human body parts' response to road-induced vibration is different from a seat response. Hence, the following comfort and health criterions selected for this study. RMS weighted head acceleration, VDV at the head, RMS seat acceleration, RMS upper torso acceleration, the amplitude ratio of head RMS acceleration to seat RMS acceleration, the amplitude ratio of upper torso RMS acceleration to seat RMS acceleration, and Crest Factor selected as comfort and health criteria. Moreover, for the ride handling, reliability and safety criteria, RMS suspension travel, RMS tire travel, and RMS IWM travel are included.

RMS weighted head acceleration (A_{wh}) is given by ISO 2631-1 (1997) as in Eq. (3.42).

$$A_{wh} = \left\{ \frac{1}{T} \int_0^T [a_{wh}(t)]^2 dt \right\}^{\frac{1}{2}} \tag{3.42}$$

Alongside RMS head acceleration, RMS upper torse acceleration (A_{ut}) is another important objective to consider when optimizing a suspension system. The effect of vibration on different body parts might differ in some situations. Hence, A_{ut} is defined as the shown in Eq. (3.43).

$$A_{ut} = \left\{ \frac{1}{T} \int_0^T [a_{ut}(t)]^2 dt \right\}^{\frac{1}{2}} \tag{3.43}$$

While the effect of vibration on the seat and body parts may be matching objectives, in some cases, conflicting behavior may be observed. RMS seat acceleration (A_s) is defined as presented in Eq. (3.44).

$$A_s = \left\{ \frac{1}{T} \int_0^T [a_s(t)]^2 dt \right\}^{\frac{1}{2}} \tag{3.44}$$

The major portion of vibration humans exposed in vehicles enter the body through the seat (Van Niekerk, Pielemeier, & Greenberg, 2003). Studies have shown that seated Whole Body Vibration (WBV) exposure affects the spine by mechanical overload and excessive muscular fatigue (Bovenzi, 2005). The time of exposure to vibrations determines the health risks. As a result of these reasons, the measurement of WBV is important. As ISO 2631-1 (1997) states, VDV is a measure for assessing vibration dose effect. VDV is given by ISO 8608 (2016) as shown in Eq. (3.45).

$$VDV_h = \left\{ \int_0^T [a_{wh}(t)]^4 dt \right\}^{\frac{1}{4}} \tag{3.45}$$

Alongside the RMS value of acceleration value, another essential factor to consider is maximum exposed acceleration. Hence, CF is our following objective function. CF is defined as the ratio of maximum head acceleration to the RMS head acceleration and given by ISO 2631-1 (1997) as shown in Eq. (3.46).

$$CF = max(a_h) \Big/ \left\{ \frac{1}{T} \int_0^T [a_s(t)]^2 dt] \right\}^{\frac{1}{2}} \tag{3.46}$$

The transmissibility ratio is another factor to be considered as an objective. The amplitude ratios of head RMS acceleration and upper torso RMS acceleration to seat RMS acceleration is AR_h and AR_{ut}, respectively. These values are defined in Eqs. (3.47) and (3.48).

$$AR_h = \left\{ \frac{1}{T} \int_0^T [a_h(t)]^2 dt] \right\}^{\frac{1}{2}} \Big/ \left\{ \frac{1}{T} \int_0^T [a_s(t)]^2 dt] \right\}^{\frac{1}{2}} \tag{3.47}$$

$$AR_{ut} = \left\{ \frac{1}{T} \int_0^T [a_{ut}(t)]^2 dt] \right\}^{\frac{1}{2}} \Big/ \left\{ \frac{1}{T} \int_0^T [a_s(t)]^2 dt] \right\}^{\frac{1}{2}} \tag{3.48}$$

Suspension system travel is defined as relative displacement between sprung mass and unsprung mass. Minimization of this value is vital for a more stable suspension system characteristic. Also, optimization of this value would improve the lifespan of the suspension system. RMS suspension travel (RMS_{st}) is calculated independently for each suspension system, and the summation is defined as a single optimization objective and defined in Eq. (3.49).

$$\begin{aligned} RMS_{st} = & \left\{ \frac{1}{T} \int_0^T [Z(t) - \Theta(t) \cdot c - \Phi(t) \cdot a - Z_{wr1}(t)]^2 dt \right\}^{\frac{1}{2}} \\ & + \left\{ \frac{1}{T} \int_0^T [Z(t) - \Theta(t) \cdot c + \Phi(t) \cdot b - Z_{wl1}(t)]^2 dt \right\}^{\frac{1}{2}} \\ & + \left\{ \frac{1}{T} \int_0^T [Z(t) + \Theta(t) \cdot d - \Phi(t) \cdot a - Z_{wr2}(t)]^2 dt \right\}^{\frac{1}{2}} \\ & + \left\{ \frac{1}{T} \int_0^T [Z(t) + \Theta(t) \cdot d + \Phi(t) \cdot b - Z_{wl2}(t)]^2 dt \right\}^{\frac{1}{2}} \end{aligned} \tag{3.49}$$

For EVs equipped with an IWM system, RMS of ADMs travel (RMS_{adm}) is a notable criterion when optimizing suspension system. RMS_{adm} is calculated independently for each motor, and the summation is defined as a single optimization objective and defined in Eq. (3.50).

$$
\begin{aligned}
RMS_{adm} = & \left\{ \frac{1}{T} \int_0^T [Z_{admr1}(t) - Z_{wr1}(t)]^2 dt \right\}^{\frac{1}{2}} \\
& + \left\{ \frac{1}{T} \int_0^T [Z_{adml1}(t) - Z_{wl1}(t)]^2 dt \right\}^{\frac{1}{2}} \\
& + \left\{ \frac{1}{T} \int_0^T [Z_{admr2}(t) - Z_{wr2}(t)]^2 dt \right\}^{\frac{1}{2}} \\
& + \left\{ \frac{1}{T} \int_0^T [Z_{adml2}(t) - Z_{wl2}(t)]^2 dt \right\}^{\frac{1}{2}}
\end{aligned} \tag{3.50}
$$

Dynamic tire forces are related to tire deflections. Tire deflection is defined as relative displacement between wheel and road. For reliable road handling characteristics, optimization of this value is essential. RMS value of tire deflection objective (RMS_{tire}) calculated as accumulation of each wheel's RMS values and defined in Eq. (3.51).

$$
\begin{aligned}
RMS_{tire} = & \left\{ \frac{1}{T} \int_0^T [Z_{wr1}(t) - Z_{rr1}(t)]^2 dt \right\}^{\frac{1}{2}} \\
& + \left\{ \frac{1}{T} \int_0^T [Z_{wl1}(t) - Z_{rl1}(t)]^2 dt \right\}^{\frac{1}{2}} \\
& + \left\{ \frac{1}{T} \int_0^T [Z_{wr2}(t) - Z_{rr2}(t)]^2 dt \right\}^{\frac{1}{2}} \\
& + \left\{ \frac{1}{T} \int_0^T [Z_{wl2}(t) - Z_{rl2}(t)]^2 dt \right\}^{\frac{1}{2}}
\end{aligned} \tag{3.51}
$$

To reduce dimension of objective space, sum of AR_{ut}, AR_h, VDV_h and A_{ut} is taken as a uni-objective. As a result, seven objective functions are defined for optimization. Objectives are defined as following:

$$
\begin{aligned}
f_1 &= A_{wh} \\
f_2 &= A_{ws} \\
f_3 &= CF \\
f_4 &= AR_{ut} + AR_h + VDV_h + A_{ut} \\
f_5 &= RMS_{st} \\
f_6 &= RMS_{tire} \\
f_7 &= RMS_{adm}
\end{aligned} \tag{3.52}
$$

For optimization of vehicle suspension systems, in addition to comfort and health criteria, ride safety is another key factor. Hence, the following parameters are defined as constraints. Baumal et al. (1998) defined required maximum suspension travel as 125 mm to avoid hitting suspension stop, and maximum seat acceleration as 4.5 m/s^2. For the minimization of dynamic tire forces, maximum tire deflection should not exceed 58 mm. For the vehicle's cornering characteristic, the roll angle should not exceed 5° for a 25-meter cornering radius at 25 m/s vehicle speed. These parameters are determined as constraints in the optimization of the suspension system. Values concerning the full vehicle model and human model are tabulated in Table 3.2.

Constraints defined for optimization problem are $max(a_{seat}) \leq 4.5m/s^2$ for maximum seat acceleration, $max(Susp.Disp.) \leq 0.125m$ for maximum suspension travel, $max(TireDisp.) \leq 0.058m$ for maximum tire deflection and $\chi \leq 5°$ for maximum roll angle.

Design parameters for the optimization are spring stiffnesses and damping coefficients of shock absorbers for vehicle suspension, IWM, and seat. These parameters are the passive parts of the suspension system. For optimizing the FLC, α and σ parameters of the Gaussian membership functions and rule list are selected.

Table 3.2. Constants of full vehicle and human model

Parameter	Value	Unit	Parameter	Value	Unit
M	1200	kg	e	0.7	m
I_x	4000	kgm^2	f	0.5	m
I_y	950	kgm^2	v	25	m/s
M_{wr1}	40	kg	R	25	m
M_{wl1}	40	kg	h'	0.2	m
M_{wr2}	40	kg	M_1	4.17	kg
M_{wl2}	40	kg	M_2	15	kg
M_{admr1}	30	kg	M_3	5.5	kg
M_{adml1}	30	kg	M_4	36	kg
M_{admr2}	30	kg	k_1	166990	N/m
M_{adml2}	30	kg	k_2	10000	N/m
M_{seat}	20	kg	k_3	144000	N/m
k_{wr1}	180000	N/m	k_4	20000	N/m
k_{wl1}	180000	N/m	k_5	49340	N/m
k_{wr2}	180000	N/m	c_1	310	$N/(m/s)$
k_{wl2}	180000	N/m	c_2	200	$N/(m/s)$
a	1.4	m	c_3	909.1	$N/(m/s)$
b	1.6	m	c_4	330	$N/(m/s)$
c	1	m	c_5	2475	$N/(m/s)$
d	1	m	h_r	0.5	m
p_f	0.2	m	p_r	0.2	m
m_f	50	kg	m_r	50	kg
h_f	0.5	m			

3.3.3. Population size and stoppage criterion

Rosenthal and Borschbach (2014) concluded that seventy to 100 population size is best for their study. Hernández-Díaz et al. (2008) experimentally determined the minimum population size as 52 for NSGA-II. Reeves and Rowe (2002) conducted their study on the principle that, at the very least, every point in search space should be reachable from the initial population. This requirement can only be satisfied if there is at least one instance of every allele at each locus in the whole population of strings. As a result, they calculated that population size seventeen is adequate for a string length of fifty to demonstrate the probability of 99.9% to satisfy the aforementioned principle. This calculation carried out according to Eq. (3.53).

$$N \approx [1 + \log(-\frac{l_s}{lnP_2^*})/\log 2] \tag{3.53}$$

Here P_2^* is defined as $P_2^* = (1 - (1/2)^{N-1})^{l_s}$ and using an exponential function approximation $P_2^* \approx exp(-l_s/2^{N-1})$ equation is established as in Eq. (3.53). In Eqs. (3.53) and (3.54), N and l_s stands for population size and GA string length, respectively.

Alander (1992) through a set of experiments, concluded an optimum population size for problems with varying complexity for GA as shown in Eq. (3.54).

$$l_s \leq N \leq 2l_s \tag{3.54}$$

According to Eq. (3.54), optimum population size has a connection to chromosome length. As an example, the range of design variable k_{sr1} is $(30,000 - 10,000) = 20,000$. Thus, via this example $2^{14} = 16,384 < 20,000 < 2^{15} = 32,768$, requirement of k_{sr1} is 15 bits for storation of its value in chromosome.

Bit requirements for other design variables and design variable ranges are shown in Tables 3.3 to 3.5. Hence, the chromosome length for passive suspension elements is 127 bits, and for FLC of k_p and k_d, the chromosome length is 273 bits each. Therefore according to Eq. (3.54), the total length of chromosome for passive suspension optimization is as stated, and the population size is 250 selected. For the optimization of FLC, total length of the chromosome is 673 bits, and population size is selected as 1300 for optimization. Criteria for the optimization stoppage is the generation number and is equal to 250.

Table 3.3. Design variable range for passive suspension elements

Design Variables	k_{sr1} k_{sl1}	k_{sr2} k_{sl2}	c_{sr1} c_{sl1}	c_{sr2} c_{sl2}	k_{admr1} k_{aml1}
upper bound	30000	30000	1800	1800	60000
lower bound	10000	10000	600	600	20000
search space	20000	20000	1200	1200	40000
bit value	15	15	11	11	16
Design Variables	k_{admr2} k_{aml2}	c_{admr1} c_{aml1}	c_{admr2} c_{aml2}	k_{seat}	c_{seat}
upper bound	60000	1500	1500	3750	2250
lower bound	20000	500	500	1250	750
search space	40000	1000	1000	2500	1500
bit value	16	10	10	12	11

Table 3.4. Design variable range of fuzzy logic controlled proportional and derivative gains

Design Variables	k_p	k_d
upper bound	60000	6000
lower bound	0	0

Table 3.5. Design variable range for fuzzy logic controller

Design Variables	E		delE		output		rule_{1-15}
	σ_{1-5}	α_{1-5}	σ_{1-3}	α_{1-3}	σ_{1-7}	α_{1-7}	
upper bound	0.24	2	0.24	1	1	6	6
lower bound	0.04	-2	0.04	-1	0.1	0	0
search space	20	400	20	200	90	600	6
total bit value	25	45	15	24	49	70	45

4. RESULTS AND DISCUSSION

After the optimization process, further action is the determination of the best members step, and since Pareto-optimal solutions cannot be said to be better than each other without further information, a straightforward approach is not possible. To select a set of population members, an additional examination of results is required. In these cases, 250 and 1300 sets of design variables are available for passive and FLC optimizations. Hence, the minimum value for each objective is tabulated in Table 4.1 for all optimizations and change in these values for all generations is shown in Fig. 4.2. To represent the findings, design variables with best RMS A_{wh} or approximations with gains in other objectives selected. Objective values and comparison of the systems tabulated and showed in Table 4.6 and Fig. 4.1.

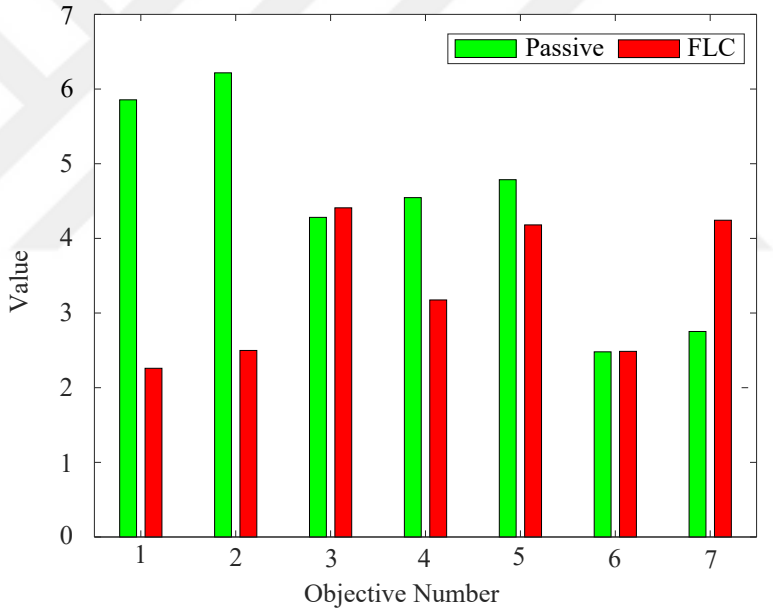


Figure 4.1. Objective values of selected members (1 and 2 scale x10 - 5 to 7 scale x100)

Table 4.1. Minimum objective values

	f_1	f_2	f_3	f_4	f_5	f_6	f_7
Passive	$0,5660$	$0,6217$	$3,7182$	$4,4382$	$0,0444$	$0,0223$	$0,0189$
FLC	$0,2260$	$0,2499$	$2,6375$	$3,1754$	$0,0328$	$0,0223$	$0,0192$
FLC vs Passive	60%	60%	29%	28%	26%	0%	-1%

Passive design variables of selected population members for passive and FLC suspension systems are shown in Table 4.2. For FLC, σ and α design variables of MFs for k_p and

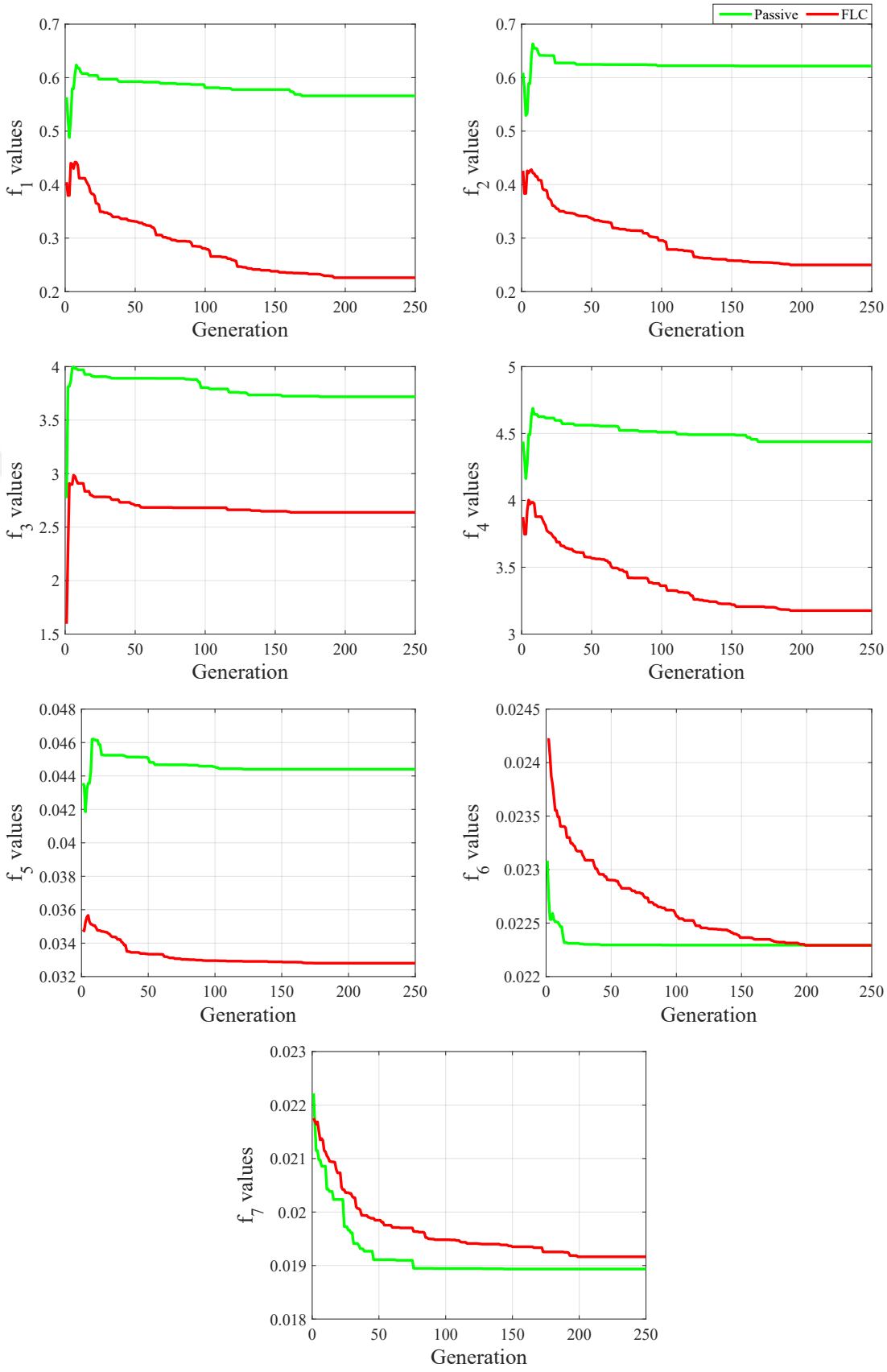


Figure 4.2. Minimum objective values of populations in all generations

k_d are shown in Table 4.3. MF names for E, delE and output are A to E, A to C, and 0 to 6, respectively. These namings are only for referencing purposes and hold no actual value concerning the operation of FL controller. In Tables 4.4 and 4.5, corresponding MF names and rule structures can be seen. $Rule_1$ for example can be written for k_p controller as *IF E is A and delE is A, THEN OUTPUT is 4*. Difference of FL from boolean logic is, instead of a binary response of boolean logic, a fuzzy response controls the system. For instance, concerning the $Rule_1$, degree of membership for E to be A and delE to be A is very important. Based on a successful optimization of rule structure and MFs, a high performing FLC is achieved.

Table 4.2. Selected passive design variables for passive and fuzzy logic controlled systems

Design Variables	k_{sr1} k_{sl1}	k_{sr2} k_{sl2}	c_{sr1} c_{sl1}	c_{sr2} c_{sl2}	k_{admr1} k_{adml1}	k_{admr2} k_{adml2}	c_{admr1} c_{adml1}	c_{admr2} c_{adml2}	k_{seat}	c_{seat}
Passive	19039	18082	1714	1363	38946	50224	867	1061	1250	750
FLC	13163	25448	855	1059	26107	25808	611	500	1340	750

MFs by characterization of fuzziness, quantify certainty of the input spaces, therefore determining the response of the system. MFs of the optimized FL controller are shown in Figs. 4.3 and 4.4. After determining the MFs and the rules, fuzzy surfaces can be created to visualize the responses of the FLC. k_p and k_d surfaces of the optimized FL controller are shown in Fig. 4.5. It is seen from the comparison of k_p and k_d surfaces, while k_d surface operates between 5200 and 5800, a rather small interval, k_p surface ranges from 5000 to 35000, quite a big interval in comparison. By this difference, it can be deduced that the effect of k_p on the system performance compared to k_d is far superior. While a relatively constant value is required for k_d gain for system control. Significant effect of proportional gain can be said to pointing the requirement of fast system response is much greater than the prediction of future errors. Furthermore, the interval with low proportional gains would prevent oscillations and system instability.

Table 4.6 shows that RMS head and seat accelerations are the most improved objectives compared to the passive suspension system. It is also seen that these values are not trade-off values. CF due to its definition is understandable to relatively stay unchanged in FLC compared to passive suspension. The reason for this is CF is ratio of RMS acceleration to

Table 4.3. Selected membership function design variables of fuzzy logic controller

		Number	K_p	K_d	MF names
E	σ	1	0,11	0,24	A
		2	0,1	0,11	B
		3	0,24	0,24	C
		4	0,09	0,17	D
		5	0,13	0,12	E
	α	1	0,36	0,9	A
		2	-0,53	1,23	B
		3	1,33	-0,07	C
		4	0,53	0,03	D
		5	-1,16	0,22	E
delE	σ	1	0,22	0,11	A
		2	0,14	0,14	B
		3	0,19	0,14	C
	α	1	-0,49	0,51	A
		2	0,95	-0,83	B
		3	0,75	-0,23	C
OUTPUT	σ	1	0,74	0,38	0
		2	0,95	0,72	1
		3	0,96	0,36	2
		4	0,12	0,18	3
		5	0,35	0,48	4
		6	0,38	0,3	5
		7	0,24	0,71	6
	α	1	1,96	5,09	0
		2	3,51	2,49	1
		3	2,64	5,63	2
		4	5,62	5,87	3
		5	0	2,45	4
		6	1,6	5,64	5
		7	3,66	1,21	6

Table 4.4. Fuzzy logic controller k_p rules of selected population member

E / delE	A	B	C	D	E
A	4	4	4	4	5
B	1	4	0	3	2
C	1	5	2	4	4

Table 4.5. Fuzzy logic controller k_d rules of selected population member

E / delE	A	B	C	D	E
A	3	5	3	2	2
B	5	3	3	2	5
C	3	3	3	3	5

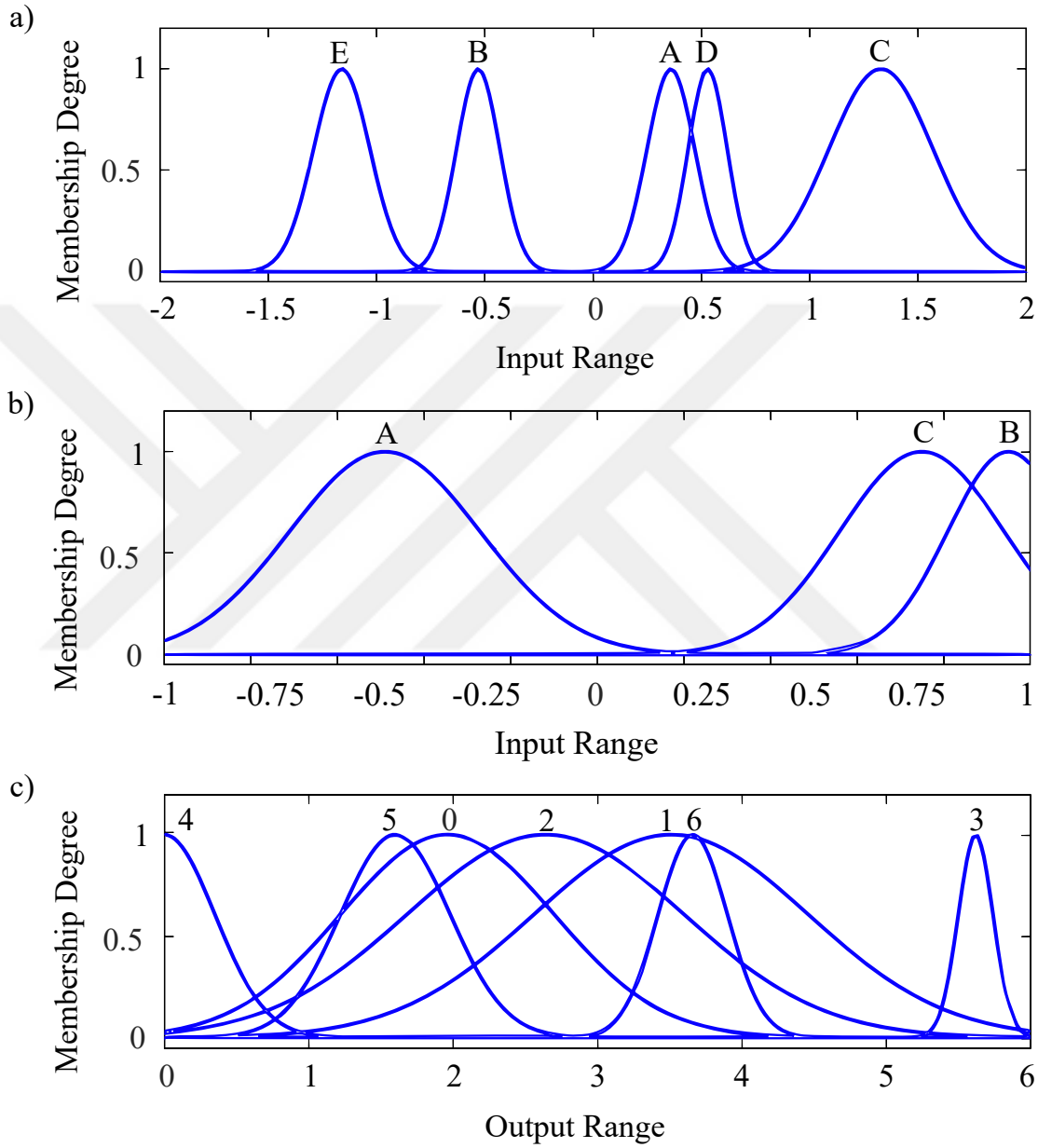


Figure 4.3. k_p fuzzy logic controller (a) E, (b) delE, and (c) output membership functions

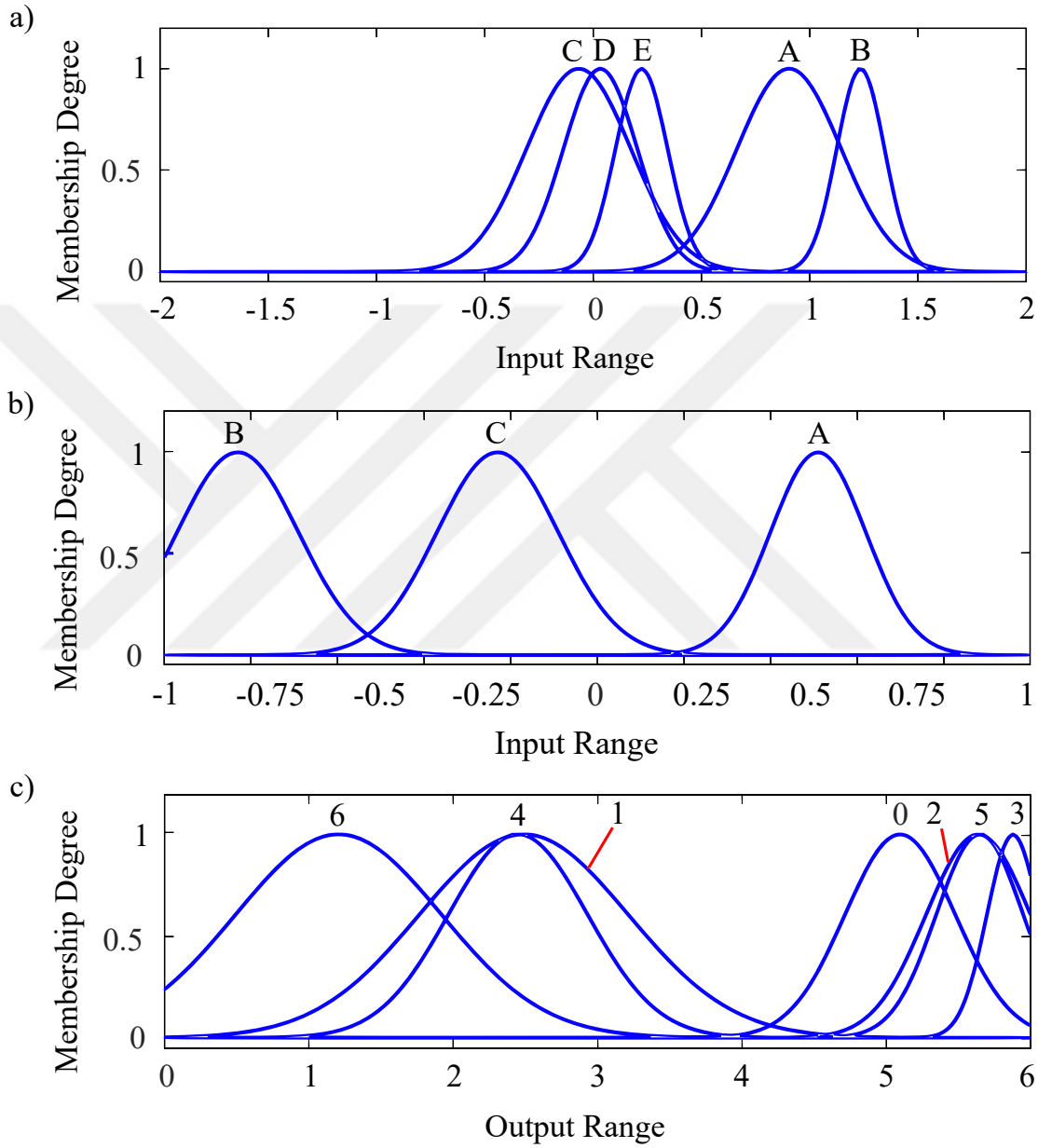


Figure 4.4. k_d fuzzy logic controller (a) E, (b) delE, and (c) output membership functions

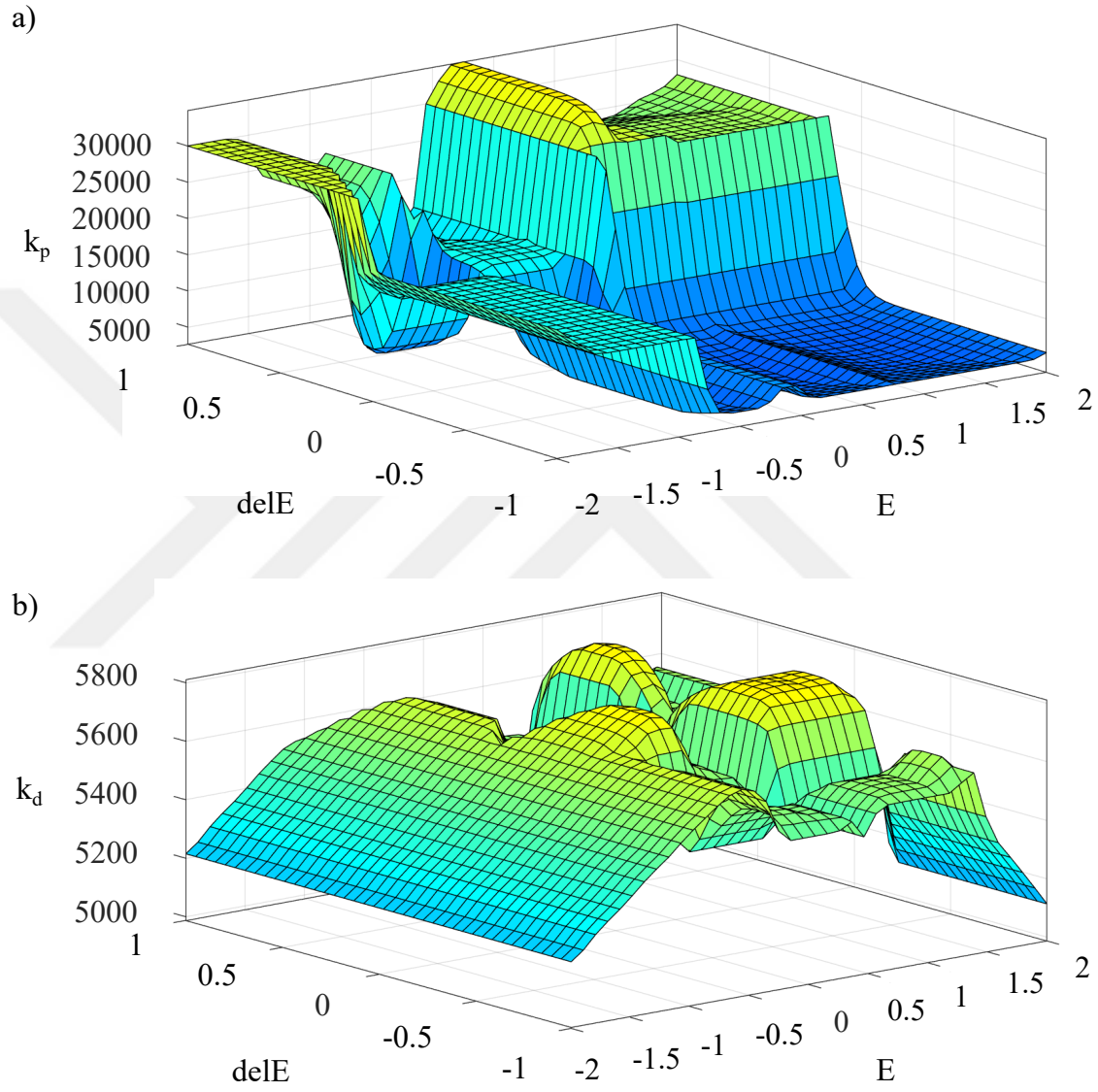


Figure 4.5. (a) k_p and (b) k_d surfaces of the fuzzy logic controller

peak acceleration. Since improvements in both RMS and peak values are seen, their ratio is relatively unchanged. Also, RMS head and upper torso acceleration graphs are shown in Fig. 4.6. It is clearly seen that FLC controller improves these values over the passive system, and improved comfort and health performance is expected.

Table 4.6. Comparison of selected members

	f_1	f_2	f_3	f_4	f_5	f_6	f_7
Passive	0.5856	0.6217	4.2816	4.5460	0.0479	0.0248	0.0275
FLC	0.2260	0.2499	4.4092	3.1754	0.0418	0.0249	0.0424
FLC vs Passive	61%	60%	−3%	30%	13%	0%	−54%

Comparison of AR_h, AR_{ut}, VDV_h, A_{ut} in Fig. 4.7 clearly displays that there is no change in values AR_h and AR_{ut} with 1,225 and 1,2 for passive, and 1,209 and 1,173 for FLC systems. These values correspond to the transmissibility of the vibration in the human body and have no relation between the type of suspension system. Unless the resonance state occurs, these values would approximately be the same for all driving conditions. However, VDV_h and A_{ut} changed drastically with 1,425 and 0,696 for passive, and 0,528 and 0,266 for FLC systems, promoting better comfort and health expectations. Improvements in VDV_h are especially significant considering it is a metric of WBVs. While WBVs practiced as a medical treatment, for instance, in order to treat back pain, even a short period of exposure can actually cause immediate adverse effects such as fatigue, nausea, and lightheadedness.

Vertical wheel forces and LTR rollover index for passive and FLC can be seen in Table 4.7. LTR index calculations made under conditions of 25 m/s vehicle speed and 50 m cornering radius. Comparing passive suspension system against FLC, FLC exhibited negligible changes, which is 0.06% increase in the LTR index. Since LTR is considered to be most reliable rollover indicator regardless of vehicle configuration and operating conditions, FL controller displayed no adverse effect against passive suspension in cornering condition.

As mentioned by W. Sun et al., comfort and stability are connected with different DOF movements; for instance, the vehicle body movement can be perilous when the sprung mass roll causes disproportionate load distribution on tires, resulting in side-slip or rollover

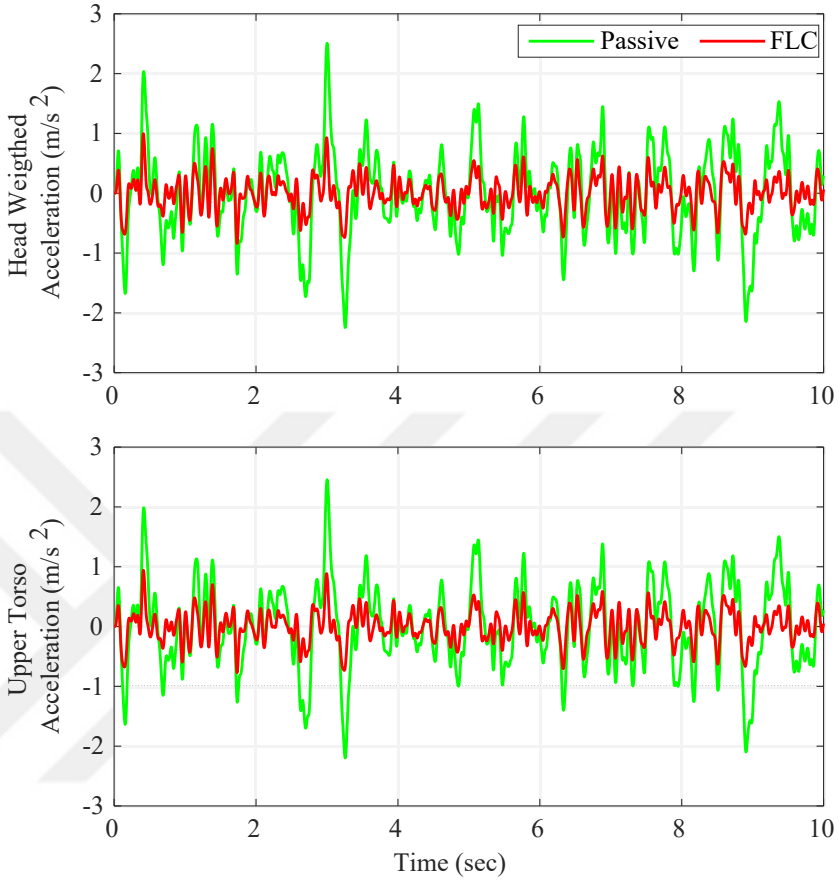


Figure 4.6. Time response of human model

Table 4.7. Vertical wheel forces and load transfer index

	$R1$	$L1$	$R2$	$L2$	LTR
$Passive$	$1388,4$	4890	1136	$4357,6$	$0,57112244$
FLC	$1655,5$	$4622,9$	$870,83$	$4622,8$	$0,57079023$

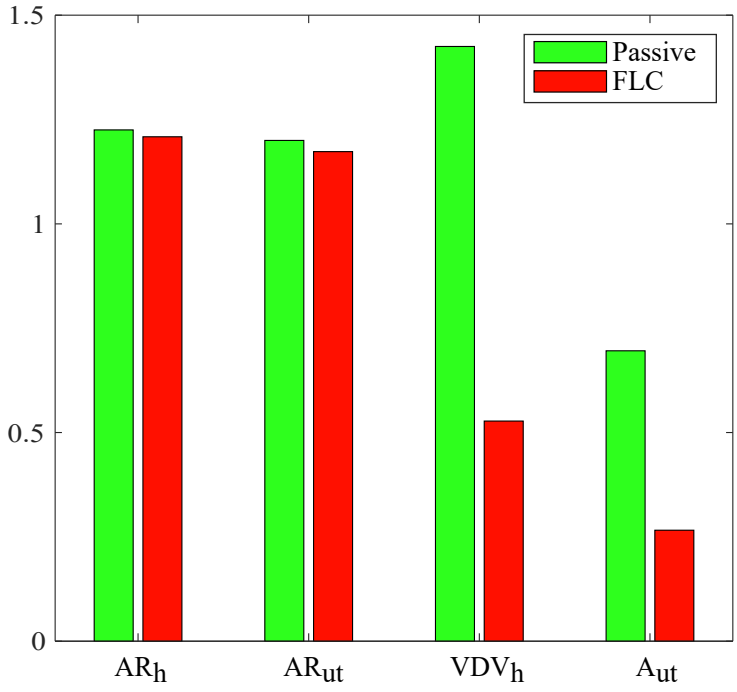


Figure 4.7. Comparison of AR_h, AR_{ut}, VDV_h, A_{ut}

of the vehicle. Hence, examination of vehicle body movement in different DOF is also an important step. Displacement graphs for vehicle body are shown in Fig. 4.8, and significant improvements in vertical displacement and phi angle and some improvement in theta angle are observed with FL controlled suspension compared to the passive system.

Suspension deflection values are significant concerning especially comfort and health criteria. Lower magnitude suspension deflection also contributes to reliability. Fig. 4.9 shows suspension deflections graph. RMS suspension displacement improved 14% for FLC system over passive suspension. As seen in Fig. 4.10, RMS tire displacement showed no significant change because it is somewhat affected by tire stiffness instead of suspension characteristic. While all objectives we discussed until now demonstrated significant improvement or negligible changes, the RMS displacement value of the IWM objective is proven to be a trade-off objective. FLC suspension RMS IWM displacement value increased 54% comparing to passive suspension. Advanced dynamic damper type IWM configuration while improving comfort and health criteria, acting of IWM as a dynamic damper increased IWM deflection. In order to overcome this, implementation of a controller for IWM could be considered. Fig. 4.11 shows the control forces of FLC.

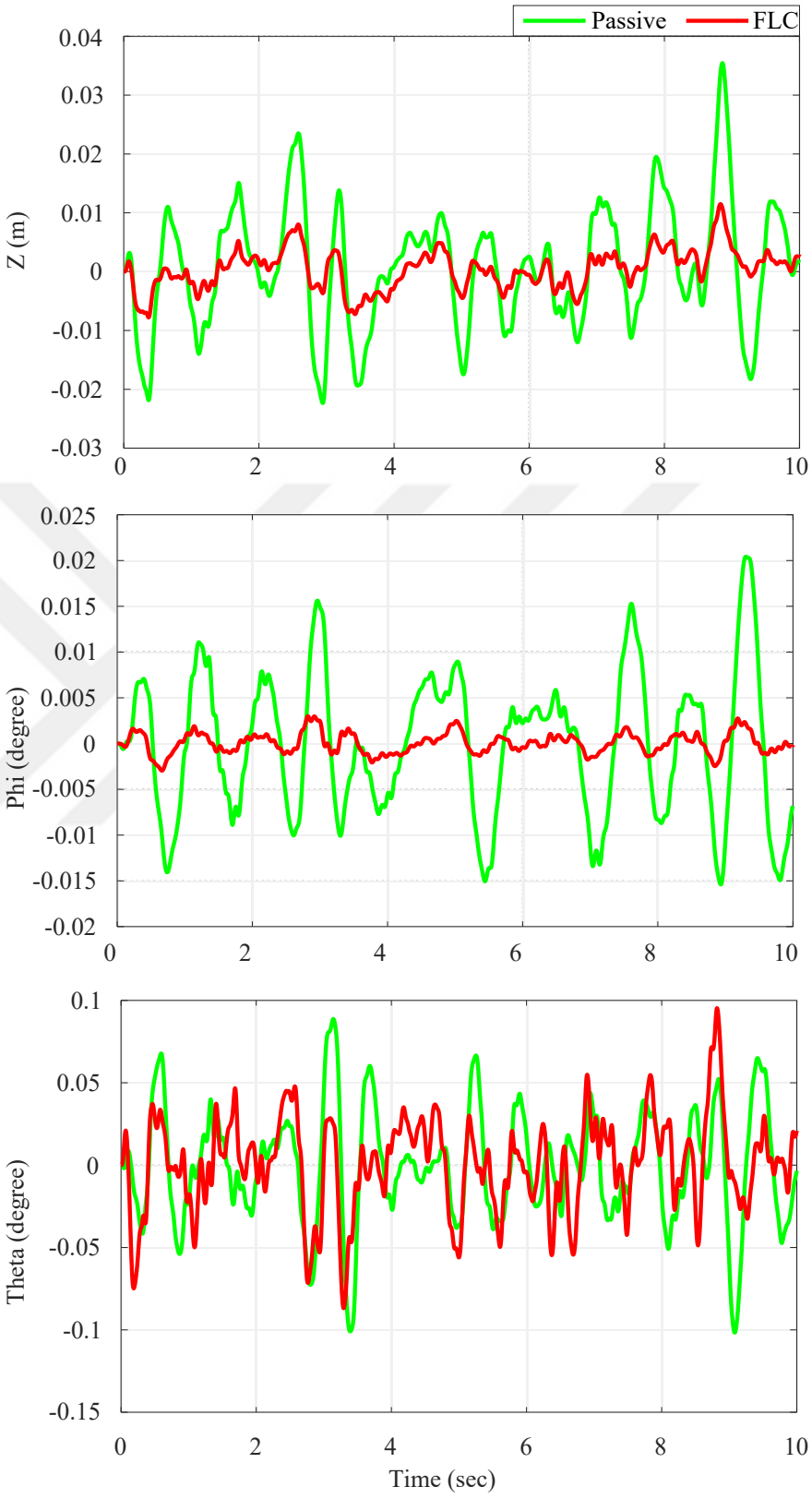


Figure 4.8. Sprung mass displacement graphs

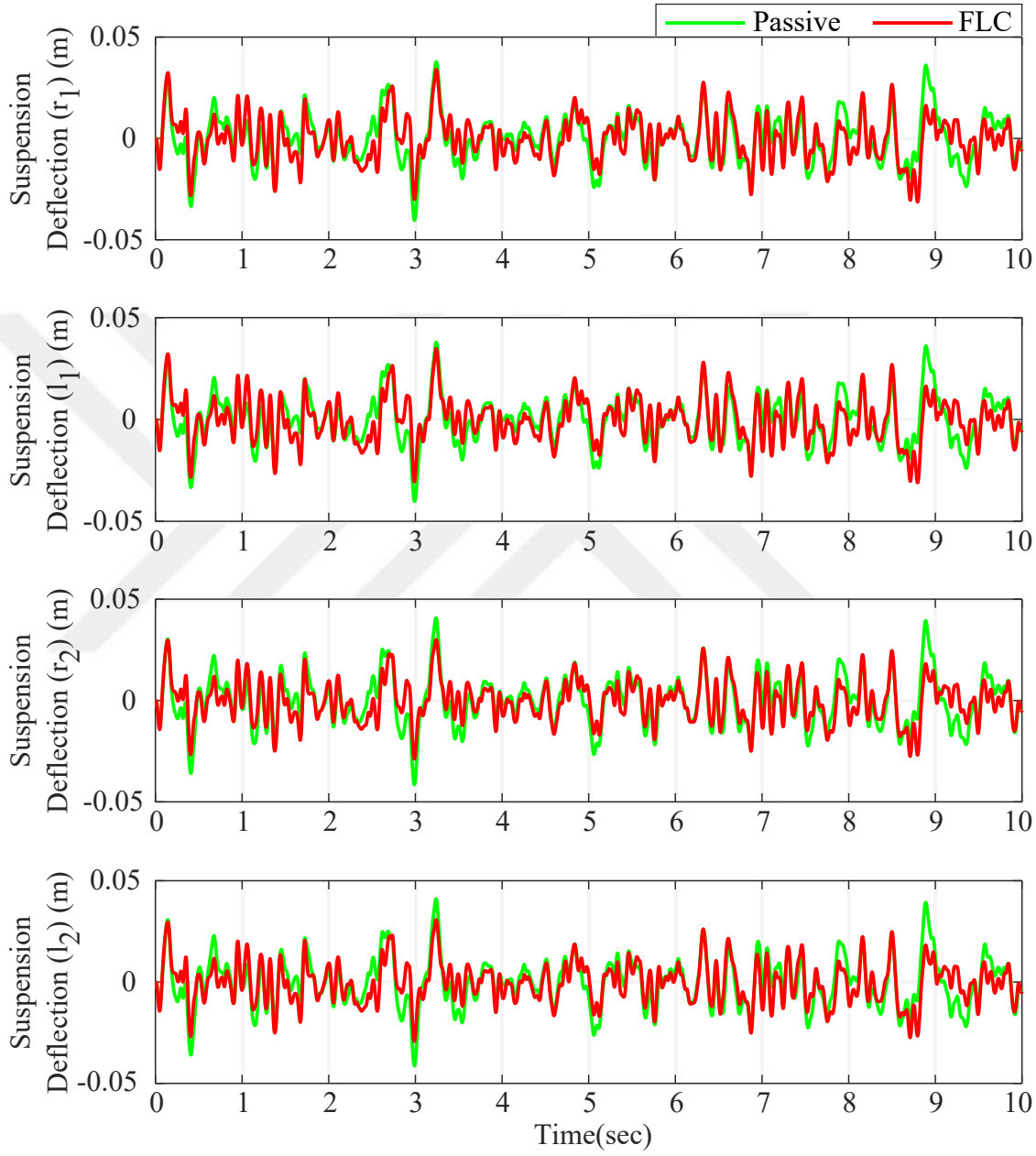


Figure 4.9. Suspension deflections

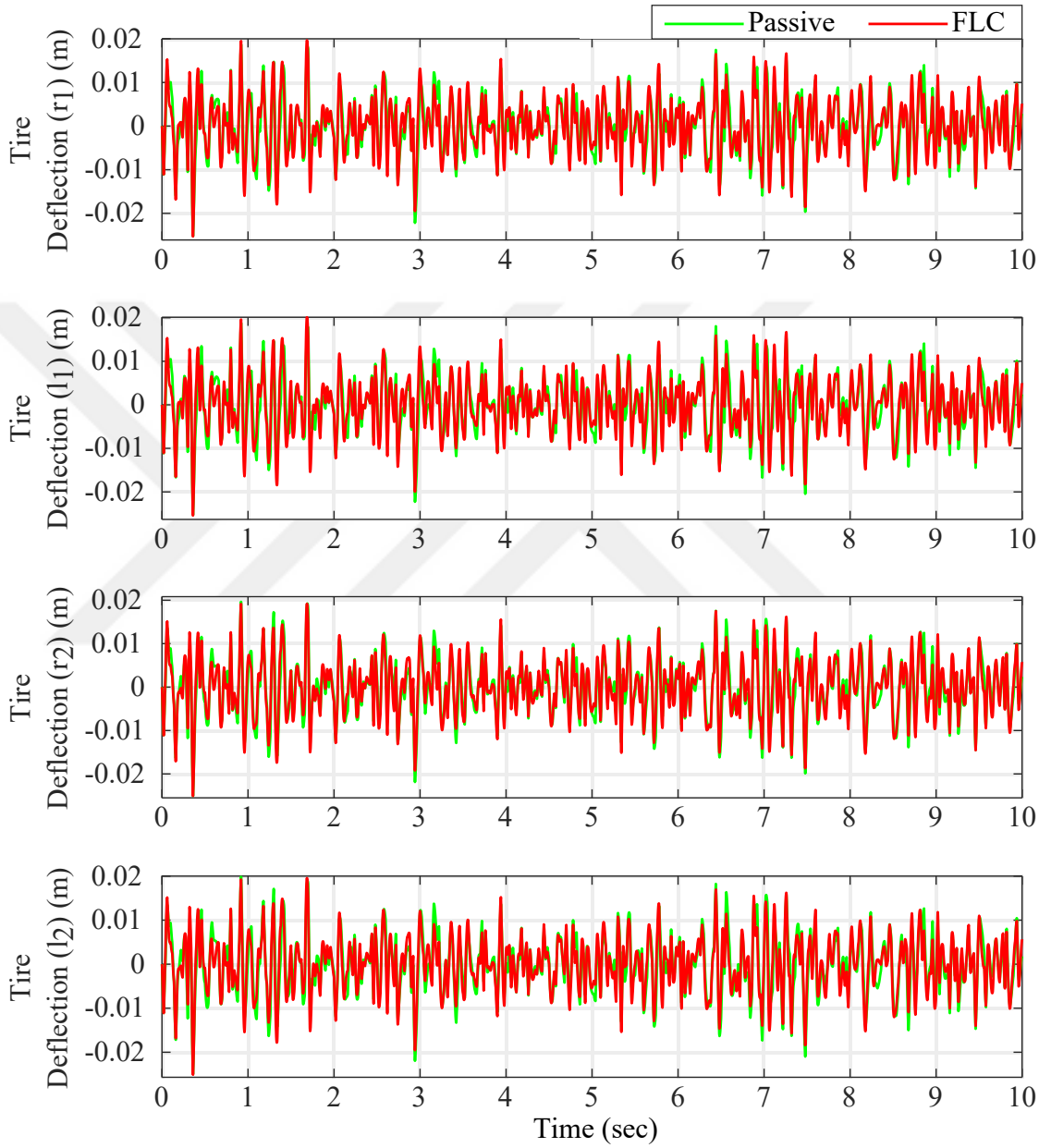


Figure 4.10. Tire deflections

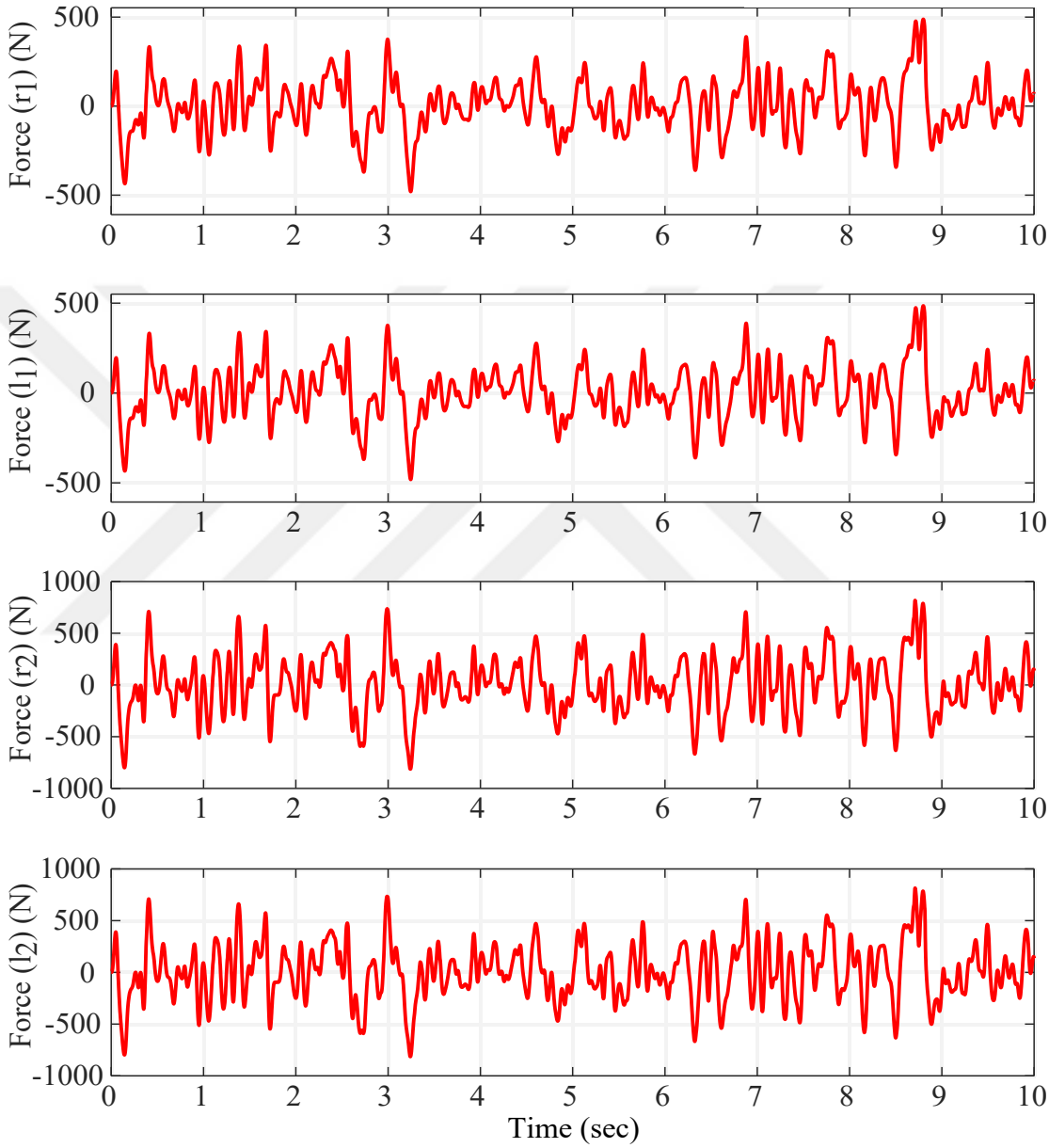


Figure 4.11. Control forces of active suspension

While the investigation of acceleration values gives an idea about expectable health and comfort criteria, further examination is required to ensure the effects of vibration meet the necessary standards. Such as the effects of various durations to exposing such vibration. ISO 2631-1 (1997) defines vibration exposure limits by Health Guidance Caution Zone (HGCZ) as shown in Fig. 4.12. In this figure, dashed lines numbered as one is exposure period and vibration magnitude as RMS weighted head acceleration, straight lines numbered as two are based on VDV_h. Here the criterion used to define exposure limit is RMS weighted head acceleration-based. This criterion has three categories for assessing vibration exposure, No Health Risk (NHR), Potential Health Risk (PHR), and Likely Health Risk (LHR). In Fig. 4.12 A_{wh} values for passive and FLC systems are presented.

Vibration exposure limits for A_{wh} is tabulated in Table 4.8. Passive system durations are 4,2 hours, 4,2 to 17,2 hours, and 17,2 to 24 hours for NHR, PHR, and LHR. FLC system exceeds the time limits and no health risk is expected over 24 hours.

Table 4.8. Time limits for vibration exposure

	$A_{wh}(m/s^2)$	Vibration exposure limits (h)		
		NHR	PHR	LHR
$Passive$	$0,5856$	$4,2$	$4,2-17,2$	$17,2-24$
FLC	$0,2260$	–	–	–

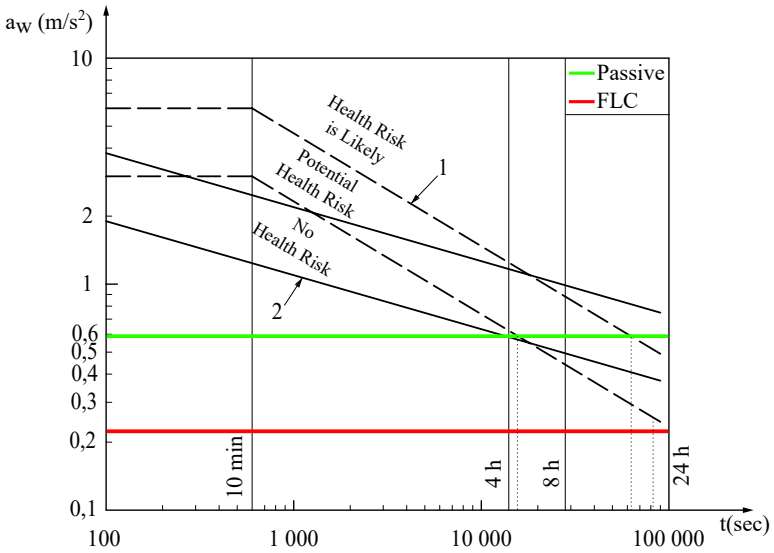


Figure 4.12. A_{wh} graph (health guidance caution zone)

5. CONCLUSION

This thesis presents the multi-objective optimization of an IWM EV. Implemented EV model is a nonlinear full car model with an active suspension system. A sixteen DOF model consists of eleven DOF nonlinear vehicle models with quadratic nonlinearities in tires and cubic nonlinearities in the suspension system, five DOF driver-seat model, and an FL controlled PD controller developed and optimized.

Optimization objectives concerning health, comfort, ride handling, and safety were selected. These objectives are A_{wh}, VDV_h, A_s, A_{ut}, Crest Factor, AR_h, AR_{ut}, and suspension, tire, and IWM deflections. Optimization of FL controlled active suspension system successfully implemented using NSGA-II algorithm with constrictions concerning ride and cornering safety such as maximum suspension deflection to prevent hitting suspension stop, dynamic tire loads concerning road holding ability by limiting tire deflection, maximum seat acceleration for comfort, and max roll angle concerning cornering characteristic. Moreover to these traditional objectives, the rarely considered rollover effect is investigated.

Presented optimization results demonstrated a significant improvement over the passive system with the FL controller. Optimized FL controller improves ride comfort and health criterion over the passive system. In addition to these, the LTR index showed no adverse change between models concerning the rollover situation. However, apart from the improvements observed, implementing a controller to reduce IWM deflection is recommended as the following study subject.

REFERENCES

2631-1, I. (1997). ISO2631-1.. Mechanical vibration and shock; evaluation of human exposure to whole body vibration in the working environment; Part 1 General requirements. *International Standard Organization, Geneva*.

8608, I. (2016). ISO 8608.. Mechanical vibration — Road surface profiles — Reporting of measured data. *International Standard Organization, Geneva*.

Abbas, W. (2010). Optimization of Biodynamic Seated Human Models Using Genetic Algorithms. *Engineering*, *02*(09), 710–719. doi: 10.4236/engineering.2010.29092

Abido, M. A. (2003). A niched Pareto genetic algorithm for multiobjective environmental/economic dispatch. In *International journal of electrical power and energy systems* (Vol. 25, pp. 97–105). doi: 10.1016/S0142-0615(02)00027-3

Abu Bakar, S. A., Masuda, R., Hashimoto, H., Inaba, T., Jamluddin, H., Rahman, R. A., & Samin, P. M. (2014). Ride comfort performance improvement of electric vehicle (EV) conversion using SAS-controlled active suspension system. *Jurnal Teknologi*, *71*(2), 113–120. doi: 10.11113/jt.v71.3729

Ahmadian, M. (2001). Active control of vehicle vibration. In S. Braun (Ed.), *Encyclopedia of vibration* (p. 37-45). Oxford: Elsevier. Retrieved from `https://www.sciencedirect.com/science/article/pii/B0122270851001934` doi: https://doi.org/10.1006/rwvb.2001.0193

Ahmed, A. A., & Özkan, B. (2017). Using of fuzzy pid controller to improve vehicle stability for planar model and full vehicle models. *International Journal of Applied Engineering Research*, *12*(5), 671–680.

Alander, J. T. (1992). On optimal population size of genetic algorithms. In *Proceedings - computer systems and software engineering: 6th annual european computer conference, compeuro 1992* (pp. 65–70). doi: 10.1109/CMPEUR.1992.218485

Anadolu Ajansı. (2021). *Varank: Ford Otosan'ın 'Yeni Nesil Ticari Araç ve Batarya Üretimi' yatırımı 2. elektrikli araç üretim tesisi olacak.* `https://www.aa.com.tr/tr/ekonomi/varank-ford-otosanin-yeni-nesil-ticari-arac-ve-batarya-uretimi-yatirimi-2-elektrikli-arac-uretim-tesisi-olacak/2177886`.

Bakar, S. A. A., & Aziz, A. A. (2014). Active suspension system to improve ride comfort performance of Electric Vehicle (EV) conversion. In *Applied mechanics and materials* (Vol. 663, pp. 208–212). Trans Tech Publications Ltd. doi: 10.4028/www.scientific.net/AMM.663.208

Balamurugan, L., Jancirani, J., & Eltantawie, M. A. (2014). Generalized magnetorheological (MR) damper model and its application in semi-active control of vehicle suspension system. *International Journal of Automotive Technology*, *15*(3), 419–427. Retrieved from `https://doi.org/10.1007/s12239-014-0044-4` doi: 10.1007/s12239-014-0044-4

Baumal, A. E., McPhee, J. J., & Calamai, P. H. (1998). Application of genetic algorithms to the design optimization of an active vehicle suspension system. *Computer Methods in Applied Mechanics and Engineering*, *163*(1-4), 87–94. doi: 10.1016/S0045-7825(98)00004-8

Bello, M. M., Shafie, A., & Khan, M. R. (2015). Electro-hydraulic pid force control for nonlinear vehicle suspension system. *International journal of engineering research*

and technology, *4*.

Bovenzi, M. (2005). Health effects of mechanical vibration. *Giornale Italiano di Medicina del Lavoro ed Ergonomia*, *27*(1), 58–64.

Cao, D., Rakheja, S., & Su, C. Y. (2010). Roll- and pitch-plane coupled hydro-pneumatic suspension. *Vehicle System Dynamics*, *48*(3), 361–386. Retrieved from https://doi.org/10.1080/00423110902883251 doi: 10.1080/00423110902883251

Cao, D., Song, X., & Ahmadian, M. (2011). Editors' perspectives: Road vehicle suspension design, dynamics, and control. *Vehicle System Dynamics*, *49*(1-2), 3–28. Retrieved from https://doi.org/10.1080/00423114.2010.532223 doi: 10.1080/00423114.2010.532223

Cao, J.-T., Liu, H.-H., Li, P., Brown, D. J., & Dimirovski, G. (2007). A study of electric vehicle suspension control system based on an improved half-vehicle model. *International Journal of Automation and Computing*, *4*(3), 236–242. Retrieved from https://doi.org/10.1007/s11633-007-0236-8 doi: 10.1007/s11633-007-0236-8

Chen, H., & Guo, K. H. (2005). Constrained H∞ control of active suspensions: An LMI approach. *IEEE Transactions on Control Systems Technology*, *13*(3), 412–421. doi: 10.1109/TCST.2004.841661

Chen, P. C., & Huang, A. C. (2005). Adaptive sliding control of non-autonomous active suspension systems with time-varying loadings. *Journal of Sound and Vibration*, *282*(3-5), 1119–1135. doi: 10.1016/j.jsv.2004.03.055

Chiou, J. S., & Liu, M. T. (2009). Using fuzzy logic controller and evolutionary genetic algorithm for automotive active suspension system. *International Journal of Automotive Technology*, *10*(6), 703–710. doi: 10.1007/s12239-009-0083-4

Choi, S. B., Choi, Y. T., & Park, D. W. (1998, apr). A Sliding Mode Control of a Full-Car Electrorheological Suspension System Via Hardware in-the-Loop Simulation . *Journal of Dynamic Systems, Measurement, and Control*, *122*(1), 114–121. Retrieved from https://doi.org/10.1115/1.482435 doi: 10.1115/1.482435

Choi, S. B., & Han, Y. M. (2007). Vibration control of electrorheological seat suspension with human-body model using sliding mode control. *Journal of Sound and Vibration*, *303*(1-2), 391–404. Retrieved from https://www.sciencedirect.com/science/article/pii/S0022460X07000909 doi: 10.1016/j.jsv.2007.01.027

Choi, S. B., Lee, H. S., & Park, Y. P. (2002). H∞ control performance of a full-vehicle suspension featuring magnetorheological dampers. *Vehicle System Dynamics*, *38*(5), 341–360. Retrieved from https://www.tandfonline.com/doi/abs/10.1076/vesd.38.5.341.8283 doi: 10.1076/vesd.38.5.341.8283

Cole, D. J. (2000). Evaluation of design alternatives for roll-control of road vehicles. *Avec*, 561–568.

Daniyan, I. A., Mpofu, K., & Osadare, D. F. (2018). Design and simulation of a controller for an active suspension system of a rail car. *Cogent Engineering*, *5*(1), 1–15. Retrieved from https://doi.org/10.1080/23311916.2018.1545409 doi: 10.1080/23311916.2018.1545409

Deb, K., Pratap, A., Agarwal, S., & Meyarivan, T. (2002). A fast and elitist multiobjective genetic algorithm: NSGA-II. *IEEE Transactions on Evolutionary Computation*, *6*(2), 182–197. doi: 10.1109/4235.996017

Ding, R., Wang, R., Meng, X., & Chen, L. (2020). Mode-switching control and

stability analysis of a hybrid electromagnetic actuator for the vehicle suspension. *JVC/Journal of Vibration and Control*, *26*(19-20), 1804–1814. Retrieved from https://doi.org/10.1177/1077546320906296 doi: 10.1177/1077546320906296

Djellal, A., & Lakel, R. (2018). Adapted reference input to control PID-based active suspension system. *Journal Europeen des Systemes Automatises*, *51*, 7–23. doi: 10.3166/JESA.51.7-23

DOE and EPA. (2021). *All-Electric Vehicles.* https://www.fueleconomy.gov/feg/evtech.shtml.

Du, H., Yim Sze, K., & Lam, J. (2005). Semi-active H∞ control of vehicle suspension with magneto-rheological dampers. *Journal of Sound and Vibration*, *283*(3-5), 981–996. Retrieved from https://www.sciencedirect.com/science/article/pii/S0022460X04005589 doi: 10.1016/j.jsv.2004.05.030

Du, H., & Zhang, N. (2009). Fuzzy control for nonlinear uncertain electrohydraulic active suspensions with input constraint. *IEEE Transactions on Fuzzy Systems*, *17*(2), 343–356. doi: 10.1109/TFUZZ.2008.2011814

Du, H., Zhang, N., & Wang, L. (2014). Switched control of vehicle suspension based on motion-mode detection. *Vehicle System Dynamics*, *52*(1), 142–165. Retrieved from https://doi.org/10.1080/00423114.2013.866258 doi: 10.1080/00423114.2013.866258

El Majdoub, K., Ghani, D., Giri, F., & Chaoui, F. Z. (2014, sep). Adaptive Semi-Active Suspension of Quarter-Vehicle With Magnetorheological Damper. *Journal of Dynamic Systems, Measurement, and Control*, *137*(2). Retrieved from https://doi.org/10.1115/1.4028314 doi: 10.1115/1.4028314

Elattar, Y., Metwalli, S., & Rabie, M. (2016). PDF Versus PID Controller for Active Vehicle Suspension. In *The international conference on applied mechanics and mechanical engineering* (Vol. 17, pp. 1–18). doi: 10.21608/amme.2016.35163

Fidanciogullari, S., & Yildiz, A. (2021). Characterization of the torsional vibration behavior of circular and rectangular cross-sectional arc springs: Theory and experiments. *Materials Testing*, *63*(2), 113–118. Retrieved from https://doi.org/10.1515/mt-2020-0018 doi: 10.1515/mt-2020-0018

Fonseca, C. M., & Fleming, P. J. (1993). Genetic Algorithms for Multiobjective Optimization :. In *Icga* (Vol. 93, pp. 416–423).

Gillespie, T. D. (1992). Fundamentals of Vehicle Dynamics. *Fundamentals of Vehicle Dynamics*. doi: 10.4271/r-114

Gomes, H. M. (2009). a Swarm Optimization Algorithm for Optimum Vehicle Suspension Design. In *20th international congress of mechanical engineering* (pp. 1–10).

Gopala Rao, L. V., & Narayanan, S. (2009). Sky-hook control of nonlinear quarter car model traversing rough road matching performance of LQR control. *Journal of Sound and Vibration*, *323*(3-5), 515–529. Retrieved from https://www.sciencedirect.com/science/article/pii/S0022460X09000236 doi: 10.1016/j.jsv.2009.01.025

Gündoğdu, Ö. (2007). Optimal seat and suspension design for a quarter car with driver model using genetic algorithms. *International Journal of Industrial Ergonomics*, *37*(4), 327–332. doi: 10.1016/j.ergon.2006.11.005

Gysen, B. L., Paulides, J. J., Janssen, J. L., & Lomonova, E. A. (2010). Active electro-

magnetic suspension system for improved vehicle dynamics. *IEEE Transactions on Vehicular Technology*, *59*(3), 1156–1163. doi: 10.1109/TVT.2009.2038706

Haemers, M., Derammelaere, S., Ionescu, C. M., Stockman, K., De Viaene, J., & Verbelen, F. (2018). Proportional-Integral State-Feedback Controller Optimization for a Full-Car Active Suspension Setup using a Genetic Algorithm. *IFAC-PapersOnLine*, *51*(4), 1–6. Retrieved from https://www.sciencedirect.com/science/article/pii/S240589631830291X doi: 10.1016/j.ifacol.2018.06.004

Harun, M. H., Ab Rahim, A. A., Abdul Halim, I. S., & Abdullah, N. E. (2019). Performance comparison of active suspension for ride comfort using linear quadratic regulator (LQR) and fuzzy logic controller (FLC). In *2018 9th ieee control and system graduate research colloquium, icsgrc 2018 - proceeding* (pp. 99–104). doi: 10.1109/ICSGRC.2018.8657528

He, P., Wang, Y., Zhang, Y., Yang, L., & Xu, Y. (2010). Integrated control of semi-active suspension and vehicle dynamics control system. *ICCASM 2010 - 2010 International Conference on Computer Application and System Modeling, Proceedings*, *5*. doi: 10.1109/ICCASM.2010.5619352

Hernández-Díaz, A. G., Coello, C. A., Pérez, F., Caballero, R., Molina, J., & Santana-Quintero, L. V. (2008). Seeding the initial population of a multi-objective evolutionary algorithm using gradient-based information. In *2008 ieee congress on evolutionary computation, cec 2008* (pp. 1617–1624). doi: 10.1109/CEC.2008.4631008

Hrovat, D. (1997). Survey of Advanced Suspension Developments and Related Optimal Control Applications. *Automatica*, *33*(10), 1781–1817. Retrieved from https://www.sciencedirect.com/science/article/pii/S0005109897001015 doi: 10.1016/S0005-1098(97)00101-5

Hsu, H. T., Coker, C., & Huang, H. (2011). Optimization of an electric vehicle suspension system using CAE. *World Electric Vehicle Journal*, *4*(1), 179–183. doi: 10.3390/wevj4010179

Isa, H. M., Mahadi, W. N. L., Ramli, R., & Abidin, M. A. Z. (2011). A review on electromagnetic suspension systems for passenger vehicle. *InECCE 2011 - International Conference on Electrical, Control and Computer Engineering*, 399–403. doi: 10.1109/INECCE.2011.5953914

Ivanov, V. (2015). A review of fuzzy methods in automotive engineering applications. *European Transport Research Review*, *7*(3), 29. Retrieved from https://doi.org/10.1007/s12544-015-0179-z doi: 10.1007/s12544-015-0179-z

Jiang, X.-Q., Mei, X.-D., & Feng, D. (2016, jan). Air pollution and chronic airway diseases: what should people know and do? *Journal of thoracic disease*, *8*(1), E31–E40. Retrieved from https://pubmed.ncbi.nlm.nih.gov/26904251https://www.ncbi.nlm.nih.gov/pmc/articles/PMC4740163/ doi: 10.3978/j.issn.2072-1439.2015.11.50

Jianhua, L. D. Z. (2008). A BP neural network model based on the adaptive PID control algorithm. *Automation technology and applications*, *8*, 8–10.

Jin, L., Yu, Y., & Fu, Y. (2016). Study on the ride comfort of vehicles driven by in-wheel motors. *Advances in Mechanical Engineering*, *8*(3), 1–9. Retrieved from https://doi.org/10.1177/1687814016633622 doi: 10.1177/1687814016633622

Kaldas, M. M., Çalişkan, K., Henze, R., & Küçükay, F. (2013). Rule Optimized Fuzzy

Logic Controller for Full Vehicle Semi-Active Suspension. *SAE International Journal of Passenger Cars - Mechanical Systems*, *6*(1), 332–344. Retrieved from https://doi.org/10.4271/2013-01-0991 doi: 10.4271/2013-01-0991

Karnopp, D., & Crosby, M. (1974). System For Controlling The Transmission Of Energy Between Spaced Members Patent Grant Karnopp , et al. April 30, 1 [Lord Corporation]. *Google Patents*. Retrieved from https://uspto.report/patent/grant/3807678

Kirli, A. (2015). Design and application of an active suspension system on a 6 DOF half vehicle model. In *2015 25th international conference on information, communication and automation technologies, icat 2015 - proceedings* (pp. 1–6). doi: 10.1109/ICAT.2015.7340500

Kulkarni, A., Ranjha, S. A., & Kapoor, A. (2018). A quarter-car suspension model for dynamic evaluations of an in-wheel electric vehicle. *Proceedings of the Institution of Mechanical Engineers, Part D: Journal of Automobile Engineering*, *232*(9), 1139–1148. Retrieved from https://doi.org/10.1177/0954407017727165 doi: 10.1177/0954407017727165

Kuznetsov, A., Mammadov, M., Sultan, I., & Hajilarov, E. (2011). Optimization of a quarter-car suspension model coupled with the driver biomechanical effects. *Journal of Sound and Vibration*, *330*(12), 2937–2946. doi: 10.1016/j.jsv.2010.12.027

Lam, Q., Wang, L., & Zhang, N. (2013). Experimental implimentation of a fuzzy controller for an active hydraulically interconnected suspension on a sport utility vehicle. In *Ieee intelligent vehicles symposium, proceedings* (pp. 383–390). IEEE. Retrieved from https://doi.org/10.1109/IVS.2013.6629499 doi: 10.1109/IVS.2013.6629499

Lee, S., Yakub, F., Kasahara, M., & Mori, Y. (2013). Rollover prevention with predictive control of differential braking and rear wheel steering. In *Ieee conference on robotics, automation and mechatronics, ram - proceedings* (pp. 144–149). doi: 10.1109/RAM.2013.6758574

Li, H., Liu, H., Gao, H., & Shi, P. (2012). Reliable fuzzy control for active suspension systems with actuator delay and fault. *IEEE Transactions on Fuzzy Systems*, *20*(2), 342–357. doi: 10.1109/TFUZZ.2011.2174244

Lin, C., Liu, W., & Ren, H. (2015). Neutral network-PID control algorithm for semi-active suspensions with magneto-rheological damper. *Journal of Vibroengineering*, *17*(8), 4432–4444.

Lin, J., Cheng, K. W. E., Xue, X., Cheung, N. C., & Zhang, Z. (2014). Estimation of inductance derivative for force control of linear switched reluctance actuator. *IEEE Transactions on Magnetics*, *50*(11), 1–4. Retrieved from https://doi.org/10.1109%2Ftmag.2014.2334312 doi: 10.1109/TMAG.2014.2334312

Lin, J., Cheng, K. W. E., Zhang, Z., Cheung, N. C., & Xue, X. (2015). Adaptive sliding mode technique-based electromagnetic suspension system with linear switched reluctance actuator. *IET Electric Power Applications*, *9*(1), 50–59. Retrieved from https://ietresearch.onlinelibrary.wiley.com/doi/abs/10.1049/iet-epa.2014.0115 doi: 10.1049/iet-epa.2014.0115

Lin, J., Cheng, K. W. E., Zhang, Z., Cheung, N. C., Xue, X., & Ng, T. W. (2013). Active suspension system based on linear switched reluctance actuator and control schemes. *IEEE Transactions on Vehicular Technology*, *62*(2), 562–572. doi:

10.1109/TVT.2012.2222682

Liu, M., Gu, F., & Zhang, Y. (2017). Ride comfort optimization of in-wheel-motor electric vehicles with in-wheel vibration absorbers. *Energies*, *10*(10), 1–21. Retrieved from https://ideas.repec.org/a/gam/jeners/v10y2017i10p1647-d115613.html doi: 10.3390/en10101647

Maciejewski, I., Glowinski, S., & Krzyzynski, T. (2014). Active control of a seat suspension with the system adaptation to varying load mass. *Mechatronics*, *24*(8), 1242–1253. Retrieved from https://www.sciencedirect.com/science/article/pii/S0957415814001664 doi: 10.1016/j.mechatronics.2014.10.008

Mahmoodabadi, M. J., & Nejadkourki, N. (2020). Optimal fuzzy adaptive robust PID control for an active suspension system. *Australian Journal of Mechanical Engineering*, *0*(0), 1–11. Retrieved from https://doi.org/10.1080/14484846.2020.1734154 doi: 10.1080/14484846.2020.1734154

Martins, I., Esteves, J., Marques, G. D., & da Silva, F. P. (2006). Permanent-magnets linear actuators applicability in automobile active suspensions. *IEEE Transactions on Vehicular Technology*, *55*(1), 86–94. doi: 10.1109/TVT.2005.861167

Marzbanrad, J., Soleimani, G., Mahmoodi-k, M., & Rabiee, A. H. (2015). Development of fuzzy anti-roll bar controller for improving vehicle stability. *Journal of Vibroengineering*, *17*(7), 3856–3864.

Mashadi, B., Mahmoudi-Kaleybar, M., Ahmadizadeh, P., & Oveisi, A. (2013). A path-following driver/vehicle model with optimized lateral dynamic controller. *Latin American Journal of Solids and Structures*, *11*(4), 613–630. doi: 10.1590/s1679-78252014000400004

Meng, Q., Qian, C., & Liu, R. (2018). Dual-rate sampled-data stabilization for active suspension system of electric vehicle. *International Journal of Robust and Nonlinear Control*, *28*(5), 1610–1623. Retrieved from https://onlinelibrary.wiley.com/doi/abs/10.1002/rnc.3974 doi: 10.1002/rnc.3974

Mihai, I., & Andronic, F. (2014). Behavior of a semi-active suspension system versus a passive suspension system on an uneven road surface. *Mechanika*, *20*(1), 64–69. doi: 10.5755/j01.mech.20.1.6591

Mitra, A. C., Desai, G. J., Patwardhan, S. R., Shirke, P. H., Kurne, W. M., & Banerjee, N. (2016). Optimization of Passive Vehicle Suspension System by Genetic Algorithm. *Procedia Engineering*, *144*, 1158–1166. Retrieved from https://www.sciencedirect.com/science/article/pii/S1877705816303046 doi: 10.1016/j.proeng.2016.05.087

Murata, S. (2012a). Innovation by in-wheel-motor drive unit. *Vehicle System Dynamics*, *50*(6), 807–830. Retrieved from https://doi.org/10.1080/00423114.2012.666354 doi: 10.1080/00423114.2012.666354

Murata, S. (2012b). Innovation by in-wheel-motor drive unit. *Vehicle System Dynamics*, *50*(6), 807–830. Retrieved from https://doi.org/10.1080/00423114.2012.666354 doi: 10.1080/00423114.2012.666354

Nagarkar, M. P., Vikhe Patil, G. J., & Zaware Patil, R. N. (2016). Optimization of nonlinear quarter car suspension–seat–driver model. *Journal of Advanced Research*, *7*(6), 991–1007. Retrieved from https://www.sciencedirect.com/science/article/pii/S2090123216300236 doi: 10.1016/j.jare.2016.04.003

Nagaya, G., Wakao, Y., & Abe, A. (2003). Development of an in-wheel drive with

advanced dynamic-damper mechanism. *JSAE Review*, *24*(4), 477–481. doi: 10.1016/S0389-4304(03)00077-8

Naudé, A. F., & Snyman, J. A. (2003). Optimisation of road vehicle passive suspension systems. Part 2. Qualification and case study. *Applied Mathematical Modelling*, *27*(4), 263–274. Retrieved from https://www.sciencedirect.com/science/article/pii/S0307904X0200121X doi: 10.1016/S0307-904X(02)00121-X

Nguyen, L. H., Park, S., Turnip, A., & Hong, K. S. (2009). Application of LQR control theory to the design of modified skyhook control gains for semi-active suspension systems. *ICCAS-SICE 2009 - ICROS-SICE International Joint Conference 2009, Proceedings*, 4698–4703.

Niu, X. J. (2014). The optimization for PID controller parameters based on genetic algorithm. In *Applied mechanics and materials* (Vol. 513-517, pp. 4102–4105). Trans Tech Publications Ltd. doi: 10.4028/www.scientific.net/AMM.513-517.4102

Özcan, D., Sönmez, Ü., & Güvenç, L. (2013). Optimisation of the nonlinear suspension characteristics of a light commercial vehicle. *International Journal of Vehicular Technology*, *2013*. doi: 10.1155/2013/562424

Papageorgiou, A. M.-c. C. (2006). Evolutionary Algorithms and Bilinear Matrix Inequalities for a Passive Suspension. In *Optimization* (pp. 386–391).

Patil, M. K., & Palanichamy, M. S. (1985). Minimization of human body responses to low frequency vibration: Application to tractors and trucks. *Mathematical Modelling*, *6*(5), 421–442. doi: 10.1016/0270-0255(85)90063-6

Paulides, J. J., Encica, L., Lomonova, E. A., & Vandenput, A. J. (2006). Design considerations for a semi-active electromagnetic suspension system. *IEEE Transactions on Magnetics*, *42*(10), 3446–3448. doi: 10.1109/TMAG.2006.879963

Peng, J., He, H., & Feng, N. (2013). Simulation research on an electric vehicle chassis system based on a collaborative control system. *Energies*, *6*(1), 312–328. Retrieved from https://www.mdpi.com/1996-1073/6/1/312 doi: 10.3390/en6010312

Pillai, S. R., Pon Selvan, C., & Madara, S. R. (2019). Design of PID Control to Improve Efficiency of Suspension System in Electric Vehicles. In *Proceedings of 2019 international conference on computational intelligence and knowledge economy, iccike 2019* (pp. 570–575). doi: 10.1109/ICCIKE47802.2019.9004322

Quynh, L. V., Cuong, B. V., Liem, N. V., Long, L. X., & Dung, P. T. T. (2019). Effect of in-wheel motor suspension system on electric vehicle ride comfort. *Vibroengineering Procedia*, *29*, 148–152. Retrieved from https://doi.org/10.21595%2Fvp.2019.21175 doi: 10.21595/vp.2019.21175

Reeves, C. R., & Rowe, J. E. (2002). *Genetic algorithms: Principles and perspectives: A Guide to GA theory* (Vol. 20). Springer US. Retrieved from https://books.google.com.tr/books?id=gu1DLIzoJDQC

Ren, H., Chen, L., & Zhou, Q. (2020, may). Fuzzy Control for Uncertain Electric Vehicle Systems with Sensor Failures and Actuator Saturation. *International Journal of Fuzzy Systems*, *22*(5), 1444–1453. Retrieved from https://doi.org/10.1007%2Fs40815-020-00869-y doi: 10.1007/s40815-020-00869-y

Rosenthal, S., & Borschbach, M. (2014). Impact of Population Size and Selection within a Customized NSGA-II for Biochemical Optimization Assessed on the Basis of the Average Cuboid Volume Indicator. In *Biotechno 2014 : The sixth international conference on bioinformatics, biocomputational systems and biotechnologies im-*

pact (Vol. I, pp. 1–7).

Senthil Kumar, P., Sivakumar, K., Kanagarajan, R., & Kuberan, S. (2018). Adaptive neuro fuzzy inference system control of active suspension system with actuator dynamics. *Journal of Vibroengineering*, *20*(1), 541–549. Retrieved from https://doi.org/10.21595%2Fjve.2017.18379 doi: 10.21595/jve.2017.18379

Shao, X. (2018). *Active suspension control of electric vehicle with in-wheel motors* (Doctoral dissertation, Doctor of Philosophy thesis, School of Electrical, Computer and Telecommunications Engineering, University of Wollongong, Wollongong, Australia). Retrieved from https://ro.uow.edu.au/theses1/377

Shao, X., Naghdy, F., & Du, H. (2017). Reliable fuzzy H∞ control for active suspension of in-wheel motor driven electric vehicles with dynamic damping. *Mechanical Systems and Signal Processing*, *87*, 365–383. doi: 10.1016/j.ymssp.2016.10.032

Shao, X., Zhang, N., Du, H., & Wang, L. (2013). Fuzzy control of hydraulically interconnected suspension with configuration switching. In *Proceedings of 2013 ieee international conference on vehicular electronics and safety, icves 2013* (pp. 66–71). doi: 10.1109/ICVES.2013.6619605

Simon, D. E., & Ahmadian, M. (1998). *Experimental Evaluation of Semiactive Magnetorheological Primary Suspensions for Heavy Truck Applications by* (Unpublished master's thesis). VA: Virginia Tech.

Sinha, P. K., & Pechev, A. N. (2004). Nonlinear H∞ controllers for electromagnetic suspension systems. *IEEE Transactions on Automatic Control*, *49*(4), 563–568. doi: 10.1109/TAC.2003.822865

Smith, M. C., & Walker, G. W. (2005). Interconnected vehicle suspension. *Proceedings of the Institution of Mechanical Engineers, Part D: Journal of Automobile Engineering*, *219*(3), 295–307. doi: 10.1243/095440705X6578

Smith, W. A., & Zhang, N. (2010). Recent developments in passive interconnected vehicle suspension. *Frontiers of Mechanical Engineering in China*, *5*(1), 1–18. doi: 10.1007/s11465-009-0092-z

Smith, W. A., Zhang, N., & Hu, W. (2011). Hydraulically interconnected vehicle suspension: Handling performance. *Vehicle System Dynamics*, *49*(1-2), 87–106. doi: 10.1080/00423111003596743

Sosthene, K., Josee, M., & Hui, X. (2018). Fuzzy Logic Controller for Semi Active Suspension Based on Magneto-Rheological Damper. *International Journal of Automotive Engineering and Technologies*, *7*(1), 38–47. doi: 10.18245/ijaet.438045

Srinivas, N., & Deb, K. (1994). Muiltiobjective Optimization Using Nondominated Sorting in Genetic Algorithms. *Evolutionary Computation*, *2*(3), 221–248. doi: 10.1162/evco.1994.2.3.221

Sun, W., Gao, H., & Shi, P. (2020). *Advanced Control for Vehicle Active Suspension Systems* (Vol. 204) (No. 2). Retrieved from http://ieeexplore.ieee.org/lpdocs/epic03/wrapper.htm?arnumber=5428778%0Ahttp://link.springer.com/10.1007/978-3-030-15785-2 doi: 10.1007/978-3-030-15785-2

Sun, W., Gao, H., & Yao, B. (2013). Adaptive robust vibration control of full-car active suspensions with electrohydraulic actuators. *IEEE Transactions on Control Systems Technology*, *21*(6), 2417–2422. doi: 10.1109/TCST.2012.2237174

Sun, W., Li, Y., Huang, J., & Zhang, N. (2017). Efficiency improvement of vehicle active suspension based on multi-objective integrated optimization. *JVC/Journal*

of Vibration and Control, *23*(4), 539–554. Retrieved from https://doi.org/10.1177/1077546315581731 doi: 10.1177/1077546315581731

Sun, W., Pan, H., & Gao, H. (2016). Filter-Based Adaptive Vibration Control for Active Vehicle Suspensions with Electrohydraulic Actuators. *IEEE Transactions on Vehicular Technology*, *65*(6), 4619–4626. doi: 10.1109/TVT.2015.2437455

Sun, X. Q., Cai, Y. F., Yuan, C. C., Wang, S. H., & Chen, L. (2018). Fuzzy sliding mode control for the vehicle height and leveling adjustment system of an electronic air suspension. *Chinese Journal of Mechanical Engineering (English Edition)*, *31*(2), 25. doi: 10.1186/s10033-018-0223-8

Sun, Y. Q., Zhao, L. F., & Xiang, W. (2013). A fuzzy logic controller for vehicle-active suspension systems. In *Advanced materials research* (Vol. 805-806, pp. 1645–1649). Trans Tech Publications Ltd. doi: 10.4028/www.scientific.net/AMR.805-806.1645

Sung, H. K., Lee, S. H., & Bien, Z. (2005). Design and implementation of a fault tolerant controller for EMS systems. *Mechatronics*, *15*(10), 1253–1272. Retrieved from https://www.sciencedirect.com/science/article/pii/S0957415805000814 doi: 10.1016/j.mechatronics.2005.04.003

Sung, K. G., Han, Y. M., Cho, J. W., & Choi, S. B. (2008). Vibration control of vehicle ER suspension system using fuzzy moving sliding mode controller. *Journal of Sound and Vibration*, *311*(3-5), 1004–1019. Retrieved from https://www.sciencedirect.com/science/article/pii/S0022460X0700795X doi: 10.1016/j.jsv.2007.09.049

Sung, K. G., Han, Y. M., Lim, K. H., & Choi, S. B. (2007). Discrete-time fuzzy sliding mode control for a vehicle suspension system featuring an electrorheological fluid damper. *Smart Materials and Structures*, *16*(3), 798–808. Retrieved from https://doi.org/10.1088/0964-1726/16/3/029 doi: 10.1088/0964-1726/16/3/029

Taghavifar, H. (2021). EKF estimation based PID Type-2 fuzzy control of electric cars. *Measurement: Journal of the International Measurement Confederation*, *173*, 108557. Retrieved from https://www.sciencedirect.com/science/article/pii/S0263224120310800 doi: 10.1016/j.measurement.2020.108557

Taghavifar, H., Hu, C., Qin, Y., & Wei, C. (2020). EKF-Neural Network Observer Based Type-2 Fuzzy Control of Autonomous Vehicles. *IEEE Transactions on Intelligent Transportation Systems*, 1–13. doi: 10.1109/tits.2020.2985124

Tan, D., Lu, C., & Zhang, X. (2016). 2169. Dual-loop PID control with PSO algorithm for the active suspension of the electric vehicle driven by in-wheel motor. *Journal of Vibroengineering*, *18*(6), 3915–3929. Retrieved from https://doi.org/10.21595%2Fjve.2016.16689 doi: 10.21595/jve.2016.16689

Termous, H., Moreau, X., Francis, C., & Shraim, H. (2018). From the standard PID to the CRONE first generation controller: Application to an anti-roll system for Electric Vehicles. *IFAC-PapersOnLine*, *51*(4), 733–738. Retrieved from https://www.sciencedirect.com/science/article/pii/S2405896318305068 doi: 10.1016/j.ifacol.2018.06.209

Tian, M., & Nguyen, V. (2020). Control performance of suspension system of cars with PID control based on 3D dynamic model. *Journal of Mechanical Engineering, Automation and Control Systems*, *1*(1), 1–10. Retrieved from https://doi.org/10.21595%2Fjmeacs.2020.21363 doi: 10.21595/jmeacs.2020.21363

TOGG. (2020). *TOGG*. http://www.togg.com.tr/content/automobile.

TOKSOY, M. T., & YILDIZ, A. (2020). TekerleİçiMotorlElektrikliBir AracinAktifSüspansiySisteminin Pid Ve Bulanik Mantik Tabanli Kontrolü. *Uludağ University Journal of The Faculty of Engineering*, *25*, 1373–1390. doi: 10.17482/uumfd.789019

Türkiye Elektrikli ve Hibrid Araçlar Derneği. (2020). *Markaların Elektrikli Araç Üretim Planlaması*. https://www.tehad.org/2020/03/21/markalarin-elektrikli-arac-uretim-planlamasi/.

Van Der Sande, T. P., Gysen, B. L., Besselink, I. J., Paulides, J. J., Lomonova, E. A., & Nijmeijer, H. (2013). Robust control of an electromagnetic active suspension system: Simulations and measurements. *Mechatronics*, *23*(2), 204–212. Retrieved from https://www.sciencedirect.com/science/article/pii/S0957415812001031 doi: 10.1016/j.mechatronics.2012.07.002

Van Niekerk, J. L., Pielemeier, W. J., & Greenberg, J. A. (2003). The use of seat effective amplitude transmissibility (SEAT) values to predict dynamic seat comfort. *Journal of Sound and Vibration*, *260*(5), 867–888. doi: 10.1016/S0022-460X(02)00934-3

Verros, G., Natsiavas, S., & Papadimitriou, C. (2005). Design optimization of quarter-car models with passive and semi-active suspensions under random road excitation. *JVC/Journal of Vibration and Control*, *11*(5), 581–606. doi: 10.1177/1077546305052315

Vos, R., Besselink, I. J. M., & Nijmeijer, H. (2010). Influence of in-wheel motors on the ride comfort of electric vehicles. In *the 10th international symposium on advanced vehicle control (avec10)* (pp. 835–840).

Wan, Y., & Schimmels, J. M. (1995). Simple model that captures the essential dynamics of a seated human exposed to whole body vibration. In *American society of mechanical engineers, bioengineering division (publication) bed* (Vol. 31, pp. 333–334).

Wang, L., Zhang, N., & Du, H. (2012). Experimental Investigation of a Hydraulically Interconnected Suspension in Vehicle Dynamics and Stability Control. *SAE International Journal of Passenger Cars - Mechanical Systems*, *5*(2), 759–768. doi: 10.4271/2012-01-0240

Xu, Y., Ahmadian, M., & Sun, R. (2014). Improving vehicle lateral stability based on variable stiffness and damping suspension system via MR damper. *IEEE Transactions on Vehicular Technology*, *63*(3), 1071–1078. doi: 10.1109/TVT.2013.2282824

Yang, G., & Zhao, Y. (2012). Fuzzy control of vehicle suspension system. In *Advanced materials research* (Vol. 383-390, pp. 2012–2017). Trans Tech Publications Ltd. doi: 10.4028/www.scientific.net/AMR.383-390.2012

Yatak, M. Ö., & Şahin, F. (2021). Ride Comfort-Road Holding Trade-off Improvement of Full Vehicle Active Suspension System by Interval Type-2 Fuzzy Control. *Engineering Science and Technology, an International Journal*, *24*(1), 259–270. Retrieved from https://www.sciencedirect.com/science/article/pii/S221509862034235X doi: 10.1016/j.jestch.2020.10.006

Yildiz, A. (2019a). A comparative study on the optimal non-linear seat and suspension design for an electric vehicle using different population-based optimisation algorithms. *International Journal of Vehicle Design*, *1*(1), 1. doi: 10.1504/ijvd.2019.10031168

Yildiz, A. (2019b). Optimum suspension design for non-linear half vehicle model using particle swarm optimization (Pso) algorithm. *Vibroengineering Procedia*, *27*, 43–

48. Retrieved from https://doi.org/10.21595%2Fvp.2019.21012 doi: 10.21595/vp.2019.21012

Yildiz, A. (2021). Parametric synthesis of two dıfferent trunk lid mechanisms for sedan vehıcles using population-based optimisation algorithms. *Mechanism and Machine Theory*, *156*, 104130. Retrieved from https://www.sciencedirect.com/science/article/pii/S0094114X20303475 doi: 10.1016/j.mechmachtheory.2020.104130

Yildiz, A., & Özel, M. A. (2021). A comparative study of energy consumption and recovery of autonomous fuel-cell hydrogen–electric vehicles using different powertrains based on regenerative braking and electronic stability control system. *Applied Sciences (Switzerland)*, *11*(6). Retrieved from https://www.mdpi.com/2076-3417/11/6/2515 doi: 10.3390/app11062515

Yokoyama, M., Hedrick, J. K., & Toyama, S. (2001). A model following sliding mode controller for semi-active suspension systems with MR dampers. In *Proceedings of the american control conference* (Vol. 4, pp. 2652–2657). doi: 10.1109/ACC.2001.946276

Yoshimura, T., Kume, A., Kurimoto, M., & Hino, J. (2001). Construction of an active suspension system of a quarter car model using the concept of sliding mode control. *Journal of Sound and Vibration*, *239*(2), 187–199. Retrieved from https://www.sciencedirect.com/science/article/pii/S0022460X00931171 doi: 10.1006/jsvi.2000.3117

Yıldız, A. S., Sivrioğlu, S., Zergeroğlu, E., & Çetin, □. (2015). Nonlinear adaptive control of semi-active MR damper suspension with uncertainties in model parameters. *Nonlinear Dynamics*, *79*(4), 2753–2766. Retrieved from https://doi.org/10.1007/s11071-014-1844-9 doi: 10.1007/s11071-014-1844-9

Zhang, J., Yang, Y., Hu, M., Fu, C., & Zhai, J. (2021). Model predictive control of active suspension for an electric vehicle considering influence of braking intensity. *Applied Sciences (Switzerland)*, *11*(1), 1–19. Retrieved from https://www.mdpi.com/2076-3417/11/1/52 doi: 10.3390/app11010052

Zhang, N., Smith, W. A., & Jeyakumaran, J. (2010). Hydraulically interconnected vehicle suspension: Background and modelling. *Vehicle System Dynamics*, *48*(1), 17–40. doi: 10.1080/00423110903243182

Zhang, N., Wang, L., & Du, H. (2014). Motion-mode energy method for vehicle dynamics analysis and control. *Vehicle System Dynamics*, *52*(1), 1–25. Retrieved from https://doi.org/10.1080/00423114.2013.847468 doi: 10.1080/00423114.2013.847468

Zhu, S., Wang, L., Zhang, N., & Du, H. (2013). H∞ control of a novel low-cost roll-plane active hydraulically interconnected suspension: An experimental investigation of roll control under ground excitation. *SAE International Journal of Passenger Cars - Mechanical Systems*, *6*(2), 882–893. Retrieved from https://doi.org/10.4271/2013-01-1238 doi: 10.4271/2013-01-1238

Zitzler, E., Deb, K., & Thiele, L. (2000). Comparison of multiobjective evolutionary algorithms: empirical results. *Evolutionary computation*, *8*(2), 173–195. doi: 10.1162/106365600568202